# Developing Membrane Active Peptides for Endosomal Escape of Macromolecules

by
Gregory R Wiedman

A dissertation submitted to Johns Hopkins University in conformity with the requirements for the degree of Doctor of Philosophy

Baltimore, Maryland
March 2015

Abstract

Membrane Active Peptides (MAPs) are an important class of short protein sequences that hold the potential to be used for a number of varied purposes such as antibacterial, antiviral, and drug delivery based therapies. Despite this great potential, the development of MAPs has been hindered by a lack of consensus about their mechanisms of activity. Herein we proposed that MAPs can be categorized into several categories differentiating how they interact with model cell membranes. In this dissertation we examined how these activities can be regulated by pH. We used this information to design and test MAPs with pH-dependant activity for drug delivery through both rational design and high-throughput screening. Finally, we tested our peptides both with model biophysical characterization techniques as well as cell based assays and made connections between the two. Our intention is that the work conducted in this dissertation will provide a framework for the development of effective and efficient Membrane Active Peptides.

Readers:

Dr. Martin Ulmschneider

Dr. Kalina Hristova

Summary Chapter 6

## Chapter 7 Biophysical and Cell-based Studies of Positive Screen Results

List of Figures

List of Abbreviations

AF: Alexafluor (488)

ANTS: 8-aminonapthalene-1,3,6 trisulfonic acid

CD: Circular Dichroism

CH: Cholesterol

DPX: p-xylene-bis-pyridinium bromide

FD: Fluorescein Dextran

kDa: kiloDalton (mass)

TA/TAMRA: Carboxytetramethylrhodamine

TBD: TAMRA-Biotin-Dextran (10 and 40kDa)

LC/MS: Liquid Chromatography Mass Spectroscopy

MS: Mass Spectroscopy

MAP: Membrane Active Peptide

nm: nanometers (length)

nmol: nanomoles (number)

nM: nanomolar (concentration)

POPC: -palmitoyl-2-oleoylphosphatidylcholine

POPG: 1-hexadecanoyl-2-(9Z-octadecenoyl)-sn-glycero-3-phospho-(1'-rac-glycerol)

SA: Streptavidin-Alexafluor488

The Cell Membrane: Key Component of Cell Survival

The existence of the cell membrane is both a blessing and a curse to human physiology.  Since the evolution of the very first prokaryotic organism, the cell membrane has provided a barrier to separate a cell's internal components from the outside world.  While this barrier offers a degree of protection to the cell from harmful molecules, it also impedes the diffusion of potentially beneficial particles.  We have begun to develop a greater understanding of cell biology and cellular engineering, which has created a desire to add exotic components to our cells.  We understand the free energy penalties associated with binding/insertion into the cell membrane and we can determine the kinetic rates of these pathways.  This begs the question; how far can we go with this knowledge and can we control the way in which molecules interact with the cell membrane?

Cell membranes, the outer barrier of a cell, are conventionally thought of as liquid crystalline materials.[1] The main component of these liquid crystals are small amphiphilic molecules known as phospholipids.  These are molecules that have both a hydrophilic phosphate head group and hydrophobic alkyl chain tails.  Of these phospholipids, 1-palmitoyl-2-oleoylphosphatidylcholine (POPC) is the most abundant in cell membranes.[2]  Phospholipids that compose the cell membrane are found in a bilayer structure with head groups facing the aqueous environments of the cell cytosol or the outside of the cell and with alkyl chains facing inwards.  The driving force for phospholipids to form this phase of liquid crystal stems from the manner in which water molecules can coordinate about the head groups/tails: the hydrophobic effect.  X-ray

diffraction studies show that the tail groups associate with each other to exclude nearly all water molecules from the inside, hydrophobic core of the cell membrane.[3] Though these forces are strong enough to stabilize membranes on the order of several microns in length, other lipid types are needed for further stabilization.

Even though the most prevalent component of the cell membrane, POPC, comprises nearly 75% of the molecules in the membrane, it is not the only component needed for stabilization. One other important component of the cell membrane is cholesterol. Cholesterols are small organic molecules that is known to form a chiral liquid crystalline phase from which the term "cholesteric liquid crystal" is derived.[4] Cholesterol acts as a mediator to stabilize the cell membrane when it would encounter varying temperatures in its environment. At temperatures approaching the gel-crystalline phase of a pure POPC membrane, cholesterol serves to prevent the complete ordering of the phospholipids by inhibiting packing of phospholipids. Thus, cholesterol allows the membrane to retain its liquid crystalline "fluidity" at lower temperatures. In addition, at higher temperatures where phospholipid liquid crystals tend to become more highly disordered, cholesterol allows the membrane to obtain rigidity by impeding diffusion of the phospholipids. Cholesterol is an important component of membranes of multi-cellular organisms because it can allow the cells of these organisms to remain stable in a range of temperature conditions.

The final, important component of cell membranes discussed in this work is another phospholipid called 1-hexadecanoyl-2-(9Z-octadecenoyl)-sn-glycero-3-phospho-(1'-rac-glycerol) (POPG). This phospholipid's head group has a net negative charge,

unlike POPC or even cholesterol. POPG is important because it is a major component of bacterial cell membranes, sometimes between 10-20% of total molecules but is rarely found in mammalian cells (<2%).[5] Due to the relative abundance of charged phospholipids on bacterial membranes as compared to mammalian membranes the possibility of localizing charged molecules to a cell surface exists. Much work has gone into targeting positively charged molecules to the negatively charged bacterial cell membrane.[6, 7] For this reason, we have sought to investigate the effects of having cholesterol (mammalian cell membrane) or POPG (bacterial cell membrane) inside of our model cell membranes. These lipid components of the cell membrane allow it to maintain a liquid crystalline structure and give it very useful properties for a cell's existence.

The cell membrane provides a crucial barrier for the cell to section off its internal components from the outside environment. At the very basic level, the cell membrane prevents the free diffusion of molecules across it. This property allows the cell to prevent its internal components, DNA, enzymes, organelles, and etc from diffusing away. The cell membrane affords the cell a restricting volume in which it can undergo a vast array of chemical reactions.[8] Theories such as the endosymbiotic theory propose that the development of cell membrane was a key evolutionary step in the development of higher-order cell types.[9] This theory suggests that existence of this barrier to keep large components together led to the rise of complex cell structures. Cell membranes not only afford the cell an internal compartment in which it can control and direct chemical reactions, they also create a site for molecular/chemical reactions to occur.

Selective permeability makes the cell membrane a site for the establishment of chemical gradients.  Due to its liquid crystalline amphiphilic structure, cell membranes have a defined hydrophilic outer layer and a strongly hydrophobic inner core.  This bilayer structure prevents the free diffusion of large, polar molecules across it. This is because in order for a polar molecule to pass through the membrane it would have to coordinate about the hydrophobic tail group of the cell membrane phospholipids. Coordination of polar groups about hydrophobic groups reduces the molecule's ability to coordinate with water molecules.  This interaction decreases the entropy of the system and is thus, energetically unfavorable.[10]  Similarly, the diffusion of large molecules is unfavorable due to the displacement of lipids by the large molecules. Such displacement would require the lipids to interact, unfavorably, with water in a similar entropy-decreasing manner to a polar-hydrophobic interaction.[11]  With this ability to restrict the motion of molecules, the cell membrane is able to become the site of sharp chemical gradients.  Cells can take advantage of the chemical potential of these separated species to regulate its internal state.

An electrical potential exists across intact cell membranes due to the membrane's ability to inhibit the diffusion of charged molecules.  Cells can take advantage of the energetic penalties of moving a charged molecule across the cell membrane to develop gradients of charged molecules and a net potential across the cell membrane.  This net potential is useful to a cell for catalyzing transport interactions, for energy production interactions, for signaling interactions, and for a wide variety of other purposes.[12-14]  Without the ability to maintain this potential, cells become susceptible to

apoptosis and eventual cell death.  The hallmark of a cell with a ruptured membrane is a decrease in the membrane potential.[15, 16]  The cell membrane is essential to establishing electrochemical gradients from the outside to the inside of the cell and for cell survival.

Mechanisms of Cell Entry

Cell membranes, being selectively permeable liquid crystalline bilayers, are able to restrict the motion of molecules across them.  Just because the membrane limits the diffusion of molecules across it, however, does not mean that molecules cannot reach the inside of the cell.  Other than diffusion through the membrane, there are two canonical classes of particle entry into the cell: direct transport and endocytosis.[17]  The first class, direct transport, can be either an energy consuming (Active) process or non-energy consuming (Passive).  These pathways involve molecules other than lipids, e.g. proteins, which exist in the cell membrane and allow the molecules to pass through them instead of through the membrane.  The work discussed in this dissertation focuses on the second class of transportation into the cell: endocytosis.

Endocytosis can be categorized by the type of molecules being up taken and by the manner in which they are up taken.  Pinocytosis, a type of endocytosis, refers to cellular uptake of liquids and well dissolved aqueous components.  In this case, the cell membrane becomes invaginated allowing the liquid to fill a small pocket, before eventually being closed by the fission of an endosome from the cell membrane.  One other endocytosis process is phagocytosis.  In this case, the cell membrane protrudes outward to surround a large solid particle.  Eventually the two ends of the protrusion are able to meet when the molecule is fully engulfed; the ends fuse together again forming a free endosome.  Finally, the last major class of endocytosis involves receptor-mediated endocytosis.[17]  In the case of receptor-mediated endocytosis, molecules bind to receptor present on the cell membrane.  The binding of molecules to these receptors

elicits a response from the cell telling it to begin an invagination process. The invagination process terminated with the receptor-captured molecules becoming encased in an endosome inside of the cell. In each of these three types of endocytosis, the components entering the cell become encased in vesicle-phase lipid particle known as an endosome.

What happens to a particle when it gets into a cell by way of endocytosis? The fate of endocytosed particles varies but very few particles will simply diffuse out of the endosome. The endosomes have a similar composition to the cell membrane from which they are derived; they are made of phospholipids. Rather than existing in a semi-planar bilayer phase these phospholipids are now in a vesicle phase. This vesicle phase still maintains the bilayer structure of having external hydrophilic layers and a hydrophobic core. Due to this fact; large, polar molecules that would not readily be able to diffuse across the cell membrane are still restricted from diffusion across the endosomal membrane. It is up to the cell's internal machinery to deliver the contents of endosomes to where it is needed within the cell.

Endosomal cargo that cannot be used by the cell must be disposed of via endosomal maturation pathways.[18, 19] Foreign molecules that cannot be released from the endosome will remain entrapped until the endosome undergoes a natural maturation process. Over time, endosomes will become acidified to a lower pH level than the inside cytosol of the cell. As this process occurs, endosomes become "late endosomes" when new lipids and components are trafficked to the endosome. If the components are not able to escape from late endosomes they will eventually be

subjected to the harsh conditions of lysosomes.  As a late endosome matures further, they can be trafficked to various organelles, one of which is the lysosome.  A late endosome can fuse with the cells lysosome and uptake degradation enzymes.  At the low pH of the endo-lysosome these enzymes activate and serve to degrade the cargo that was previously encapsulated inside of the endosome.[20]  Therefore, molecules that cannot diffuse out of the endosome and cannot reach a different organelle are destined to be degraded by natural cell machinery.

Escape from Endosomes

Molecules that cannot escape from the endosome and that are not trafficked to other organelles face eventual degradation in lysosomes.  This is not a productive fate for medicinal molecules, which often need to enter the cytosol to achieve their therapeutic function.  One promising group of such molecules are siRNA sequences. Sequences of siRNA can target and bind to specific mRNA molecules in the cell cytosol, thus treating certain genetic disorders.[21, 22]  If these siRNA sequences are degraded, however, they cannot interact with their target and will not have any effect on the cell. Therapeutic siRNA sequences often contain several dozen individual nucleic acids. Given that the phosphate backbone of siRNA contains a number of charged groups, it is unlikely that it would be able to readily diffuse out of the endosome. How can molecules such as siRNA effectively escape?

Fortunately for the field of siRNA-based gene therapy, several schemes have been developed by which molecules may exit the endosome.  Certain types of drug delivery devices that are currently being developed can cause endosomal escape via a "proton-sponge effect".[23-25]  In this case, drug molecules are encapsulated within a large, charged polymer network.  As the endosome matures and it begins to acidify, the protons that are pumped in are absorbed by the polymer network.  The selective absorption of one type of charged ion leads to a buffering effect on the endosome, promoting the influx of more ions.  As these ions build up inside of the endosome, a large osmotic pressure gradient builds up across the membrane.  The endosome will begin to swell with water over time to compensate for this buildup in osmotic pressure.

Eventually the polymer network present inside of the endosome induces lysis. Current theories suggest that when the endosome swells and lyses due to the "proton-sponge effect" its contents are able to diffuse into the cytosol. Evidence for this has been seen with studies using large dextran molecules encapsulated with one polymer network PEI as well as siRNA knockdown of genes in model cell systems.[26] Little direct evidence has been discovered, to date, to show this mechanism in action *in vivo* and it is still debated.

Other than osmotic pressure based lysis of the cell, extreme concentrating of solutes on the membrane may lead to endosomal escape. There are certain peptide sequences such as TAT and Arg9 that are known to promote endosomal uptake of molecules.[27, 28] Originally these molecules were thought to pass through cell membranes directly without the need for endocytosis.[29] The scientific consensus now states that molecules such as Arg9 are able to bind to components on either the cell membrane or the extracellular matrix to induce uptake.[30-32] These molecules, and therefore any molecule conjugated to them, are able to reach extremely high localized concentrations. Once inside of an endosome, the concentration of these molecules would be much higher than had they been endocytosed via non receptor/receptor-like pathways. Having molecules in such a high concentration leads to a increased number of molecules escaping from the endosome. The escape of an individual molecule may be extremely unlikely but the escape of one molecule out of two or three orders of magnitude more molecules be more likely. In essence, putting more molecules into an endosome leads to a higher probability that a molecule will be observed escaping via

diffusion.  This pathway still relies on diffusion of molecules through the endosomal membrane and leaves substantial room for improvement.

Of the various methods to cause endosomal escape, creating a pathway for molecules to escape through direct transport holds the most promise.  The creation of stable, long lived pores in an endosomal membrane would allow for the contents to escape quickly without having to depend on membrane rupture or transmembrane diffusion of molecules.  Several types of molecules have been studied for their pore-forming ability.  Membrane active peptides are such molecules.  Some types membrane active peptides were found to interact with cell membranes in a pH-dependant manner; they held promise as use for use as drug delivery agents.  Many studies have attempted to prove the potential for membrane active peptides or derivatives thereof to cause endosomal escape.[33-35]  While they may hold therapeutic purpose for other reasons, such molecules were not initially designed to cause endosomal escape.  The drawback in using pH-sensitive peptides to form pores in endosomes is that their pores are either small or transient in nature.  They are not suited for the transport of large, polar molecules such as siRNA sequences or plasmid DNA.  If we can understand the ideal mechanism by which membrane active peptides would need to interact with the endosomal membrane we might finally achieve effective endosomal escape.

<u>History of Membrane Active Peptides</u>

Membrane active peptides (MAPs) are a well-studied class of biomolecules which have been investigated for a variety of uses. The study of MAPs dates back to the 1960's when the synthesis of bulk, pure peptides from individual amino acids became available.[36] As soon as it was possible to generate large amounts of short amino acid sequences, the field began to look at the ways in which these molecules interacted with model membrane systems. These early studies focused on peptides known to cause cytotoxic effect in humans such as Melittin and Alamethicin.[37, 38] By the 1980's the focus shifted from naturally occurring cytotoxic peptides to synthetic peptides such as GALA.[39] More recently, combinatorial library screening has yielded peptides with even stronger activity than those previously mentioned.[40] Each of these peptides has been lauded for having the ability to interact with cell membranes in a controlled manner. New methods need to be developed in order to understand how to differentiate these classes of related but different peptides.

The first MAPs to be studied came from natural sources which were known to cause cytotoxic effects on human cells. One such peptide is Melittin, the key component of European Honey Bee venom. Early studies highlighted the ability of Melittin to disrupt the integrity of cell membranes.[41] One other peptide that groups began investigating was a potent pore forming peptide purified from the fungus *Trichoderma viride*: Alamethicin. Studies using patch-clamp devices showed that Alamethicin induced the flow of charge across model cell membranes.[38] Several sources hypothesized that, under certain conditions, these peptides are able to form pores in

membranes, causing the effects observed years prior.[41]  These studies lead to the idea

that such peptides constituted what was believed to be a class of "pore forming

membrane active peptides".  Eventually this work spawned the development of artificial

MAPs.

Work on MAPs in the 1980s started to have an eye towards developing novel,

synthetic membrane active peptides.  The Membrane Active Peptide GALA was one such

peptide to be developed based on principals discovered in the 1960s and 1970s.  GALA

is a peptide so named because of its repeating sequence of glycine-alanine-lucine-

alaninie, which is a motif (small part of a peptide sequence) believe to promote alpha

helical structure formation and membrane activity.  Several glutamic acid residues were

incorporated into the sequence due to the fact that they are charged at neutral pH and

protonated at low pH.  The initial attempt was to create a peptide that could bind to a

membrane in a pH dependant manner.[39]  GALA can bind to cell membranes in a pH

dependant manner and it can form pores similar to melittin or alamethicin.  It remains

to be seen, however, what the exact extent of pore formation can be, and the ability of

GALA to become a clinically useful peptide remains doubtful.[42]

In an effort to create extremely active MAPs, Wimley et al began using

combinatorial library screening of long-studied MAP sequences to find sequences with

enhanced activity.  The peptide libraries in these studies were created by taking a

known sequence and allowing the residues to vary in during the solid phase synthesis.

By screening a library based on the sequence of Melittin, the Wimley group was able to

take find a peptide, MelP5, which had improved pore-forming ability at low

concentrations.[40]   The development of this peptide begs the need for a method of characterizing the mechanisms by which MAPs interact with model membranes.

Chapter 1: The Categorization of Membrane Active Peptides as Stable vs Transient Pore

formers

The quest to create the ideal pore-forming membrane active peptide begins with

developing a method of categorizing the ways in which MAPs can interact with model

cell membranes.  Peptide pores can assume many different structures from tight

toroidal pores to diffuse membrane disruptions.[43] In fact, the exact pore structure of

certain peptides is still a contentious subject.[44]  Few reliable methods of determining

peptide pore structure exist, and the structure of the peptide pore might not be the

most important factor for developing useful MAPs.  The temporal nature of the pore

structure is more important to designing peptide-based drugs.  A pore may be toroidal,

barrel stove, or detergent-like but its long-term stability will dictate its usefulness in

allowing the passage of molecules.  Therefore, the first important categories of MAPs

are transient pore-forming MAPS and long-lived pore forming MAPS.

EIS and Time-dependant Pore Stability

We chose to study pore stability using Electrical Impedance Spectroscopy (EIS).

EIS allowed for the detection of small changes in impedance over large time scales.[45]

Impedance responses of bilayers were tracked every two minutes for up to one hour,

though responses could be tracked for even longer than this time. We were able to

expose our system to 20mV AC over a range of frequencies from $10*10^6$ Hz to 0.1Hz in

this two minute time period.[46]  In addition, using this method, transmembrane helix

dimerization and the size of gramicidin channels in a model system was determined.[47, 48]

EIS proved to be a useful method for studying even minute changes in membrane

permeability over long time periods.  Since MAPs pore structures were likely to be on the same size scale as a gramicidin channel or smaller EIS offered a useful way of studying them.  More than these factors, EIS was used due to the ability to interface with robust model membrane systems with which MAPs could interact.

<u>1.1 Supported Bilayers as Model Membranes</u>

The most useful information about membrane active peptides can be gained when they are able to interact with biologically relevant membrane systems. In the past studies have shown that MAPs can interact with black lipid membranes (BLMs) as well as tethered lipid bilayers.[49, 50] In these instances, however, the lipids were either not stable enough so as to prevent long-term studies (e.g. BLMs) or so stable that they could not accurately mimic the fluidity of the cell membrane (e.g. tethered lipids). To circumvent these problems, Lin *et al* developed a method to deposit lipid membranes on to a surface with a supportive polymer cushion.[51] In these membranes, lipid molecules could sit on top of a polymer cushion just below its collapsing pressure point. This cushion allowed the lipids to flow freely and fluidly more like the normal liquid crystalline phase seen in cell membranes.

Supported lipid bilayers could be created with a variety of different lipid compositions, mimicking both mammalian as well as bacterial cell membranes. Supported bilayers contained mostly POPC as this molecule is the most prevalent lipid in cell membranes. For mammalian membranes, supported bilayers were created with 75% POPC and 25% Cholesterol. To mimic bacterial membranes, bilayers were created using 90% POPC and 10% POPG. These membranes could be deposited using a Langmuir-Blodgett trough to deposit an initial monolayer at a surface pressure of 32mN/cm on top of <111> silicon.[52] After this, vesicles could be fused to the top of this surface to create a model cell membrane. In principal the deposited monolayer and the vesicles could have different compositions, thus creating distinct "inner" and "outer"

leaflets of the membrane. The greatest success was found with uniform membrane, though future work with asymmetric bilayers is warranted. These supported lipid bilayers were created for use in electrochemical cells as part of our EIS studies.

Electrochemical cell construction and model circuit

Previous work done by Lin et al outlined the method by which supported bilayers could be used as a component of electrical impedance spectroscopy. Once the monolayer of lipids was deposited onto <111> silicon, a custom electrochemical cell was carefully clamped in place over top of the silicon. A solution of vesicles was placed on top of this and allowed to fuse for up to one hour to form a bilayer. After this, the electrochemical cell would be filled with an electrolyte solution (100mM potassium chloride with 10mM sodium phosphate buffer pH7). Impedance signals were measured using a three point probe technique with one probe attached to the silicon (working electrode) one attached to a silver/silver chloride reference electrode, and a third probe attached to a platinum counter electrode. We found that allowing the electrochemical cell to equilibrate overnight generated the most robust bilayers.

Bilayer robustness was determined by measuring the impedance and using a model cell circuit to determine the bilayer conductance. Cell membranes are selectively permeable and therefore have a high resistance to charge flow across them. We also knew that cell membranes have a potential across them due to separation of charged solutes. Therefore, a cell membrane can be modeled as a capacitor and a resistor in parallel. In this instance $R_m$ is the resistive component of the membrane response and $C_m$ is the capacitive component. In our model system, the bilayer sits on top of a

polymer cushion on a silicon substrate.[53]   This silicon substrate/polymer cushion

experiences a certain charge transfer rate and also creates some charge separation.   We

denoted the contributions of the substrate/polymer as $R_{ct}$ and $C_p$ respectively.   Finally,

there were inherent resistive contributions of the bulk silicon and the system itself;

denoted as $R_s$.   We were able to fit our impedance data to this model to calculate

individual components of the impedance.
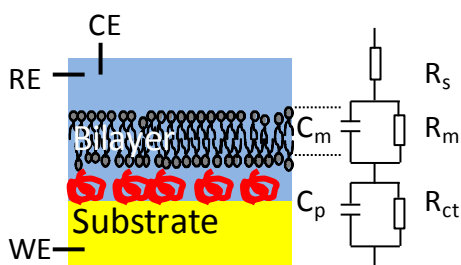


Figure 1.1 Model EIS Circuit.  This figure shows the mode circuit of our electrochemical cells.  CE, RE, and WE are the Counter Electrode, Reference Electrode, and Working Electrode connections.  $R_m$, and $C_m$ are contributions from the membrane and $R_{ct}$ and $C_p$ are contributions from the substrate/polymer.

1.2 Determining Supported Bilayer Stability

To make useful statements about our peptides, we needed supported bilayers that accurately mimicked the properties of naturally occurring cell membranes.  POPC molecules have a known length of approximately 2.5 nm, and a normal cell bilayer is close to 5 nm in thickness.  This bilayer thickness could be calculated from our impedance data by noting that there is a capacitive component of the response.  The capacitance depends on the thickness of a capacitor by: $C = \epsilon_o * \frac{A}{t}$ (capacitance C equals the dielectric constant $\epsilon_o$ multiplied by the ratio of the area A to the thickness t). Knowing these values we can determine the expected capacitance of the bilayer in our model setup.  For a capacitor of thickness 5 nm with our defined electrochemical cell area of 0.8 cm$^2$ in a 100mM potassium chloride solution we expect the capacitance to be between 0.8-1.2 µF*cm$^2$.  Figure 1.2 shows example capacitance values from 100% POPC (PC), 75%POPC 25%CH (PC:CH), and 90%POPC 10%POPG (PC:PG) bilayers obtained by measuring impedance when exposed to a 20mV AC current.  For each bilayer type, capacitances of between 0.8-1.2 µF*cm$^2$ were regularly observed. We were able to create bilayers with a thickness comparable to natural cell membranes.
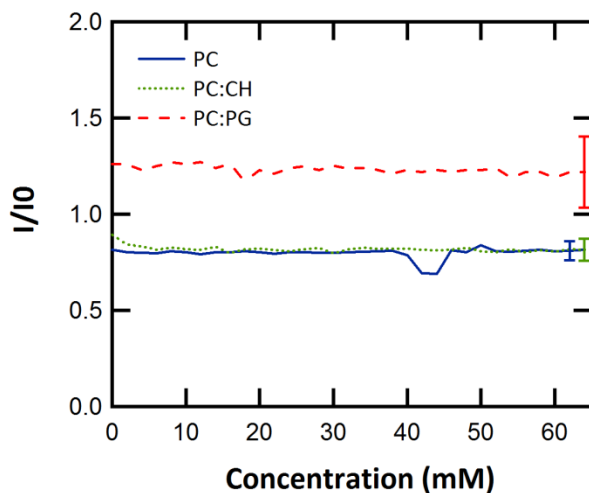


Figure 1.2 Capacitance of Biologically Relevant Bilayers.  This figure shows the capacitance of PC, PC:CH and PC:PG bilayers measured up to one hour.  Each type of bilayer fell between 0.8-1.2 µF*cm$^2$ in capacitance.

Not only did our supported bilayers need to be the proper thickness, they also needed to be uniform, without intrinsic pores. Supported bilayer uniformity was measured by the resistive component of the impedance response, or inversely by the conductance. Cell membranes are selectively permeable and naturally should have a low conductance. Admittedly, tethered bilayers form membranes with lower conductance values than supported bilayers due to strong adhesion to the substrate.[54, 55] Nevertheless, the bilayers we used had sufficiently low conductance values as shown in Table 1.1. Any change in the resistance (conductance) was due to disruptions of the membrane. Thus, when we added MAPs to our supported bilayer EIS system and saw a change in the conductance we concluded that the MAPs were forming a disruption or pore in the membrane.

| Composition | Resistance (Ohm*cm$^{-2}$) | Conductance (mS*cm$^{-2}$) |
|---|---|---|
| PC | 7300±3800 | 0.13 |
| PC:CH | 17100±6300 | 0.05 |
| PC:PG | 9600±4100 | 0.10 |

Table 1.1 Resistance/Conductance of Supported Bilayers. These are initial Conductance values for supported bilayers, values were no higher than 0.15 mS*cm$^{-2}$. Given a gramicidin pore size of 0.5 A and 10 pS conductance this equates to less than $1*10^{-9}$ cm$^2$ of "pore area".[56]

## 1.3 Studies of Stable Pore-forming MAPs using EIS

Electrical impedance spectroscopy allowed us to determine the response of a supported cell bilayer, a model cell membrane, to membrane active peptides. Due to the fact that initial bilayer resistances can vary depending on the preparation, we determined that the most important parameter would be the final resistance normalized by the initial resistance (R/R0).[57] The formation of small pores in the membrane, induced by MAPs, would lead to a decrease in normalized resistance (or an increase in capacitance) over time. We could calculate the number of pores in the bilayer by knowing the change in resistance/conductance, the conductivity of the solution, and the average pore size. This information proved valuable for previous studies using gramicidin wherein the pore size was well defined.[53, 56] For certain types of MAPs where the response is not long-lived, however, the pore size cannot be directly determined. This further highlights in importance of studying the kinetics of bilayer response using EIS rather than the importance of trying to get structural information about the pores.

Not all membrane active peptides interact with cell membranes in the same manner. We tested a group of four membrane active peptides, Alamethicin, GALA, Melittin, and MelP5. Within this group we believed that our model cell membranes, supported bilayers, would exhibit a long lived response to the first peptide, Alamethicin. As stated in the Introduction, Alamethicin is a peptide known to form stable pores in membranes. This fact has been confirmed by patch-clamp experiments as well as by leakage assays and by a number of other biophysical characterization techniques.[58-61]

We expected that upon adding Alamethicin to our system, the normalized bilayer resistance would decrease as a function of time. Again, this response was consistent with an increase in capacitance due to pores opening and allowing the free flow of charge carriers (electrolytes) to the silicon substrate. As expected, at peptide:lipid ratios of 1:500 to 1:1000 supported bilayers exposed to Alamethicin showed a long-lived decrease in normalized resistance (Figure 1.3a). The response of the bilayer depended on the amount of Alamethicin added in a dose-dependent manner; adding more Alamethicin caused a greater resistance change (Figure 1.3b). Alamethicin formed long-lived pores in model cell membranes, validating the usefulness of this technique in categorizing MAPs.
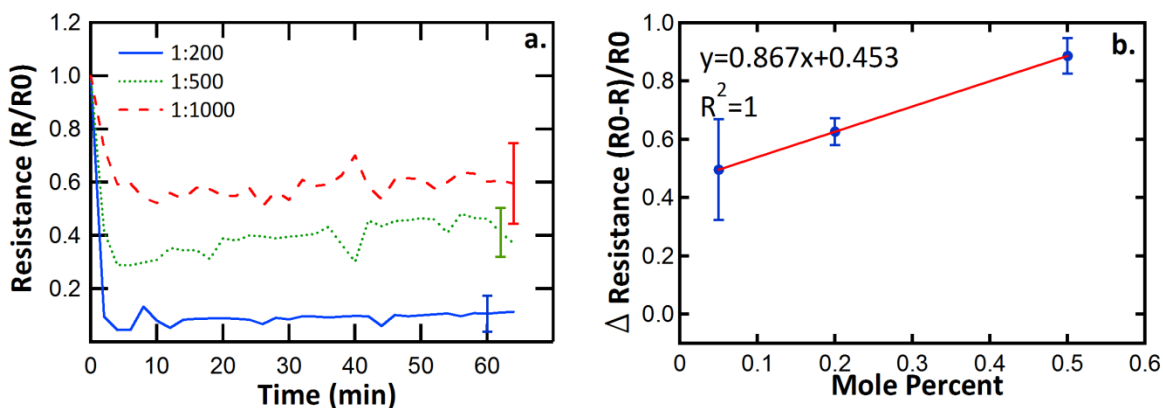


Figure 1.3 Effect of Alamethicin on Supported Lipid Bilayers. Alamethicin causes long-lived decrease in resistance over a period of 60 minutes (a). In addition, adding increasing mole percent of Alamethicin causes increased bilayer response (b).

With the identification of Alamethicin as a stable pore-forming peptide we sought to examine more exotic systems using EIS. We created supported bilayers in solutions about both pH 7 phosphate buffer as well as pH 5 phosphate buffer to study the pH-sensitive peptide GALA. These supported bilayers formed acceptable samples in

both pH conditions as determined by both their thickness and initial resistive properties

(Figure 1.4). This proved that the supported bilayers were not inherently weaker or

more porous at one pH value as compared to the other. We added GALA in

peptide:lipid ratios between 1:500 and 1:5000 to bilayers in pH 7 buffer. We found that

even at the highest peptide:lipid ratios there was no significant response of the bilayers.

GALA was not able to cause membrane disruption at pH 7. When these same

experiments were performed in pH 5 buffer, however, bilayers showed a significant

decrease in normalized resistance. Not only did GALA cause a bilayer response by

interacting with the bilayers, it also did so in a dose-dependent manner as did

Alamethicin (Figure 1.4b). From this we concluded that GALA is a stable pore-forming

peptide that can only interact with membranes in buffers of low pH values. This result

was consistent with both binding data as well as leakage assay studies of the GALA

peptide.[62] After determining that GALA and Alamethicin were stable pore-forming

peptides; we sought to test peptides with unknown pore-forming kinetics.
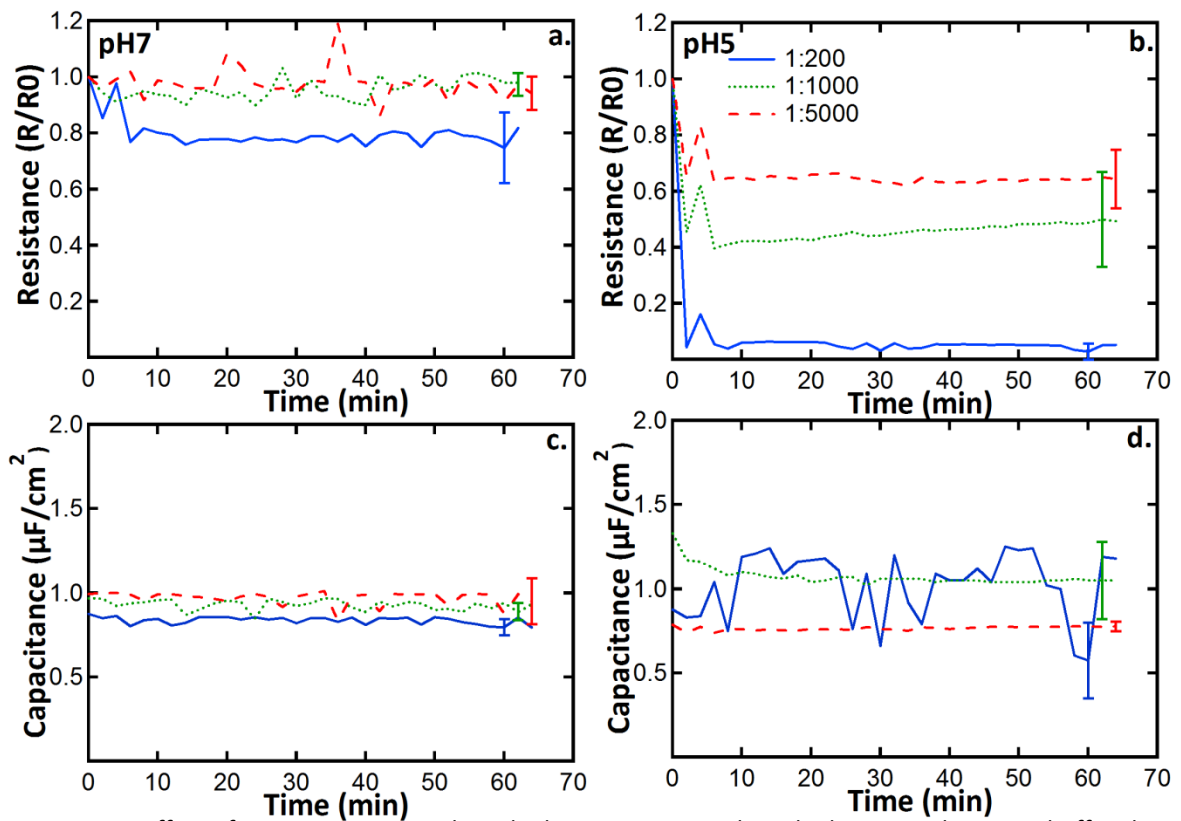
Figure 1.4 Effect of GALA on Supported Lipid Bilayers. Supported Lipid Bilayers made in pH7 buffer show no response to GALA, no decrease in normalized resistance (a). At pH5, Bilayers show a substantial, long lived decrease in resistance which persists for at least one hour (b). Bilayers are stable at both pH conditions, proving that the bilayer response is caused by the peptides and not by the pH of the buffer (c and d).

<u>1.4 Transient Pore-forming MAPs</u>

Melittin is a peptide with controversial pore-forming kinetics; it was a perfect choice for these studies. Though Melittin was known to form pores at high peptide:lipid ratios, often of greater than 1:20, its activity at low concentrations is debated.[63] We utilized EIS with supported POPC bilayers to determine the nature of Melittin pore formation. Melittin was added to our model cell membrane system at peptide: lipid ratios of 1:5000 to 1:100 in order to determine whether or not Melittin formed pores in these bilayers. At times of up to 4 minutes Melittin caused destabilizations in the membranes. These destabilizations were evidenced by a drop in the normalized resistance of the membrane. Such results were consistent with vesicle binding assays, leakage assays, and cytotoxcicity assays, which all suggested that Melittin could permeabilize cell membranes.[64-66]
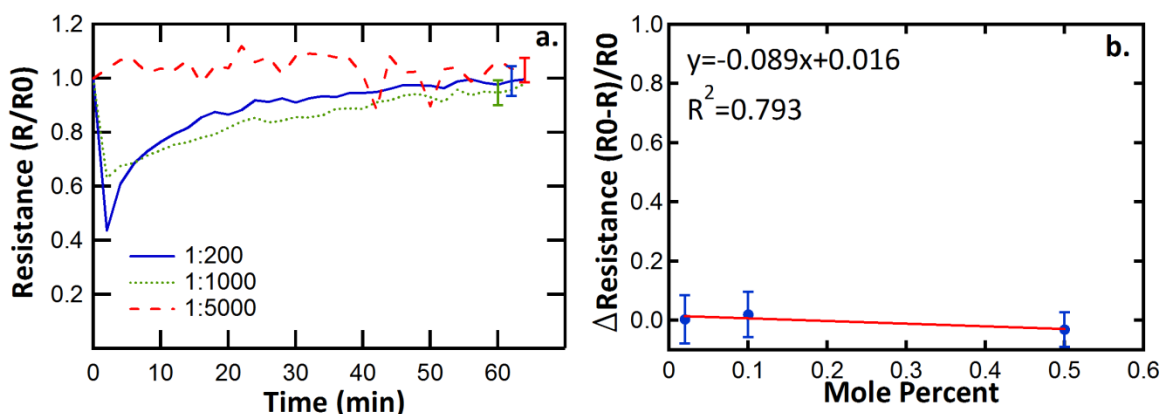


<u>Figure 1.5</u> Effect of Melittin on Supported Bilayers. Bilayers exposed to Melittin show a decrease in resistance over a short time period of up to 4 minutes, after this time the resistance returns to the initial value (a). The final resistance change does not depend on the concentration of peptide within the peptide:lipid ratio range studied (b).

At longer times, however, bilayers exposed to Melittin recovered normalized resistance Figure 1.5. Even though the membranes suffered a temporary disruption,

they regained their initial resistance by closing the openings formed when initially exposed to Melittin. Moreover, the bilayers consistently returned to their initial normalized resistance values regardless of the concentrations tested (Figure 1.5b). Melittin did not cause a dose-dependent response as was seen with Alamethicin and GALA nor did bilayers exposed to Melittin have a long-lived destabilization as with Alamethicin and GALA. From these EIS studies we were able to identify Melittin as a transient pore-forming peptide at low peptide:lipid ratios. Though Melittin is a peptide of similar size to GALA and Alamethicin its amino acid sequence causes it to act in a completely different manner.

We saw that our model cell membranes responded differently to peptides that were significantly different, Alamethicin; GALA; and Melittin and asked: would sequences with only slight differences vary this much?  To this end we examined MelP5, a gain-of-function analogue of Melittin described previously as a peptide that caused leakage at lower peptide:lipid ratios.[40]    MelP5 has only a few residue changes as compared to Melittin.  Most notably, MelP5 has a better defined hydrophobic face due to the changes such as Arginine 22 to Alanine ( denoted R22A) and Lysine 23 to Alanine (K23A) (Figure 1.6).  These changes allowed MelP5 to be more active in terms of the extent of leakage it could cause, but how the pores formed was unknown.  MelP5 bound to membranes with similar affinity as compared to Melittin; the binding interaction is not significantly more favorable for either (see Chapter 4).  These data suggested that the pore formation kinetics, rather than the binding affinity, accounted for the differences between the two.
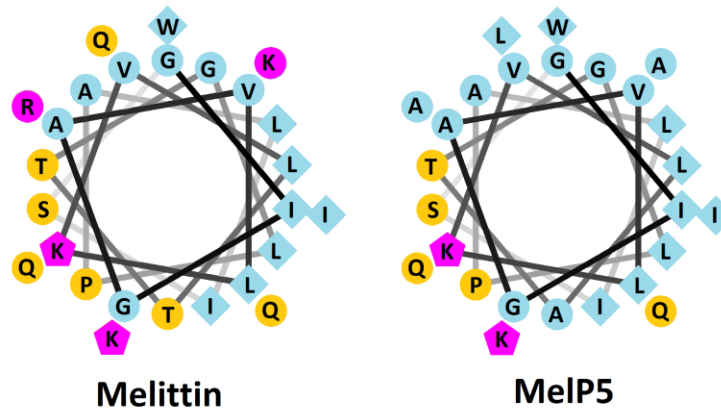


Figure 1.6 Structures of Melittin and MelP5.  These are projections of Melittin and MelP5 down a helix. Yellow residues are hydrophilic, Blue residues are hydrophobic and Magenta residues are charged.  MelP5 has a much more defined hydrophobic face as evidenced by the absence of Yellow and Magenta residues on the Blue side.

In order to probe the kinetic nature of MelP5 pore formation, we added MelP5 to supported bilayers at various peptide:lipid ratios of 1:25000 to 1:1000. These values were even lower than the values studied for Melittin. At peptide:lipid ratios below 1:1000 MelP5 caused an initial drop in the normalized resistance. MelP5 showed the same initial destabilization event as was observed with Melittin. In contrast to what was seen with Melittin, disruptions caused by MelP5 persisted and even continued to cause a decrease in resistance over time. These changes were seen not only in PC supported bilayers but also in PC:CH as well as PC:PG bilayers (Figure 1.7).[67] Figure 1.7 also shows the decrease in membrane resistance caused by MelP5 over a range of peptide:lipid ratios, displaying a dose-dependent response as was seen with Alamethicin and GALA and, in fact, at an order of magnitude lower concentration. The response of bilayers to MelP5 was fit to a simple two-exponential rate equation used by Almeida and colleagues to studying transiently active peptides.[68] Indeed there was an initial response on the order of 2 minutes in terms of half-time and a long lived response with a halftime of 20 minutes. This response was not seen in any other peptide group studied. MelP5, despite sequence similarities to Melittin, acts more like a stable pore forming peptide instead of a transient pore forming peptide.
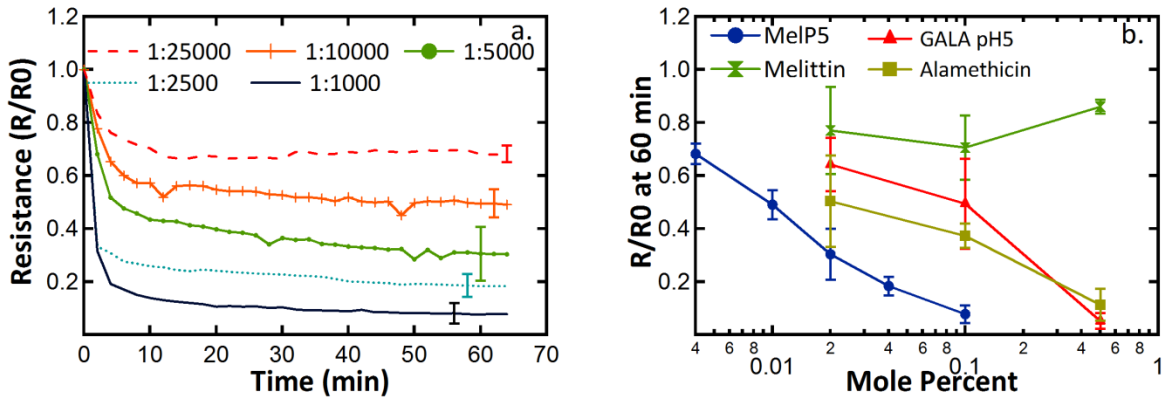
Figure 1.7 Supported Bilayer Responses to MelP5. In contrast to Melittin, MelP5 was shown to cause stable decreases in the initial resistance of supported bilayers (a). The decrease in resistance occurred at mole percent concentrations much lower than for Alamatehcin or GALA (b). These data confirmed that MelP5 formed pores at low concentrations and acted differently than Melittin.
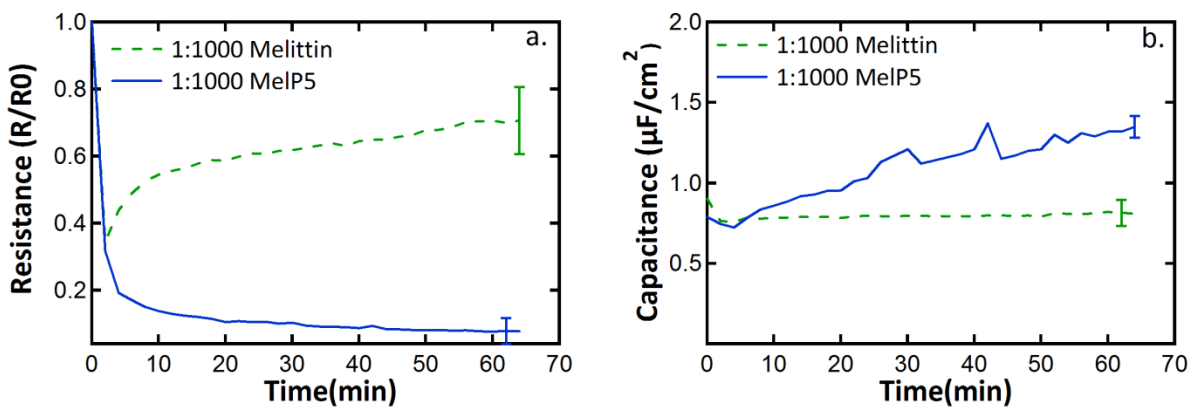


Figure 1.8 Response to Melittin and MelP5. Unlike with Melittin, supported bilayers exposed to MelP5 showed a decrease in resistance that persisted for up to 60 minutes (a). In addition, the capacitance increased over time (b). This result was due to extensive disruption of the membrane.

In addition to low peptide:lipid ratio pore formation, MelP5 caused a new type of response unlike any of the previous peptides. With each other type of peptide, at the concentrations tested, the bilayer capacitance remained constant. This result meant that even though the resistance of the bilayers dropped due to pore formation, the membrane remained intact. Unlike with Melittin, membranes exposed to MelP5 at peptide:lipid ratios of 1:1000 saw an increase in capacitance over time (Figure 1.8). This

result could come from two possibilities: an increase in bilayer thickness or a change in the permittivity of the bilayer. We reasoned that since the supported bilayers we used were well defined in work by Lin et al and since they are known to be stable for greater than 24 hours bilayer thickness was likely unchanged.[53] Rather than change size, the extent of pore formation caused by MelP5 was so great that the response of the bilayer was to change its bulk permittivity. While MelP5 did not cause large scale destabilizations of the membrane, the small, localized pore formations were enough to cause a change in the bilayer properties.

Summary of Chapter 1
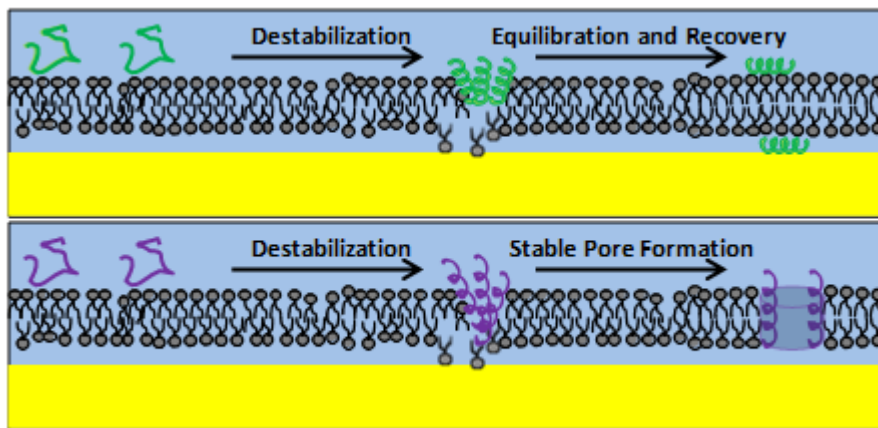


Figure 1.9 Proposed Mechanisms of Bilayer response to peptides.

Though many peptides are hypothesized to be pore forming membrane active peptides, few true pore forming peptides are confirmed. Rather than focus on finding pore structures, we categorized peptides by their kinetic nature in model cell

membranes, supported bilayers (see Figure 1.9). Using Electrical Impedance Spectroscopy found that supported bilayers exhibit a long-lived response to stable pore forming peptides such as GALA and Alamethicin. We were able to determine that transient pore-forming peptides like Melittin cause a temporary drop in bilayer resistance that is recovered over time. Finally we found that peptides with small sequence differences such as Melittin and MelP5 can be separated in terms of kinetic activity, the latter causing both a temporary and long-lived destabilization of the membrane. This information allows us to better understand the mechanisms by which these peptides cause their cytotoxic/membrane permeablizing effects.

Chapter 2: The Categorization of Membrane Active Peptides by Extent of Leakage

Membrane active peptides are an interesting class of molecule because of their ability to cause membrane permeabilization and/or cytotoxic effects in cells. The classical way of modeling the interactions of MAPs with cells in a reduced platform is to use vesicle leakage assays. By-and-large vesicle leakage assays involve lipids such as POPC, POPG, and Cholesterol in a unilamellar (one membrane) vesicle phase of defined size.[69, 70] Vesicles assays range from nanometers to microns in size to model the curvature of the cell membrane. Vesicles lack a cell's internal cytoskeleton and external extracellular matrix and as such are not stable above theses sizes. In addition, there is a thermodynamic limitation to the ability to create vesicles. Lipids have a critical micelle concentration (CMC), above which a micellular phase is favored over a vesicle phase.[71] Vesicle assays are limited in terms of the maximum concentration of vesicles that can be formed. Despite the size and concentration limitations vesicles around 100nm contain enough volume at 1-100mM to encapsulate a large number of secondary reporters for assays. The response in these systems is not as direct as with and EIS experiment; we do not see the bilayer itself opening up. We can vary the contents, however, to assess the extent of leakage that has occurred. By doing this, we are able to create a synthetic system of categorizing the effective extent of pore formation caused by membrane active peptides.

Vesicles used for leakage assays described herein were created using a standard protocol modified to accommodate a given reporter molecule. In all cases, lipids were dried from concentrated stocks in chloroform on glass vials in sizes ranging from 4mL to 20mL. Reporter solutions were made using dried components re -suspended in dionized (DI) water. The use of DI water/Millipore water allowed for the direct control of solute concentrations and reduced the osmotic stress on the systems inside and outside of the vesicles. Properly made reporter solutions were then added to dried lipids in order to allow for the encapsulation of the solutes. Vesicles self assembled in the aqueous solution and encapsulated the solution in which they are resolubilized, the reporter solution. In order to improve encapsulation, vesicles would often undergo several cycles of freeze-thaw, being frozen in liquid nitrogen then thawed in a water bath. Freeze-thaw worked best to improve encapsulation of large solutes. Vesicles were then extruded through a 0.1 µM filter in order to ensure uniform size distribution. Using this method we created vesicles encapsulating different solutes at different pH values.

Once the vesicles were created to the proper size and encapsulation efficiency, excess reporter needed to be removed from the solution. Several methods exist for purifying vesicle solutions. One simple method involved dialysis or passing the vesicles through a filter membrane. Due to the fact that vesicles are large, several hundred nanometers in radius, they would not pass through small dialysis filters. Such membranes could therefore be used to exchange reporter molecule solutions with pure buffer solutions. The most robust method for purification involved the use of size

exclusion columns to filter out excess reporter molecules. Again, the vesicles were large enough that they cannot fit into the pores in most size exclusion gels such as Sephadex whereas most reporter molecules can.[72] These vesicles had a smaller mean free path and therefore could be eluted from such columns faster than reporters, allowing for purification. Finally, vesicles were purified using resin binding techniques. Certain reporters contained components that could bind to functionalized resins. In these methods non-purified vesicle solutions were incubated with resins and centrifuged to remove excess report which bound to resin. Reliable vesicle leakage assays could not have been created without reliable purification techniques.

2.2 Small Solute Leakage Assays

Vesicle leakage assays provided an important tool for categorizing membrane active peptides by extent of leakage. Though the connection between small solute leakage and actual activity on cell membranes remains unclear, small solute leakage assays were the first step to showing activity versus lack of activity. We chose to use one of the most widely used vesicle leakage assays: the ANTS/DPX leakage assay.[65, 73, 74] In this assay, two components ANTS a fluorophore with excitation at 350 nm and emission at 520 nm and a quenching molecule DPX are encapsulated inside of a vesicle. When these molecules are in the small restrictive volume of a vesicle ANTS is quenched. When a perturbation of the membrane occurs, such as by interacting with a MAP, ANTS and DPX can leak out, leading to an increase in fluorescent signal. Since both ANTS and DPX molecules are in the size range of 500 Da (>>1 nm radius), only small perturbations were needed to see any signal.

In both small leakage assays and large solute leakage assays described later, positive controls are needed as a guide to gauge relative activity. The measuring bar used for these assays was Triton 100-X (triton). Triton is a detergent molecule which can insert into lipid membranes and disrupt the order of the liquid crystalline phase. These molecules lead to the complete disruption of these phases and the preferential formation of either disk-like phases or bicelles (mixed lipid-detergent micelles). These molecules are known to cause the complete leakage of vesicle contents, therefore any change in reporter signal could be scaled to the change in reporter signal caused by

Triton 100-X. This method provided a universal scale for comparing the extent of membrane activity of MAPs.

The ANTS/DPX small solute leakage assays were used to verify the extent of leakage caused by Alamethicin, Melittin, and MelP5. Vesicles were made with the following composition: 12.5 mM ANTS, 45mM DPX, 5mM HEPES, and 20mM potassium chloride. A given peptide was added to vesicles at 1mM lipid concentration as determined by a Stewart Assay in peptide:lipid ratios from 1:500 to 1:100. The percent leakage was determined by Equation 2.1:

$$\%leakage = \frac{I_{peptide} - I_o}{I_{triton} - I_o}$$

Equation 2.1 The percent leakage equals the intensity of the solution when adding the peptide ($I_{peptide}$) minus the background intensity ($I_o$) divided by the intensity of the solution when adding Trition ($I_{triton}$) minus the background intensity.

As shown in Figure 2.1, each peptide caused 100% small solute leakage, with respect to trition, at high peptide:lipid ratios. Each peptide exhibited a dose-dependent response. These assays highlighted the importance of a kinetic characterization of MAPs as one might have believed from these data alone that Melittin formed long-lived pores. These data could not show the recovery of the vesicles over time because once the reporters escaped the signal could not be reversed. Small solute assays only verified the amount of peptide needed for activity.
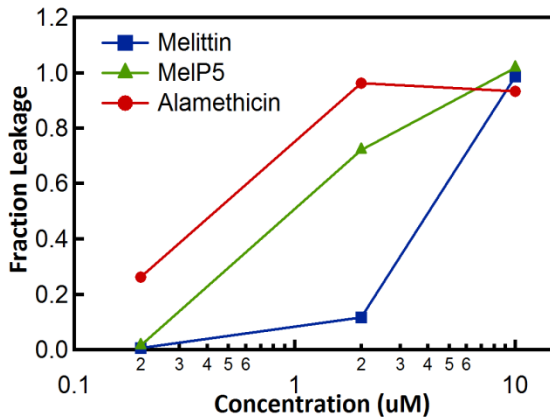


Figure 2.1 Fractional Leakage of ANTS/DPX from Lipid Vesicles. These data show the fractional leakage of small molecules ANTS and DPX from 1mM vesicles as determined by Equation 2.1. Each peptide showed a positive correlation between concentration and activity ending with 100% leakage at concentrations of 10uM.

2.3 Large Solute Leakage Assays

Small solute assays discriminated non-active from minimally active MAPs, but large solute assays were needed to further refine this category. The passage of large solutes through vesicle membranes would be akin to the flow of large molecules across the cell membrane. Only in the event of large destabilizations of the cell membrane would these molecules freely flow through. The size range for what constituted large or macromolecular leakage reporters was in the range of >10kDa. At this size, molecules are on the order of tens of nanometers in hydrodynamic radius.[75] This size range includes solid nanoparticle therapeutics, DNA plasmids, siRNA molecules, therapeutic peptides, and a host of other useful biomolecules. In this work three main assays were investigated for their ability to help characterize large scale leakage events.

2.4 Fluorescent Dextran Based Leakage Assays

The most obvious method to try first was to attempt to scale up the quenching-dequenching mechanism of the ANT/DPX assay with larger molecules. Fluorescein Dextran (FD) molecules have been used since the 1990's in leakage assays to study large molecules leakage.[76] Fluorescein was used because at high concentrations individual molecules of Fluorescein are self-quenching.[77] The assay would work by incorporating a high concentration of FD (40 kDa in size) inside of vesicle. If large disruptions occur in the vesicle membrane, FD molecules can leak out and an increase in Fluorescein signal can be observed. Though this technique works in principal, a perfectly quenched initial state proved difficult to achieve in practice. In addition, not only was this self-quenching state difficult to achieve, the Fluorescein molecules were pH sensitive. The maximum

emission at 519 nm decreases with decreasing pH when excited at 495nm.  Figure 2.2

below shows a kinetic assay wherein FD containing vesicles prepared at pH7 were

exposed to a peptide solution at pH 4 and then to Triton.  As the membrane active

molecules were added, the signal actually decreased with FD escape instead of

increasing. We measured a "Fraction Unquenched" for these data at low pH values as

described by Equation 2.2:

$$FracUnq = \frac{I_o - I_{peptide}}{I_o - I_{triton}}$$

Equation 2.2 The Fraction Unquenched equals the background intensity ($I_o$) minus the intensity of the solution when adding peptide ($I_{peptide}$) divided by the background intensity minus the intensity of the solution when adding Trition ($I_{triton}$).


These methods were met with uncertainties about whether a change in quenching was

caused by pH or by self-quenching.  Due to the drawbacks in this large molecule assay,

other methods were developed to study large scale leakage
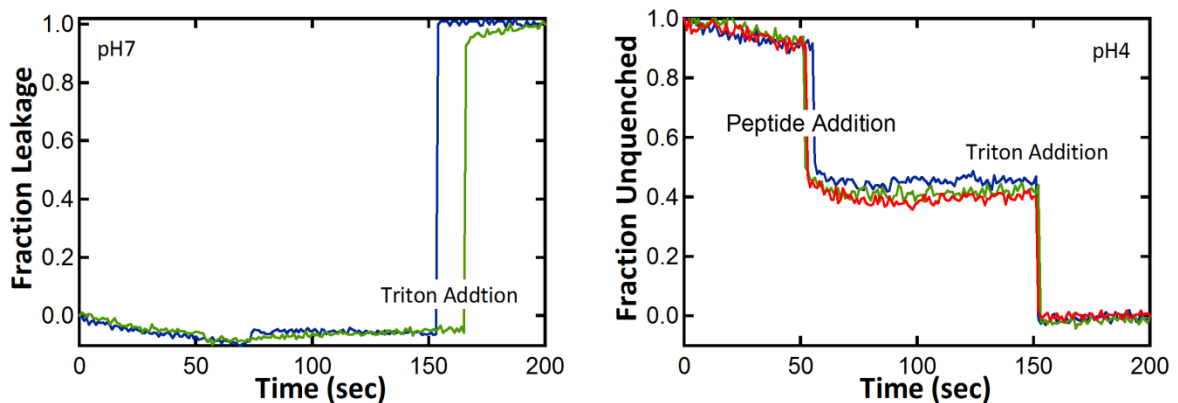


Figure 2.2 Fractional Leakage and Fraction Quenching of Large Solutes from Lipid Vesicles.  Lipid vesicles (1mM) encapsulating 40 kDa FD were exposed to the detergent Triton after approximately 150 seconds and excited at 519nm with a 495nm emission recording.  Fractional leakage data was determined as per Equation 2.1 and the Fractiona Quenching by Equation 2.2.  As described above, in pH4 solution the FD molecules were quenched even more than when they were encapsulated inside of pH7 vesicles.

2.5 Enzyme Based Leakage Assays

In order to address the limitations of the FD leakage assay, a new assay was developed involving enzyme molecules.  In this assay, a commercial kit for enzyme activity was modified to fit the role of leakage reporter.  Casein molecules (approximately 24kDa) functionalized with Texas Red fluorophore were chosen for this purpose.  Texas Red was used because as with Fluorescein this molecule is self quenching.  In this assay, however, the quenched state did not  come from being encapsulated inside of a vesicle.  Instead, Texas Red molecules were quenched because of their close proximity caused by being functionalized onto a casein backbone.  In order to achieve a dequenched state, an enzyme, chymotrypsin, was encapsulated inside of vesicles.  Chymotrypsin is a large, 26kDa, molecule which can cleave the peptide binds of hydrophobic amino acids.  In the event of a large disruption of a vesicle membrane, casein could be exposed to chymotrypsin by the leakage of either component into or out of the vesicles.  Chymotrypsin was found to be able to cleave casein, releasing Texas Red, and causing an increase in Texas Red signal.  The mechanism by which this assay operated as a leakage reporter proved to be robust.[78]

Unfortunately, several drawbacks were discovered with this method.  Due to the fact that the cleavage of casein is enzyme based, the assay was sensitive to temperature and also to time of exposure.  This fact convoluted determination of kinetic information that could be gained about interactions of MAPs with vesicle membranes.  In addition, as shown below, the addition of Trition 100-X to even the free components without vesicles caused an initial increase in signal (see Figure 2.3).  This increase was caused by

unfolding of the casein molecule, and hence slight dequenching of Texas Red, caused by Triton. Ultimately, Enzyme-Based leakage assays were optimized to find the best time of incubation, 1 hour, as well as to correct for the initial jump in signal. Theses drawbacks prompted the refinement of a different type of leakage reporter technique.
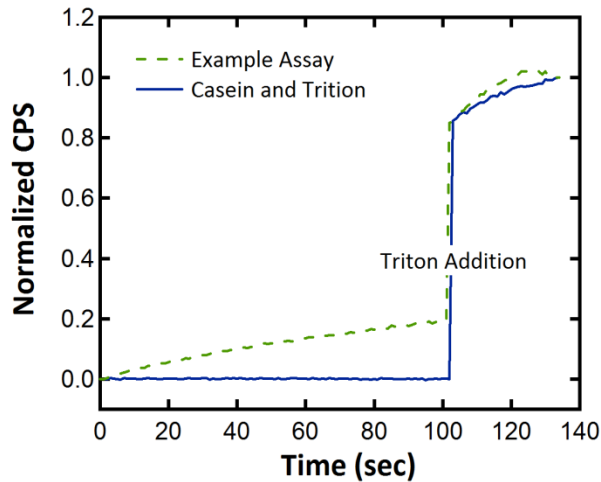


Figure 2.3 Leakage and Enzyme Cleavage of Casein Molecules. Vesicles (1mM) encapsulating chypotrypsin in and Texas Red labeled Casein in buffer were exposed to Triton detergent after approximately 100 seconds. These samples were excited at 589 nm with an emission recording of 617nm. In addition, the casein in solution without chymotrypsin was exposed to triton under the same conditions. The initial increase in fluorescence (normalized to the final value) occurred with or without the enzyme or vesicles. These data suggested that the assay could not be used as simply as the ones described in Parts 2.2 and 2.3.

## Forster Resonance Energy Transfer (FRET) Based Leakage Assays

The third iteration of large solute leakage assay, FRET-based assays, proved to be the most robust, most reliable, and easiest assay to employ to help categorize MAPs. In this assay, large TAMRA-biotin-10kD dextran (TBD) molecules were encapsulated inside of lipid vesicles.[67] Excess TBD was removed by incubating vesicles in agarose resin containing biotin's binding partner streptavidin. Streptavidin-Alexafluor488 (SA) molecules were added to the solution outside of the vesicles. Both TBD and SA are large macromolecules, +10kDa in size, and only in the case of very large perturbations of the vesicle membrane would these molecules pass through the membrane and bind with strong binding affinity ($10^{-15}$ M).[79] When TBD and SA are bound, the fluorphores on either molecule are close enough to undergo a Forster Resonance Energy Transfer interaction. The excitation and emission profiles of Alexafluor488 and TAMRA overlap such that when we excited SA at 495nm, we saw observed the non-radiative transfer of energy from an excited electron in Alexafluor488 to an electron in TAMRA (Figure 2.4). The FRET-based leakage assay provided a consistent method to track large scale membrane disruptions over time.
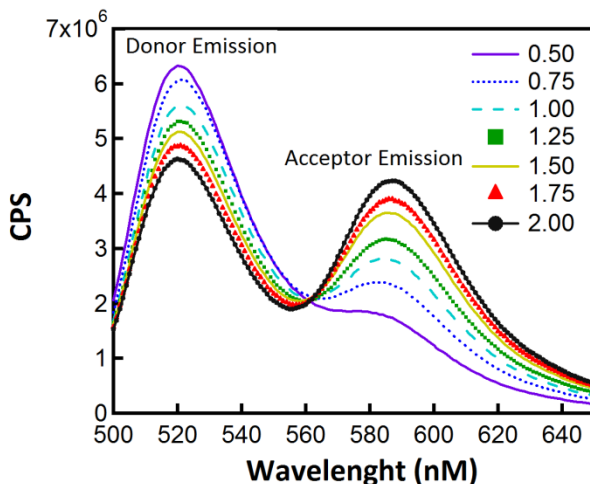


Figure 2.4 Titration of FRET Donor SA with Acceptor TBD. A solution of SA dye was prepared in phosphate buffer at pH7. Increasing aliquots of TBD, shown as a mole fraction of Donor from 0.5-2.0 were added to the solution and the dye was excited at 495 nm with emission collection from 500 to 650nm. The Donor emission decreased and the Acceptor emission increased when acceptor was added. This result showed FRET energy transfer from SA to TBD and illustrated the techniques usefulness as a leakage assay.

Having developed an effective large-solute leakage assay we tested our cohort of MAPs again to find large-scale leakage causing peptides vs small scale leakage causing peptides. TBD vesicles were prepared by making a 1 mg/mL solution of TBD in phosphate/acetate buffer with 100mM potassium chloride and adding this to vesicles to a final concentration of 100mM. In these assays, peptides were added to a solution of 1mM TBD vesicles with 6 nM SA at peptide:lipid ratios of 1:1000 to as high as 1:20 (Figure 2.5). The leakage was determined by Equation 2.3:

$$\%FRETleakage = \left(\frac{I_{SA,o} - I_{SA,peptide}}{I_{SA,o}}\right)/\left(\frac{I_{SA,o} - I_{SA,triton}}{I_{SA,o}}\right)$$

Equation 2.3 The percent leakage equals the initial SA signal $I_{SA,o}$ minus the signal when adding peptide $I_{SA,peptide}$ divided by the initial signal, scaled by the SA signal minus the triton control $I_{SA,triton}$ divided by the initial SA signal.

Figure 2.5 shows the aggregate results for several different peptides. From this data it was clear that even though Alamethicin and GALA (at pH5) were able to form small pores in membranes, they were not able to cause large membrane disruptions. Both Melittin and MelP5 caused large scale disruptions in POPC vesicle membranes at concentrations much lower than those needed for Alamethicin or GALA to have any activity. In addition, as was seen with the small solute leakage assay, Melittin and MelP5 caused a dose-dependent response, showing increased leakage at higher concentrations. The maximum MelP5 leakage occurred at a lower concentration than Melittin, suggesting that MelP5 can form large scale disruptions more readily than Melittin. The FRET-based leakage assay allowed us to find true large scale disruptive peptides.
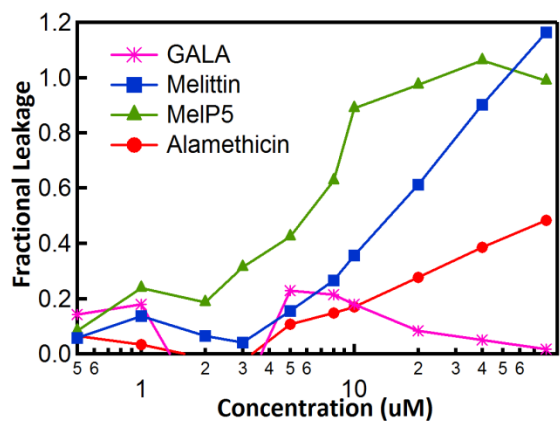
Figure 2.5 Leakage of FRET-based Assay Components from Lipid Vesicles. These data show the fractional leakage of large, 10kDa TBD molecules from 1mM vesicles as determined by excitation of the sample at 495 nm and emission at 519 nm. These data were fit to Equation 2.3 and plotted as a function of concentration. Both Melittin and MelP5 were able to cause close to 50% leakage at less than 10uM concentration. GALA and Alamethicin did not cause leakage of large molecules.

Summary of Chapter 2

The second degree of categorization of membrane active peptides concerns their leakage-causing abilities.  Leakage assays are thought of as a biophysical characterization technique to gauge cell membrane permeabilization abilities of MAPs. In this work we showed that MAPs can be categorized by the extent of the pore formation or membrane disruption.  Peptides such as Alamethicin and GALA form small pores on membranes that can only allow the passage of small solutes like ANTS and DPX.  Other peptides like Melittin and MelP5 can cause large disruptions in membranes capable of letting large solutes like TBD molecules to flow out freely.  When scaling the reporter signal elicited by these peptides to something like Triton-100x, the effects become directly comparable.  When combining these data with our EIS experiments, we developed a method to differentiate small scale stable pore forming peptides from large scale transient/stable pore forming peptides.  This categorization method will help future efforts to engineer desired properties into membrane active peptides.

Chapter 3: The Rational Design of Membrane Active Peptides for Efficient Endosomal Escape

Numerous medical molecules fail to become effective therapies solely due to their inability to cross the cell membrane and reach the cell cytosol. Molecules that are not able to diffuse across the cell membrane become endocytosed, and molecules that cannot escape endsomes are degraded or trafficked back outside of the cell. We envisioned membrane active peptides as being the needle tip to puncture endosomes as a needle would puncture skin. Properly designed MAPs could cause release of large, polar cargo before it is degraded. This method of escape is preferable to concentrating molecules in endosomes as it relies on less material to achieve similar amounts of release. In our first attempt to design a MAP to for endosomal escape and drug delivery, we utilized our knowledge of the biophysical characteristics and categories of MAPs to rationally engineer a pH-sensitive peptide.

3.1 Membrane Partitioning and Endosomal Release

When developing our initial peptide design, we first postulated that such a peptide needed to cross or insert into the cell membrane itself. As mentioned in the introduction, large polar molecules are the types of molecules unable to diffuse readily across the membrane. The canonical method of categorizing the ability of molecules to diffuse across cell membranes is to examine their partitioning coefficient. Partitioning coefficients, often represented as log(P), are a measurement of the concentration of a given molecule in a polar environment as compared to the concentration in a hydrophobic environment. Table 3.1 highlights the partitioning coefficients of several

important biomolecules.  Peptides have widely varying partitioning coefficients.  This is because, while the backbone of the peptide structure contributes a standard amount to the ability of the peptide to partition to a membrane, the side groups contribute significantly.  Understanding the contribution of side groups to peptides' partitioning coefficients was key to the design of our novel peptide.

| Molecule | Log(P) | [lipids]/[water] |
|---|---|---|
| Cholesterol | 7.11 | 1.29E+07 |
| Adenine | -0.57 | 2.69E-01 |
| Glycine | -3.4 | 3.98E-04 |
| Sucrose | -4.5 | 3.16E-05 |

Table 3.1 Partitioning Coefficients of Various Biomolecules

Amino acid side groups and peptide backbone structure dominate a peptide's partitioning coefficient and free energy of insertion.  The relationship between the partitioning coefficient and free energy follows the standard Gibbs Free Energy equation wherein the reaction quotient is the partitioning coefficient of a molecule $\Delta G = RTlnP$. Several scales of partitioning free energy per amino acid residue exist.  We chose to use the Wimley-White scale to calculate the total free energy of peptide partitioning to the membrane.[80]  Using this scale, we were able to determine which residues were important for a membrane active peptide that could disrupt endosomal membranes. Residues with hydrophobic side groups such as Alanine and Leucine provide enough of a favorable free energy of partitioning to drive the interaction of a peptide with a membrane.  We sought to prevent peptides from interacting with the membrane at neutral pH so as not to disrupt the cell membrane.  Amino acids such as Glutamic acid and Aspartic acid are charged at neutral pH, leading to an unfavorable free energy of partitioning.  These aminio acids are referred to as "acidic" residues.  At low pH these

47

residues can become protonated and do not contribute unfavorably to the partitioning free energy. Thus the ideal peptide would contain some mixture of these types of residues such that the total partitioning free energy, the sum of the contributions of each amino acid, would be greater than zero at neutral pH but less than zero at low pH values.

3.2 Ideal Mechanism of Peptide-Membrane Interaction

We utilized our understanding of partitioning free energy combined with our knowledge of MAP categories to determine the ideal mechanism for peptide-endosome interactions. The first iteration of peptides needed two components: pH sensitivity and large scale, stable membrane disruption. One or both of these characteristics are lacking in the representative group of peptides tested in Chapters 1 and 2 of this dissertation. The peptide GALA was found to be able to interact with membranes in a pH-dependant manner, but only formed small pores that would be unsuitable for delivery of large cargo (Figure 2.5). MelP5 forms the types of large scale disruptions that GALA cannot, but is not pH sensitive. We sought to combine these activities to develop the ideal mechanism of interaction allowing for both pH-sensitivity as well as large scale disruption capabilities.

The ideal mechanism of interaction takes advantage of the known binding-insertion coupling of membrane active peptides.[81] In order for MAPs to become active on a cell or endosomal membrane, such peptides must first bind to the surface, obtain secondary alpha-helical structure, and insert/partition into the membrane. Adding acidic amino acids to a sequence of largely or mostly hydrophobic amino acids disrupts

the insertion of the peptide into the membrane. The acidic residues would remain charged at high pH due to having an acid dissociation constant (pKa) of approximately 4.5.[82] Below pH 4.5, protons would be bound to these amino acids, making the peptide less charged and thus allowing it to interact with the hydrophobic core of a lipid bilayer. In our ideal mechanism, peptides in the low pH environment of an endosome would become protonated, bind to the periphery, insert into the membrane, and cause large scale disruptions.

## 3.3 Development of Peptides MelP5_Δ4 and MelP5_Δ6

Rather than design a completely new peptide *De Novo*, we created new peptide designs from existing peptides that had part of our desired characteristics. We had one initial hypothesis: the characteristics of large scale membrane disruption and pH-sensitivity are additive. Additive properties imply that a single sequence could encompass both activities without the diminishing of either property. Since MelP5 already has the large scale pore forming property, we used this sequence as a template to design two new peptides named MelP5_Δ4 and MelP5_Δ6. The MelP5 template and both designed peptides are shown below in a projection down the alpha helix in Figure 3.1. Acidic residues, glutamic acid and aspartic acid were positioned about the helix mimicking the placement of acidic residues in the pH-sensitive peptide GALA. The total partitioning free energies in neutral pH from the Wimley-White scale were calculated using MPEX and found to be +7.8 kcal/mole and +8.99 kcal/mole. These values were extremely unfavorable compared to the partitioning free energy of MelP5 and its parent sequence Melittin, which is -7.0 to -9.0 kcal/mole.[83] Protonation of these residues was expected to drive the partitioning free energy into the favorable range, less than 0 kcal/mole, so that peptide insertion would be favorable. We postulated that adding these changes to the sequence of MelP5 would allow it to become pH-sensitive.
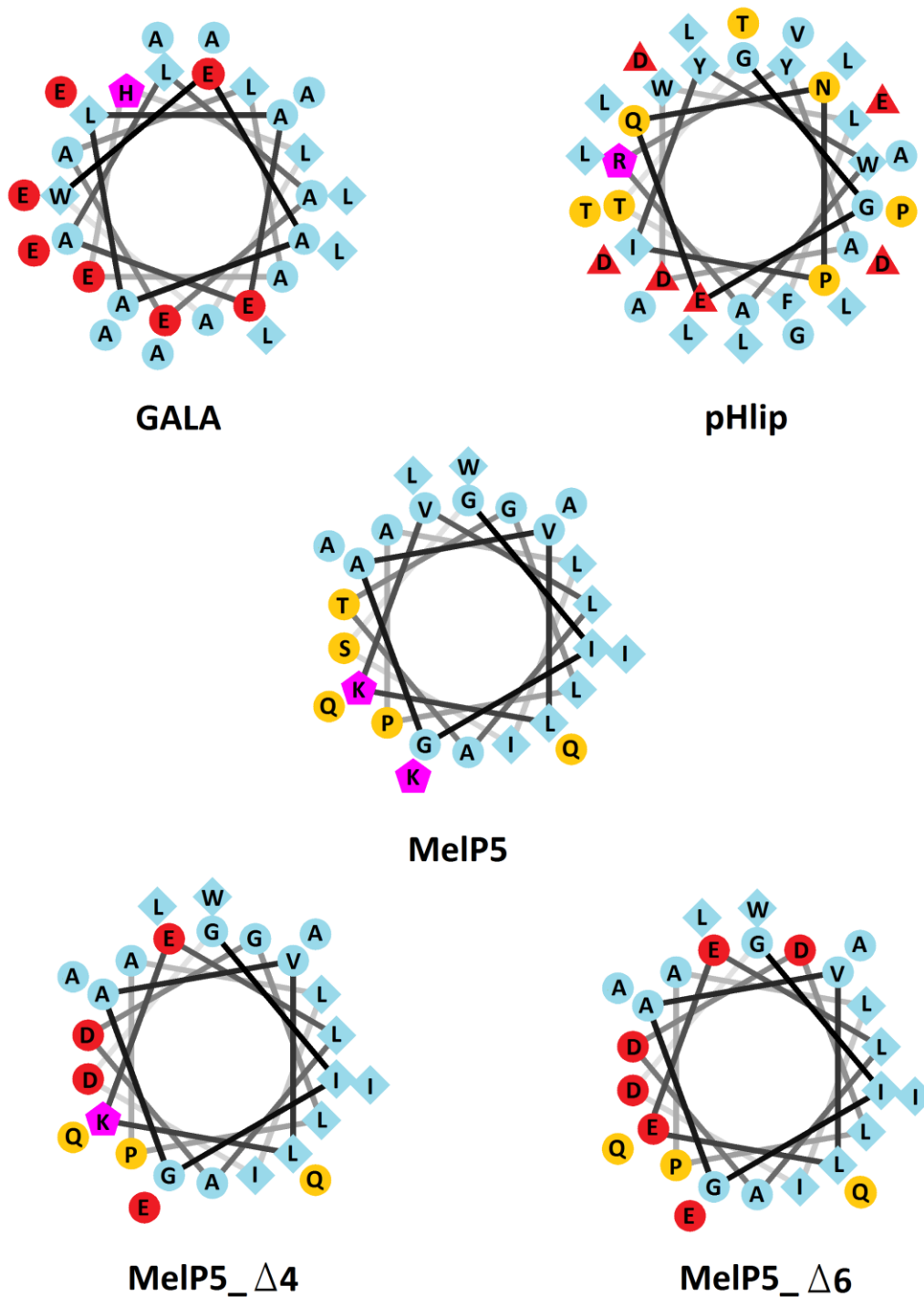
**Figure 3.1** Rationally Designed Peptides and Parent Sequences. This figure shows helical projections of the peptides discussed in Chapter 3. Blue residues are hydrophobic, yellow residues are hydrophilic, Magenta residues are positively charged and Red residues are acidic, negatively charged at neutral pH.

Certain components of our design were explicitly engineered to retain the large-scale pore forming ability of MelP5.  The main component of MelP5 activity is the amphipathic nature of the peptide.  MelP5 is able to form pores due to having a well define hydrophobic face about the alpha helical structure of the peptide.  The hydrophobic face of the peptide does not inhibit hydrogen bonding between water molecules if it faces the hydrophobic lipid bilayer core.  At the same time, the hydrophilic face of the amphiphilic peptide can turn inwards toward each other, allowing the formation of column of water molecules stretched across the membrane. Acidic residues within the hydrophobic face of the peptide helix would promote unfavorable interactions between charged residues and the hydrophobic core and would inhibit pore formation.  Taking these facts into consideration, residues on or near the hydrophobic face, mostly charged or polar residues were chosen as sites to add acidic residues.  We theorized that these additions would allow MelP5_Δ4 and MelP5_Δ6 to retain large scale pore forming abilities and tested this hypothesis in the following section.

## Ideal mechanism of Activity
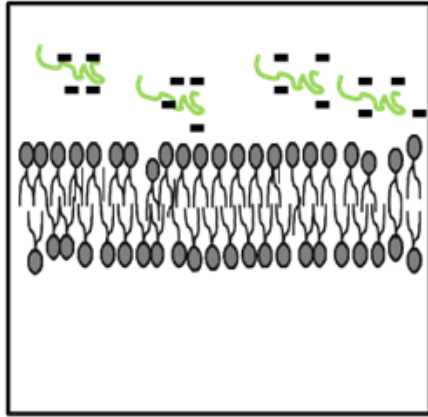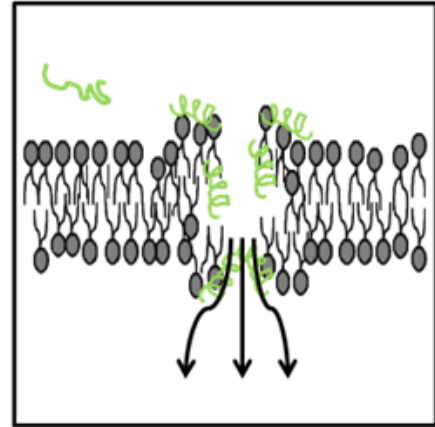


High pH
Low pH

Chapter 4: Testing the Limits of Rational Design of Peptides

Our first attempt at designing a peptide for efficient endosomal escape was an exercise in rational design of peptides. We hypothesized that two properties: large scale membrane disruption and pH-sensitivity were additive. By merging the sequences of GALA and MelP5 we hoped to obtain a peptide with both properties. We began testing this hypothesis by synthesizing peptides MelP5_ Δ 4 and MelP5_ Δ 6, which were described in Chapter 3. These peptides were first tested for their ability to bind to membranes in a pH dependant manner, which would indicate pH sensitivity. Next, MelP5_Δ4 and MelP5_Δ6 were tested for their ability to form secondary structure and insert into membranes, evidence of the binding-insertion coupling. Finally, we sought to test these peptides for their large-scale leakage properties to confirm that they were as active as the parent MelP5 sequence. This set of experiments would determine the biophysical characteristics of these peptides and would show their usefulness as endosomal escape agents.

4.1 Binding of MelP5_ Δ4 and MelP5_ Δ6 to Model Cell Membranes

Peptides which are pH sensitive bind strongly to cell membranes in one pH range and bind less readily at another pH range.[84] In our studies we believed that MelP5_Δ4 and MelP5_Δ6 would be unable to bind to membranes at neutral pH due to their high calculated partitioning free energy and positive charge. At lower pH values, however, acidic residues in the peptide sequence could become protonated, thus lowering the partitioning free energy. Though the total partitioning free energies of peptides have been shown to depend on the amino acid sequence of the peptide, the relationship

between the free energy and pH is not as direct.  The pKa or effectively the pH at which 50% of the amino acid residues are protonated depends not only on the individual amino acids but also upon neighboring amino acid environment.  Ideally these peptides would bind only at a pH between pH 6.0 and pH 5.5, the pH of late endosomes.  We could not determine the pKa of the peptides from the sequence alone, so we measured the binding of the peptides at various pH values.

Peptide binding was measured using a standard tryptophan fluorescence assay conducted at various pH values between pH7 and pH4.[85]  The model membrane in this assay was POPC lipid vesicles created as described in Chapter 2 but without any encapsulated reporter.  Tryptophan, an aromatic amino acid, has an excitation of 280nm and an emission maximum between 300nm and 450nm.  The maximum emission wavelength and intensity vary depending on the hyrdophobicity of the environment of the tryptophan.  If a peptide can bind to a membrane and burry the tryptophan residue in the hydrophobic core of the lipid bilayer then the fluorescence signal from the tryptophan residue will increase.  Titrations of increasing amounts of vesicles between 1uM and 10mM were added to a known amount of peptide (10uM) in buffer solution.  For pH values between pH7 and pH6 we used 10mM Sodium Phosphate buffer and for pH values between pH5.5 and pH3.5 we used 10mM Sodium Acetate buffer.  Buffers at all pH values contained 100mM potassium chloride to mimic the salinity of biological tissues, which is approximately 150mM.[86] We used two different buffers because the buffering capacity of Sodium Phosphate is highest between pH7-pH6, and the buffering capacity of Sodium acetate is highest below pH6.[87] As increasing amounts of lipid were

added, the intensity of the tryptophan signal increased until all tryptophan residues were buried.  Once the maximum change in intensity was determined, the data could then be used to calculate partitioning coefficients.

We calculated mole fraction partitioning coefficients by fitting to Equation 4.1:

$$I([L]) = 1 + (I_\infty - 1) * \frac{K_x[L]}{55.3 + K_x[L]}$$

Equation 4.1 The tryptophan fluorescence change at a given lipid concentration I([L]) equals 1 plus the final fluorescence change $I_\infty$ multiplied by the ratio of the mole fraction partitioning coefficient $K_x$ times the lipid concentration [L] over the molarity of water (55.3M) plus $K_x$ times [L]

At certain concentrations the amount of vesicles in the solution was great enough to cause significant scattering of the signal. To correct for the scattering effect, the intensity values were corrected by scaling to the signal of non-binding free tryptophan as described by Ladohkin *et al.*[85]  This assay method provided a way of reliably determining the partitioning coefficient and binding free energy of the peptides at even low pH values. Figure 4.1 shows the change in tryptophan intensity at pH 4 for both peptide MelP5_Δ4 and MelP5_Δ6 (4.1a and 4.1b).  Note that the maximum signal both increases and shifts to a shorter wavelength, which was indicative of peptide binding to our endosomal-like membranes.  Figure 4.1c shows the change in tryptophan intensity maximum with respect to lipid concentration at over a range of vesicle concentrations. Partitioning coefficients that were calculated from Equation 4.1 were then used to calculate the free energy displayed in 4.1d as a function of pH.
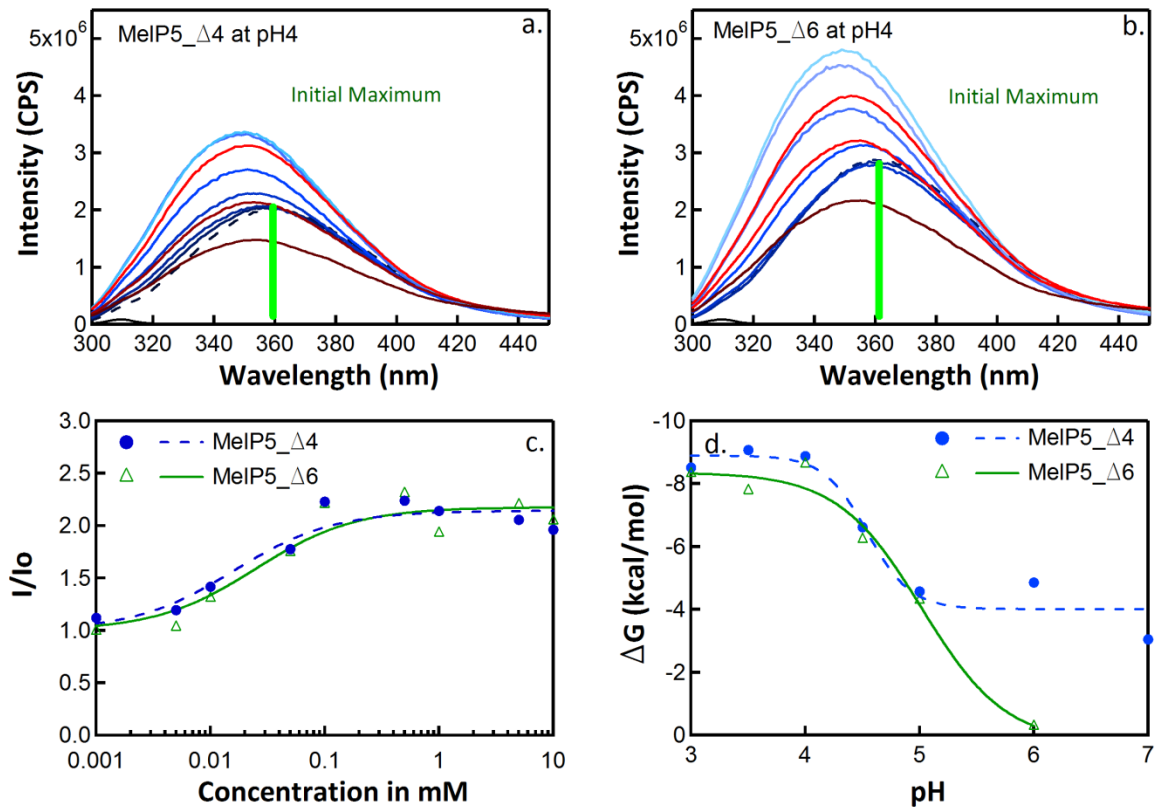
Figure 4.1 Binding of MelP5_Δ4 and MelP5_Δ6 to POPC Vesicles.  Peptides MelP5_Δ4 and MelP5_Δ6 were prepared in buffer solutions at pH 4 and pH 7.  Vesicles were titrated into the solution in increasing amounts from 1uM to 10mM.  At pH 4, as the vesicle concentration increased, the fluorescence intensity of the tryptophan residue (excited at 280 nm) increased and shifted to a lower wavelength maximum (a and b).  This result indicated tryptophan binding to the membrane. The values of the fluorescence change ($I/I_o$ at 335nm) at pH 4 over the titration range are shown in c.  These data were fit to equation 4.1 producing a plot of free energy as a function of pH shown in d.

These binding free energies of MelP5_Δ4 and MelP5_Δ6 were found to depend on pH in a manner that was consistent with our ideal mechanism of activity for efficient endosomal escape causing peptides. The parent sequence, MelP5, was found to bind to membranes with a free energy of -8.9 kcal/mole at pH7.  This value is similar to the known value of Melittin binding to small lipid vesicles.[85]  For a modest peptide:lipid ratio of 1:100 (1mM) this corresponded to complete binding of the peptide to the membrane or a capacity of nearly 60 peptides bound per lipid molecule.  MelP5_Δ4 and MelP5_Δ6

57

had partitioning free energies of -3.0 kcal/mole and -0.3 kcal/mole respectively, which was higher than the values predicted from the Wimley-White scale. These values, despite being on the favorable side of binding, were much less than that of MelP5 or Melittin. With a free energy of -3.0 kcal/mole only one peptide per 350 lipids would be bound, or less than 0.2% peptide bound. For MelP5_Δ6, with a free energy of -0.3 kcal/mole, only one peptide per 30000 lipids or 0.003% of the peptide could be expected to bind to the membrane at a peptide:lipid ratio of 1:100 (1mM). In other words, MelP5_Δ4 and MelP5_Δ6 bound much less favorably to model cell membranes at pH 7 as compared to MelP5. At low pH values, the free energy becomes more favorable. MelP5_Δ4 has a partitioning free energy of -9.0 kcal/mole at pH 4 and MelP5_Δ6 has a partitioning free energy of -8.6 kcal/mole, both of which are similar to MelP5. The fraction of bound peptide at low pH for these peptides was found to be five to six orders of magnitude higher than the fraction bound at pH7. Given this significant difference in free energy at low pH verses high pH, these peptides were classified as pH-sensitive.

Even though these peptides were found to be pH-sensitive, the apparent pKa of the peptides were found to be lower than ideal. We modeled the pH dependence of peptide binding as a simple pH-titration curve with first-order rate kinetics and fit the data in Figure 4.1 to a sigmoid function. The midpoint of the fit to these data was taken to be the "effective pKa" of the peptides, hereafter always referred to as "pKa". We found that the transition pH of MelP5_Δ4 and MelP5_Δ6 were pH 4.8 and pH4.6 respectively. The pKa of the side groups of aspartic acid and glutamic acid are in the

range of pH4.5; the pH-sensitivity appeared to be dominated by these side groups. Again, this transition pH was lower than the pH of late endosomes, pH6-pH5.5 from which cargo would need to escape. Less than 100% of the peptide would be charged at pH5.5 and therefore less than 100% of the peptide would be bound to the endosomal membrane. This fact suggested that, while adding acidic residues to an existing peptide sequence can cause it to become pH-sensitive, doing so must be attempted with a light hand. Once we confirmed that these peptides bound to the membrane in a pH-dependant manner we needed to examine whether or not they were active in the model membranes.

4.2 Dependence of Secondary Structure of MelP5_Δ4 and MelP5_Δ6 on pH

Secondary structure formation is a crucial indicator part of membrane active peptide activation. The reasons for this are twofold. The formation of a alpha helix allows peptides to order themselves in an amphiphatic structure of defined hydrophobic and hydrophilic faces. This structure would not be present if the peptides were in a random coil or globular configuration. Secondly, the formation of secondary structure lowers the portioning free energy of the peptide. An individual peptide bond requires +1kcal/mole of energy to partition to a hydrophobic environment.[88] The partitioning of free peptide bonds is unfavorable. If a peptide's backbone structure can undergo hydrogen bonding due to a favorable orientation of amino acid side groups, this energy penalty can be elevated. Peptides which can form alpha helical structure not only have the correct structure to associate within a membrane, they also have the correct structure to insert into the membrane as well. The formation of secondary structure is a crucial part of the ideal endosomal escape causing MAP mechanism of activity as described in Chapter 3.

We examined the secondary structure of our peptides using circular dichroism (CD) spectroscopy conducted in buffers at varying pH values. CD spectroscopy allows for the determination of the chirality of molecule's structure based on the preferential absorption of left or right polarized light.[89] Alpha helical peptides form known chiral structures with a complete turn at every i to i+4 amino acid in the sequence. The absorption is reported as molar ellipticity per amino acid reside because the intensity of the absorbance depends on total length of the peptide helix. In this way the signals

from different peptide sequences can be normalized to determine a percent alpha-helical structure. Alpha helices have well defined minima when excited with polarized light at 222 nm and 208nm wavelengths and a well defined maximum at 200nm wavelength. We determined that the ratio of the signal at 200nm verses 208nm would describe the relative alpha helical nature of the peptide in various pH buffers and from this we made conjectures about the dependence of alpha helical structure on pH value.

Peptides MelP5_Δ4 and MelP_Δ6 were found to gain increased alpha helical secondary structure preferentially at low pH values. Solutions of peptides were prepared at various pH values between pH7 and pH3.5 using either 10mM sodium phosphate buffer or 10mM sodium acetate buffer. Potassium chloride cannot be used in these experiments because small anions interfere with the CD absorbance spectrum between 200-180nm wavelengths. As seen in Figure 4.2a the parent sequence MelP5 exhibits strong alpha helical structure at even a high pH of pH 7. This again confirmed the fact that MelP5 was not inherently pH-sensitive. The structure of MelP5_Δ4 and MelP_Δ6 at pH 7 was a random coil structure, lacking the characteristic alpha helical minima at 222nm and 208nm wavelengths (Figure 4.2b and c). The minima at 200nm wavelength, as opposed to a maximum at 200nm, indicated a random coil structure of these peptides. In buffer at pH 4, MelP5_Δ4 and MelP5_Δ6 showed alpha helical structure, evidenced by lower minima at 222nm and 208nm wavelengths. Empty lipid vesicles of 0.1 um radius were added to the solutions to determine if the peptides gained additional alpha helical structure with model membranes added to the system. The CD spectra did not change with the addition of vesicles, suggesting that the peptide

did not gain additional alpha helical structure in the presence of membranes. The peptide binding and secondary structure formation was therefore controlled by the protonatable amino acid side groups on the peptides.
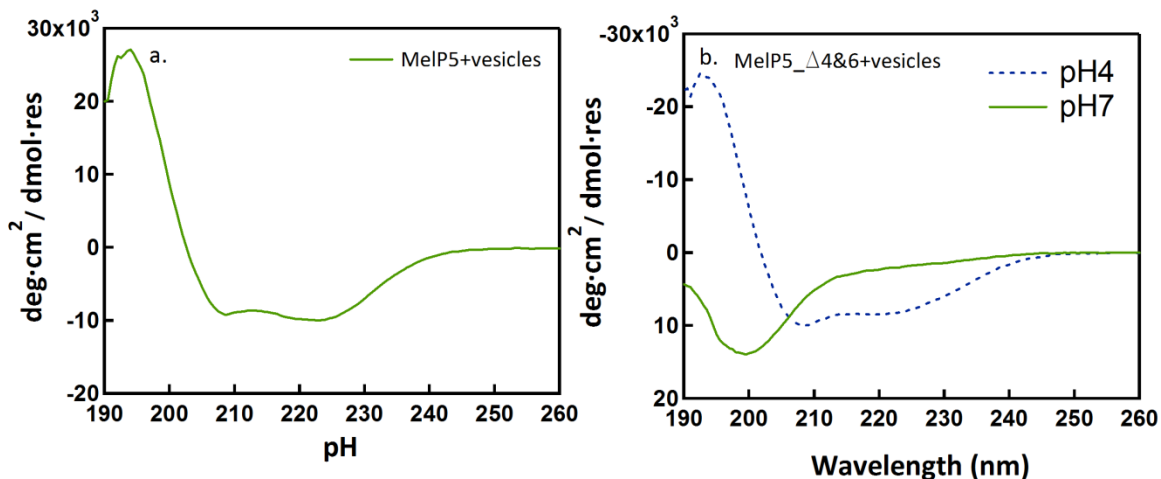


<u>Figure 4.2</u> CD Spectra of MelP5 and Variants. These are representative CD spectra of MelP5 as compared to MelP5_Δ4 and MelP_Δ6. MelP5 exhibits the characteristic alpha helical minima at 222nm and 208nm in pH7 buffer whereas the other peptides only show a minimum at 200nm. In pH 4 buffer, however, MelP5_Δ4 and MelP_Δ6 show a signal similar to MelP5, indicating that they are alpha helical.

As with the binding affinity, the extent secondary structure of these peptides was found to be a function of pH. We quantified secondary structure as the ratio of the signal at 200nm to the signal at 208nm and normalized this to the maximum 200nm/208nm value. This is called "%alpha helicity". Such a measurement was more applicable for this experiment because L-amino acids were used to synthesize MelP5_Δ4 and MelP_Δ6, complicating the normal CD signal. In neutral pH environments the peptides were random coil in structure, having a low %alpha helicity (Figure 4.3). In acidic environments, the %alpha helicity increased to a maximum at pH 4. We fit these data to a sigmoid curve and determined that the transition pH of alpha helical structure formation was similar to the transition pH of the binding curve: pH5.1 to pH5.9. The fact

that these peptides bind to membranes and form secondary structure at roughly the same pH values suggest that binding and insertion were coupled. The values at which these transitions occur were lower than the pH of late endosomes. In an endosome MelP5_Δ4 and MelP5_Δ6 would not be fully alpha helical in structure. Though these peptides exhibited pH-dependant in terms of their partitioning free energy and secondary structure, further studies of the extent of pore forming ability were needed to determine if MelP5-like activity was retained.
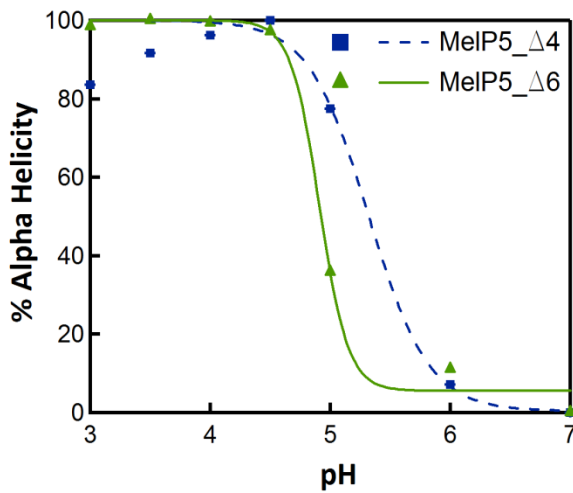


Figure 4.3 Alpha Helical Content of MelP5 Variants. Figure 4.3 shows the percent alpha helicity of the peptides as described in the text. The midpoint, where the peptides are 50% helical, appears to be between approximately pH5.1 and pH4.9.

## 4.3 Pore Forming Abilities of MelP5_Δ4 and MelP5_Δ6

Useful peptides for endosomal escape not only have a strong dependence of membrane binding affinity and secondary structure on pH, but also they must have large scale membrane disruption abilities.  The lack of large scale pore forming ability prevented GALA from becoming a clinically relevant MAP for decades.[42] Due to the fact that the molecular cargo which we would like to deliver is both polar and macromolecular, small pores are not suitable for efficient endosomal escape.  As described in Chapter 2, MelP5 caused large scale disruption of model endosomal membranes, POPC lipid vesicles. Our hypothesis predicts that by changing only a few resides of the MelP5 sequence, MelP5_Δ4 and MelP5_Δ6 could retain large scale disruption properties.  We endeavored to test this hypothesis further to see if these peptides could, in fact, disrupt membranes and allow the escape of large molecules.

Before testing for large scale disruption properties, we needed to know if MelP5_Δ4 and MelP5_Δ6 were truly inactive in neutral pH environments.  We found that these peptides neither bind to membranes nor form secondary structure at pH 7. Despite this fact, we did not know if unstructured peptides could disrupt lipid vesicle membranes in some ill-defined manner.  This would not be ideal for MAPs which would be systemically delivered to the body as they would have severe cytotoxic effects.  In order to determine if the rationally designed MelP5 derivates disrupted membranes at pH7, we prepared 0.1 um radius vesicles encapsulating the small molecule reporter ANTS and quencher DPX.  The vesicles were diluted in 10mM sodium phosphate buffer, 100mM potassium chloride buffer at pH7 and 10mM sodium acetation, 100mM

potassium chloride buffer at pH 4.  Peptides were added to 1mM vesicle solutions in peptide:lipid ratios of up to 1:100.  As shown in Figure 4.4 MelP5 caused significant leakage of reporters from vesicles at both pH7 and pH4.  These results confirmed our previous understanding of MelP5 as a characteristically large pore forming peptide.  Our new peptides, MelP5_Δ4 and MelP5_Δ6 caused no leakage above the background at pH7, and they caused leakage comparable to MelP5 at pH4.  The pH-sensitivity of these peptides allowed them to become non-damaging to cell membranes at neutral pH, close to the pH of human blood.  Our engineered pH-sensitivity caused inactivity at high pH but would the peptides become highly active at low pH?
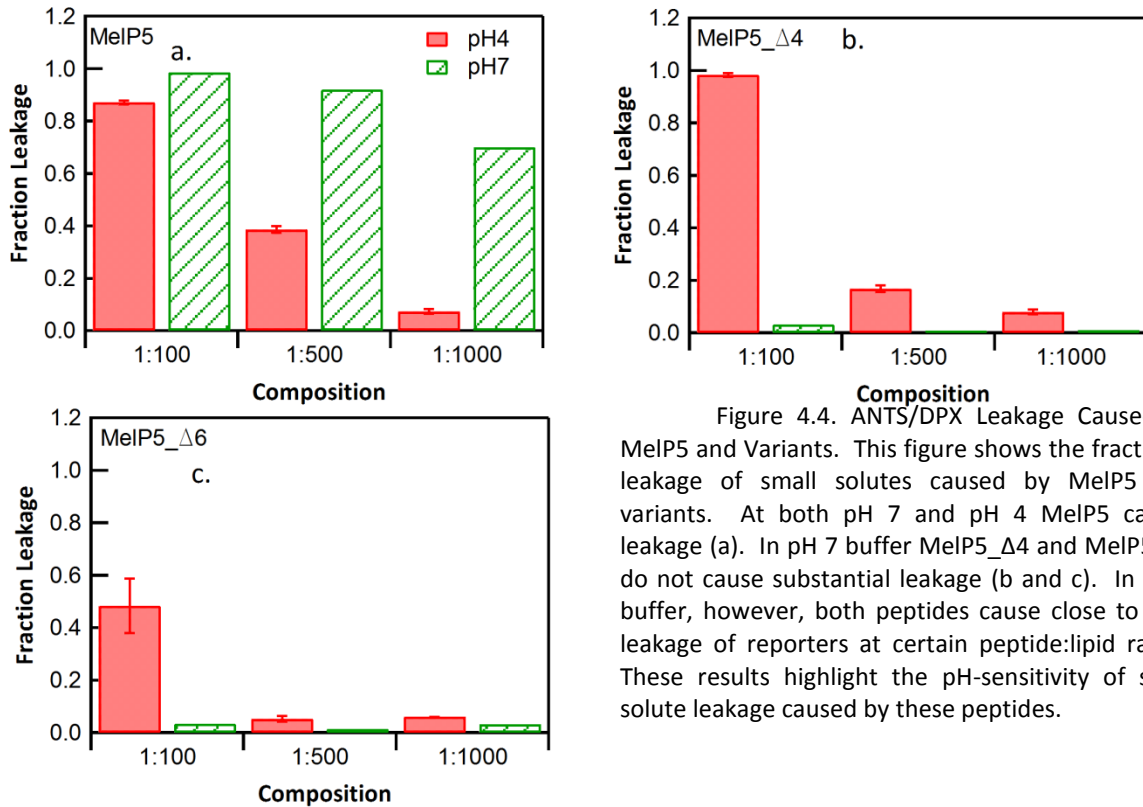


Figure 4.4. ANTS/DPX Leakage Caused by MelP5 and Variants.  This figure shows the fractional leakage of small solutes caused by MelP5 and variants.  At both pH 7 and pH 4 MelP5 causes leakage (a).  In pH 7 buffer MelP5_Δ4 and MelP5_Δ6 do not cause substantial leakage (b and c).  In pH 4 buffer, however, both peptides cause close to 50% leakage of reporters at certain peptide:lipid ratios.  These results highlight the pH-sensitivity of small solute leakage caused by these peptides.

Unfortunately, MelP5_Δ4 and MelP5_Δ6 cannot be used as peptides for efficient endosomal escape.[90] We prepared TBD containing POPC vesicles (0.1um radius) at 1mM concentration in the same buffers as described above for pH7 and pH4.  When MelP5

was added to solutions of these vesicles, nearly 100% of the large, 10kD TBD molecules were able to escape at both pH7 and pH4 (Figure 4.5). MelP5 was found to be a large pore-forming peptide in all solutions with a slight decrease in activity in acidic environments. No signal change, or small change in FRET signal was seen when MelP5_Δ4 and MelP5_Δ6 were added to vesicle solutions, even at a peptide:lipid ratio of 1:100. We knew from our binding data that almost 100% of these peptides should be bound and in an alpha helical structure at pH4. These peptides were able to associate in the membrane to cause the leakage of small molecules such as ANTS and DPX, which suggested that they formed small pores in membranes. MelP5_Δ4 and MelP5_Δ6 cannot cause large scale pores to form, which prevents large molecules such as TBD and potentially beneficial therapeutic cargo from escaping endosomal-like vesicles. In the end our rationally designed peptides failed to retain both pH-sensitivity and large scale pore forming characteristics.
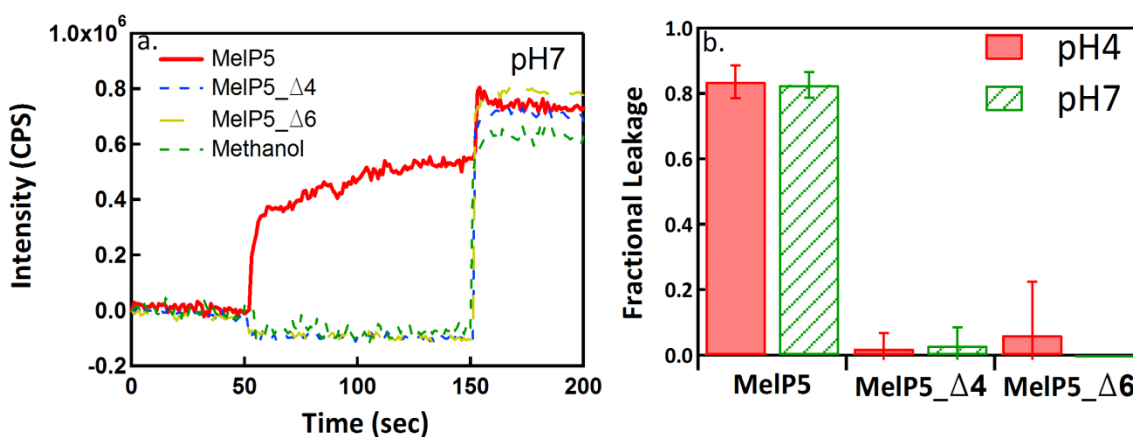


Figure 4.5 Leakage of Large Solutes Caused by MelP5 and variants. These data show that MelP5 causes leakage of close to 100% of TBD from POPC vesicles at 1:100 peptide:lipid ratio in both pH 4 and pH 7 buffer. Even at these high concentrations, MelP5_Δ4 and MelP5_Δ6 cannot cause any leakage of reporter molecules. Both variant peptides lack the large scale leakage properties of the parent sequence.

Summary of Chapter 4

Our hypothesis was refuted: pH-sensitivity and large scale pore forming activity are not additive properties of membrane active peptides.  Biophysical characterization of MelP5_Δ4 and MelP5_Δ6 showed that a modified MelP5 sequence could be made to bind to model cell membrane and form secondary structure in a pH-dependant manner. These peptides were even unable to form small pores at pH7, but could form small disruptions in membranes at pH4, similar to GALA.  Like GALA, and unlike MelP5, our newly designed peptides could not form large pores to allow macromolecular passage through membranes.  These peptides could not be used as the ideal needle tip for a drug delivery vehicle.  Adding pH-sensitivity to our peptide inherently decreased its pore forming activity; these two activities are not mutually exclusive.  From these results we determined that the development of an efficient endsomal escape causing membrane active peptide cannot be rationally designed.  The ideal balance between pH-sensitivity and pore forming ability must be discovered through peptide library screening and synthetic molecular evolution.

Chapter 5 Designing a Peptide Library to Screen for Ideal Characteristics

The characteristics we desired to combine in a peptide, large scale pore forming ability and pH-sensitivity, proved to be entangled with each other.  Creating the ideal peptide to cause endosomal release is not as simple as adding protonatable acidic residues to a preexisting peptide sequence.   In an attempt to improve our peptides we took the knowledge we gained from Chapter 3 and Chapter 4 and developed a peptide library based on the MelP5 sequence.  By designing and screening this peptide library we hoped to be able to determine which changes in the peptide sequence lead to the ideal compromise between pH-sensitivity and pore forming ability.  This approach was starkly different from the development of the current class of pH-sensitive peptides, which relied on intuition and rational design.  Rather than creating endless iterations of peptides, we decided to place selective pressure on our library as a form of synthetic molecular evolution.  We hypothesized that from this peptide library, one or a few sequences would be discovered that would have the ideal endosomal escape causing motif.

5.1 Peptide Library Design and Synthetic Molecular Evolution

The drawbacks in peptide rational design and the merits of synthetic molecular evolution were illustrated to me in a thought experiment by Dr. Chris Moser.  Suppose that there is a river crossing wherein three rocks exist to allow people to cross the river.  After some time, a wooden plank is placed over top of these rocks, improving the ability of people to cross the river.  After even more time assume the rock in the middle floats away or is removed such that the plank is suspended across only two rocks.   If a

passerby came to the river now they would notice that removing any one component of the bridge, either one of the rocks or the plank, would prevent someone from crossing the river.  New passersby might conclude that the bridge has to exist in this conformation otherwise it could not function, but they will miss the fact that a scaffold existed beforehand which allowed for the same function.  This is the case with rational design. We miss key insights and understandings of our bridges; our peptides; when we attempt to jump directly to what we perceive to be the structure-function relationship.

In order to gain as much insight as possible into this new class of peptides, we created a peptide library that allowed for multiple different changes to MelP5.  The base sequence, MelP5, was used as a design template again because we knew that it had one part of the activity we desired.  We knew based on work in Chapter 4, that by adding protonatable residues we can modulate the peptide's activity with pH.  The residues must be added in the correct places, however, to allow for the mediation between both types of non-additive activities (pH-sensitivity and pore formation).  In our library, amino acids A4, V8, T11, G12, A15, and S18 were allowed to vary with either the original residue or with aspartic acid, or with glutamic acid, or with alanine/leucine Figure 5.1. In this way, we did not preselect the ideal positions for our protonatable residues as we did with MelP5_Δ4 and MelP5_Δ6.   In addition, allowing for the incorporation of the hydrophobic residues alanine and leucine and also a change of I17Q enabled us to add back a small amount of hydrophobicity which would be lost by adding acidic residues. We hoped to apply selective pressure to our system through a library screen in order to

discover a peptide which has the ideal placing of amino acids about the peptide alpha helix.
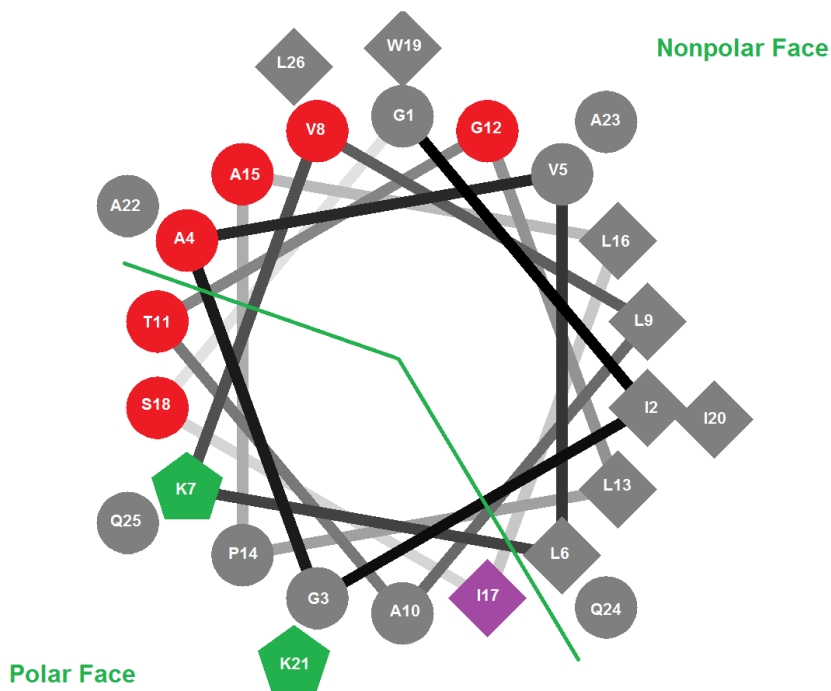


Figure 5.1 Basis for the Peptide Library. This figure shows the sequence of MelP5 with the residues that were changed. Red Residues were allowed to vary with Glutamic Acid, Aspartic Acid or the original residue. Green residues were allowed to vary with Histidine or the original Lysine residue. Finally, the Isoleucine at position 17 was allowed to vary with Glutamate the original residue.

Two other variations were allowed, K7H and K12H, along with the changes of hydrophobic residues to acidic residues. The lysine residues of MelP5 were determined to be important for the activity of MelP5 as compared to Melittin from past work.[40] Lysine, however, is a basic residue and thus could act to buffer the pH-sensitive interactions of our peptides, which we desire to activate at low pH. The pKa of lysine is 10.4, so therefore this residue would be mostly positively charged in the low pH environment of the endosome.[82] Histidine has a lower pKa of 6.2, meaning that it fewer

70

histidine residues would be charged in neutral pH environment/endosomal pH environment as compared to lysine. Since we knew that the side group pKa values would dominate the pH-sensitivity of the peptide, we believe that in allowing for the lysine-to-hisitdine variation we might achieve a higher overall peptide pKa than what we achieved with MelP5_Δ4 and MelP5_Δ6.

5.2 Hypothesized Mechanisms of Large-Pore Forming Activity Inhibition

The specific amino acid residues that we chose to vary were selected based on our understanding of peptide alpha helix formation.  The partitioning of a free peptide bond requires +1.0 kcal/mole and is thus unfavorable to peptide partitioning to lipid membranes.  Alpha helicial peptides form hydrogen bonds between side groups, which alleviates this backbone energy barrier.[91]  This is why peptides form secondary structure when binding to a membrane, and why secondary structure formation is an indication of MAP activity.  The turns of an alpha helix occur at every fourth reside, denoted as i+4 to i, so residues at these positions must be able to undergo hydrogen bonding.  Acidic residues at these distances in alpha helicial peptides experience electrostatic repulsion effects on the order of +0.45 kcal/mole.[92]  The side groups of aspartic acids or glutamic acids will repel each other enough to make the formation of an alpha helix unfavorable at neutral pH, thus interrupting peptide activity.  At low pH the residues are protonated, allowing for helix formation and thus generating pH-sensitivity.  The exact number of these helix-manipulating pairs needed to have the ideal activity is unknown.  For this reason we allowed our peptides to have acidic residues at up to 6 different spots which range from i+1 to i, to i+14 to i.  This breadth of variation allowed for different levels of activity modulation.

The number and positioning of amino acid residues in the library also took into account the potential advantages of varying the polar phase angle about the peptide alpha helix.  The hydrophobic and hydrophilic phases of MelP5 are well defined, which gives the peptide an amphipathic nature.  We allowed the residues closest to the polar

phase to vary with our acidic residues or hydrophobic residues to determine what effect modulating this phase angle would have on the peptide activity. For example, MelP5 has a hydrophobic moment of 5.91 at an angle of $50.5^{o}$ from the norm when looking at the helical projection. A theoretical peptide with all possible changes to glutamic acid would have a greater hydrophobic moment of 7.96 at a wider angle of $101.8^{o}$ when protonated.[93] A larger polar phase angle creates a larger polar surface area along the helix. We hypothesized that with more polar surface area the peptides could potentially accommodate larger volumes of polar solvent (i.e. water) and thus form larger disruptions or pores in lipid membranes. In this way, we hoped to find new mechanisms by which we could reach a compromise between the large scale disruption property and pH-sensitivity property.

## 5.3  Peptide Library Synthesis

The peptide library in discussion was synthesized using standard Solid Phase Peptide Synthesis (SPPS) techniques.  Peptides were synthesized on Tentagel megabeads with a capacity of 0.2mmoles/gram.  This process involves three main steps: washing, deprotecting, coupling, and with a final capping step at the completion of the synthesis.  The washing step involved rinsing the beads 5 times with DMF and allowing them to dry.  In order to remove the Fmoc protective groups on the beads/amino acids, a deprotecting step was used which was to add DMF+25% Piperidine to the reaction vessels.  Beads were washed again with DMF before a solution of HoBT, HBTU, DIPEA and an excess of the desired amino acid to link were added to the vessels.  A Kaiser Reagent test was used to ensure that the reaction went to completion and that no free, unprotected amide groups were present.  After certain residues the Kaiser Test can give false positive results; in this case a TNBT test was used to verify the lack of free amides.[94]  These steps were repeated until the full length peptide was created, after which time the peptide was capped with a solution of 5% acetic anhydride.

Variations in peptide residues were formed by manual splitting and differential coupling of amino acids.  The first component coupled to the bead was a photolinker molecule which would allow for cleavage of the peptides from the beads using UV light only.[95]  UV cleavage is preferable to acid-based cleavage as there were no extra reagents to interfere with the assays for screening the peptides.  At any residue that must be varied, the beads were deblocked and then split into equal amounts by mass and placed in separate reaction vessels.  We added a different amino acid to each of up

to four vessels. After the coupling reaction was complete, we mixed all of the vials together. In this manner we were able to generate a library having one unique peptide sequence per Tentagel bead. The total number of peptides in the library was 18,432 sequences. With such a large number of peptides, we set out to develop a high-throughput method to screen for the ideal endosomal escape causing activity.

Summary of Chapter 5
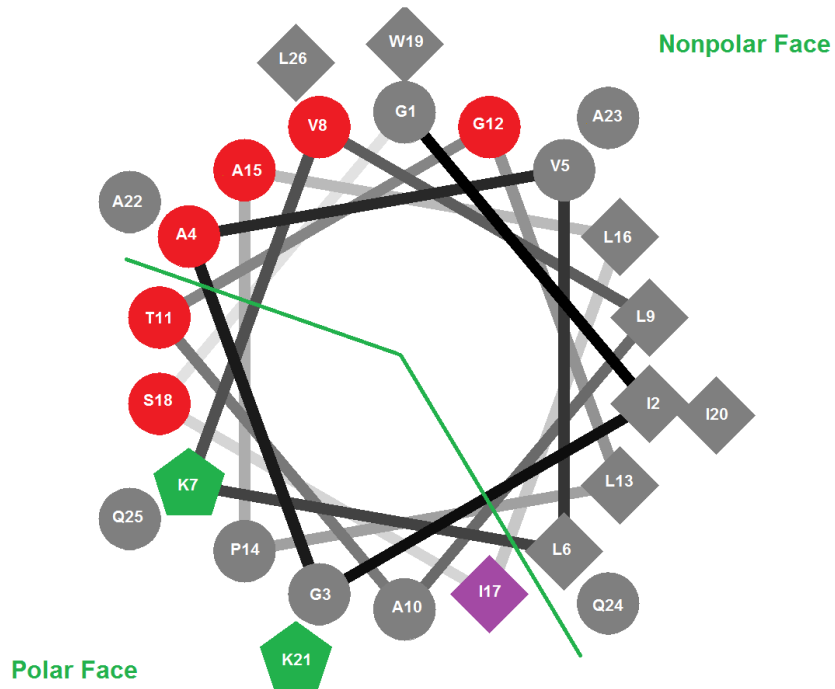
Chapter 6: Screening a Peptide Library for Efficient Endosomal Escape

Our goal was to put selective pressure on the library described in Chapter 5 to produce optimal sequences by choosing reliable assays that mimicked the conditions of endosomes. We believed that peptides from this library would exhibit the perfect compromise between pH-sensitivity and large-pore forming characteristics. We defined biophysical methods of describing these characteristics in Chapter 3. The characteristic of pH sensitivity can be described by a lack of small solute leakage from endosome-like lipid vesicles at high pH and increased activity at low pH values. Large scale pore forming ability can be described by having significant amounts of large solute leakage from lipid vesicles.[67] Again POPC lipid vesicles served as our model endosomal membrane system. We screened peptides at low concentrations using these assays as a method of selecting only the sequences which were both strongly pH-dependant and strongly pore-forming. We hypothesized that a peptide which could cause large solute leakage in a pH-dependant manner from vesicles at low concentrations could cause efficient endosomal release of macromolecules.

6.1 Peptide Library Screening Assays

Our screen process required at minimum two assays to compensate for the two characteristics that we sought to combine. The first assay used in this screen was an ANTS/DPX assay at pH 7. Lipid vesicles encapsulating ANTS and DPX as reporters were made in phosphate buffer as described above. These vesicles were added to peptide solutions and assayed for release. Peptides which were pH sensitive would not allow the small, approximately 500 Da ANTS and DPX molecules to escape from the vesicles.

For the second component of the screen we needed an assay that could tell us if large pores formed in a low pH environment. We made vesicles in pH 4 buffer containing TBD as a reporter with SA on the outside as described above.[67] When the two types of assays are combined, the overall pH of the solution was found to be pH 5, which was close to the pH of a late endosomal compartment. The ANTS/DPX in pH 7 buffer were added in 1mM concentration or 1:200 peptide:lipid ratio and allow to incubate for 1 hour before the percent leakage was determined. After this, the vesicles containing TBD in pH 4 buffer were added to the same peptide solutions at 3mM concentration for a final peptide:lipid ratio of 1:800 and the percent leakage was determined. With this two step assay, vesicles that caused low percent leakage of ANTS and high percent leakage of TBD could be discovered and selected as positive results.

These methods afforded us the additional benefit of allowing us to screen for soluble peptides. The assays above were all prepared in aqueous solutions of either phosphate or acetate buffer. Due to the fact that the library contained the possibility of increasing the hydrophobic nature of a given peptide, an insoluble peptide may have been made. Peptides which are insoluble would aggregate in phosphate buffer or acetate buffer, preventing them from binding to and interacting with our lipid vesicles. These peptides would cause little leakage and thus would constitute a negative result in the screen. All of the positive peptides, therefore, should have reasonable solubility in aqueous solutions if they were to interact with lipid vesicles. A positive result having high solubility increases their ability to be used as systemic delivery agents in blood or in combination with other soluble delivery agents. This third component of the assay,

though not directly quantified, provided an important method of screening for a desirable feature in membrane active peptides.

With a library containing over 18,000 members even screening a simple two step assay one bead at a time could become needlessly time consuming. We chose to screen the peptide library in a high throughput method. The important parameters of our screen design were reliability, reproducibility and how much could be done in parallel. The assay components needed to be reliable otherwise the results could not be trusted to accurately reflect the biophysical characteristics which we were testing. Our assays needed to be reproducible, as inconsistencies from plate to plate would not allow for the comparison of beads the large collective data set of results. Finally, we needed to ensure that many assays could be done in parallel, to limit the effects of unknown variables which might affect a given part of the screen from day-to-day. We successfully addressed all three of these components in the design of our screen.

We knew from categorizing large versus small pore forming peptides in Chapter 2 that the two assays which we selected were reliable. The ANTS/DPX assay has been used for many years and has been consistently heralded as a method of comparing the activity of MAPs. The TBD assay devised in this work is newer than the ANTS/DPX assay and has been shown to be useful in differentiating large-pore forming peptides from small pore forming peptides.[96] In terms of reliability, however, we needed to determine if the range of responses that these peptides could cause were above background noise from the assay. Could we differentiate 1% TBD leakage from 10% TBD leakage? Initial results from the TBD assay suggested that measuring the decrease in donor (SA) fluorescence provided a higher signal-to-noise ratio than measuring the increase in

acceptor (TBD) fluorescence.  We found that the background noise was less than 20% of the initial SA signal for a S:N between 5-10 (Figure 6.1).  We concluded that these assays could be used as a reliable method of screening for pH-sensitivity and large-pore formation.
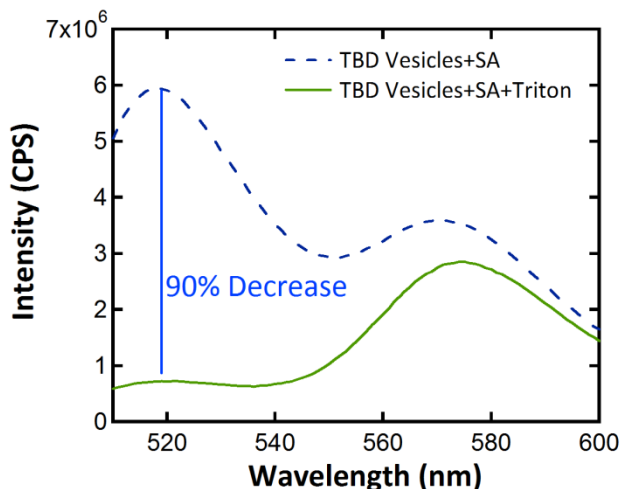


| | Intensity | Standard Deviation | S:N ratio |
|---|---|---|---|
| Control | 1.78E+04 | 5.80E+02 | 6.45E+00 |
| Triton | 2.76E+03 | 6.37E+02 | |

Figure 6.1 Tests of TBD leakage in Single vs High Throughput Methods.  The graph in this figure shows the standard decrease in SA signal that was seen when triton is added to the vesicle assay.  The signal at 519nm, the maximum emission of Alexafluor488 decreased to about 10% of the original signal.  Additionally, the table shows example data from control wells with just the TBD Vesicles+SA and wells with TBD Vesicles+SA and Triton.  The signal to noise ratio is greater than 5 and between 5-10.

At many times during the screen we took steps to measure the consistency of the results that we were achieving.  Certain plates received more or less of the assay components due to human error and could be reflected in a change in the plate average for a given assay result.  Figure 6.2 shows the results of the TBD assay at pH5 for plates from 1 to 40.  The average percent leakage of TBD for a plate falls between 10% to 20% leakage.  Several plates, such as plates 11, 12, and 13, have leakage values that are significantly higher than the other plates.  Looking at the values from these plates compared to plates from plate 20 to plate 25 we determined with a Student's T-test that these plates are significantly different (Figure 6.2).  These data suggested that the assays used for plates 11, 12, and 13 were unusual and that the results from these plates were

questionable.  We used this method of examining all plates to determine which results were true positives.
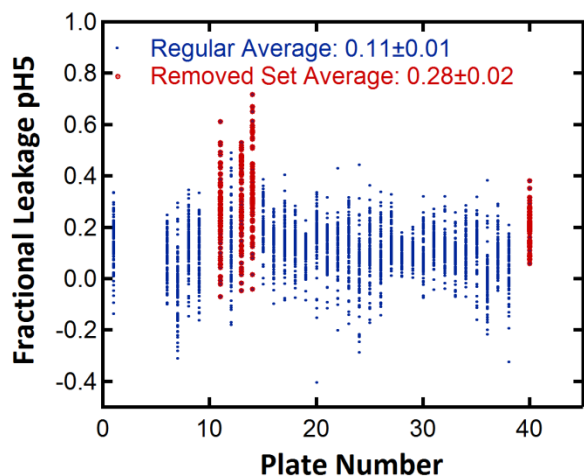


Figure 6.2 Example Data from Plates 1-40.  These data are the fractional leakage of large TBD molecules from vesicles at pH5.  The blue data are data sets that were kept, having an average of leakage of 0.11 the red data sets had an average leakage of 0.27.  Using a Student's T-test assuming equal variance, an alpha level of 0.05 and a hypothesized mean difference of 0 we found that the T-stat value was -28 as compared to a T-crit value of 1.9.  These data suggest that the data sets shown in red were statistical outliers and that peptides from those plates may be false positives.

As with many combinatorial drug libraries conducted before this work, we used multi-well plates (96-well plates) to screen numerous peptide beads in parallel.  An assay of an individual bead may take several minutes to perform using a cuvette-based fluorometer.  By using multi-well plates, one bead can be placed in each well and each well can be used as a separate reaction chamber for the assays.  Using a plate reader, many wells can be scanned simultaneously; time to screen beads is therefore decreased nearly 100-fold.  As described above, daily variations could occur with a given plate due to human error or some unforeseen circumstance.  Screening in parallel allowed us to have enough data points to determine if groups of data were outliers.  We were able to easily limit or filter out false positive results by designing a screen that was reliable, reproducible, and massively parallel.

6.3 Peptide Cleavage and Concentration

The concentration of assay components to add was determined by scaling to the average cleavage from the peptides. We utilized UV light to cleave the peptides from the beads rather than TFA or other cleavage methods. This was because residual TFA could potentially lyse vesicles or interfere with the assays. In order to cleave the peptides from the beads, a large number of dry beads was placed in a class dish and washed with methanol. The methanol was removed by drying under air and under vacuum until completely dry. The beads were placed in a 36W UV cleavage device and cleaved using 356nm wavelength light for 2.5 hours. The plate was turned upside down and the beads were cleaved using the same device for an additional 2.5 hours. After this, individual Tentagel beads were places, one-per-well, in 90 wells of a 96 well plate. We then added 25uL of Millipore water and 25uL of HFIP to each well of the plate using a multi-channel pipette. Each plate was placed in the UV cleavage device and allowed to cleave for 3.5 hours, enough time for the water and HFIP to evaporate. As a final step before the assay components were added, 25uL of Millipore water was added to each well and the plates were allowed to incubate overnight.

We used the tryptophpan fluorescence of the peptides to determine the amount of cleavage of the peptides from the beads. Solutions of the peptides which were incubated overnight could be collected and place in a cuvette in a fluorometer. The samples were excited at 280 nm and the fluorescence emission was collected from 300 to 450nm. The signal at 355nm was used for determining both a standard curve as well

as the concentrations of the samples. We found that approximately 0.5-1nmol of

peptide was cleaved from the plates (Figure 6.3).



| Well | Intensity | nmol |
|---|---|---|
| 6 | 2540 | 0.4 |
| 12 | 2520 | 0.4 |
| 18 | 3110 | 0.5 |
| 26 | 4000 | 0.6 |
| 34 | 3290 | 0.5 |
| 42 | 1830 | 0.2 |
| 50 | 2240 | 0.3 |
| 58 | 3160 | 0.5 |
| 66 | 4930 | 0.8 |
| Average | 3069 | 0.5 |
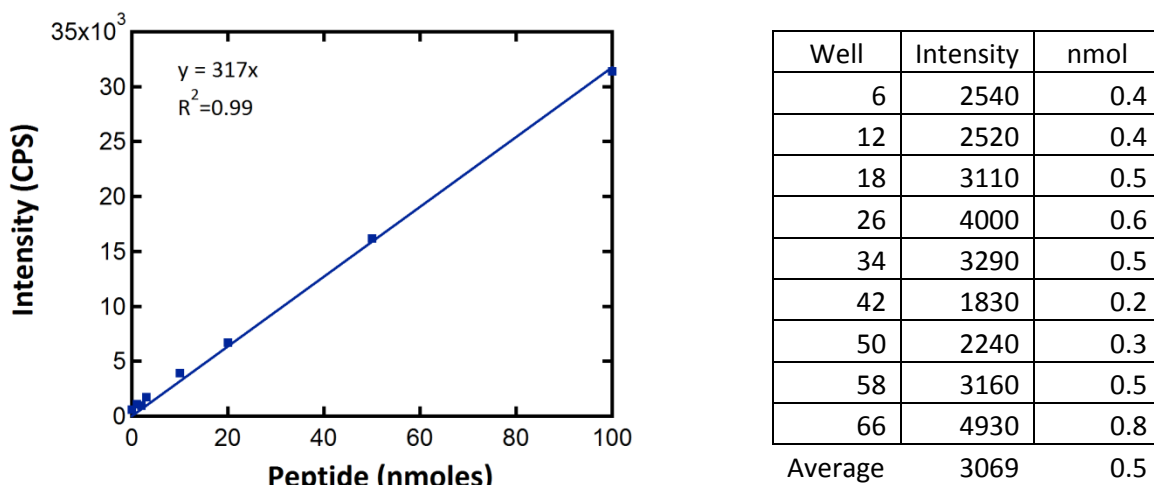
Figure 6.3 Cleavage of Peptides from Tentagel Beads. Figure 6.3 shows the standard curve calculated for tryptophan fluorescence in a 50uL cuvette over a range of known tryptophan concentrations. Sample beads were cleaved as described in the text and the fluorescence intensity of solutions of those beads is shown in the table on the left. The average cleavage from the beads was 0.5 nmoles.

Our assays used 100uL of 1mM ANTS vesicles which, for an average well, would

constitute a peptide:lipid ratio of 1:200. Adding an additional 100uL of 3mM TBD

vesicles gave a final peptide:lipid ratio of 1:800. We also performed part of the screen

using 100uL of 1mM TBD vesicles to give a final peptide:lipid ratio of 1:400. Figure 6.4

shows the results from four plates of a final condition of 1:400 and 1:800. With the

1:400 more peptides can be found with low pH 7 activity and high pH 5 activity. We

sought to set the stringency of this assay at less than one positive result per 10 plates.

Based on these results, for this amount of cleavage, decided to use a final peptide:lipid

ratio of 1:800 in order to achieve this level of stringency.
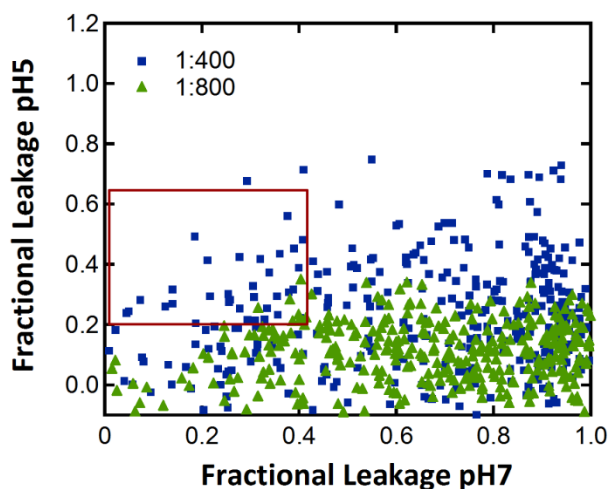
Figure 6.4 Comparison of Screen Results at Two Peptide:Lipid Ratios. These are data from screen results conducted with a final peptide:lipid ratio of either 1:800 or 1:400. Both data sets show a similar distribution of Fractional Leakage at pH7. With a peptide:lipid ratio of 1:400, however, more peptides were found to cause >20% Fractional leakage at pH5. From these data we concluded that 1:800 had a less broad distribution of activities at pH5, leading to easier identification of outliers (positive results).

We added control wells to each plate of the assay in order to ensure consistency and to ensure that results could be compared across plates. Wells A1 to A3 were used as negative controls, to which no peptide was added. The standard methods to produce the percent leakage values as described by Equations 2.1 and 2.3 require the same sample to be screened both before and after exposure to the peptides. Due the fact that in our screen design we added the vesicles to the peptide, we could not use these equations. Instead, for the first assay component we mixed the total amount of ANTS/DPX vesicle solution needed for each well together and placed an aliquot into each well. This method allowed us to have identical conditions in each well for the ANTS/DPX assay. For the TBD vesicles, the total amount of vesicles was prepared and SA was added to this total amount before it was dispensed into each well. The plates were excited twice, once at 360nm with an emission recorded at 519nm, for ANTS and a second time at 495nm with an emission recorded at 519 for SA. The negative control wells showed a lack of ANTS fluorescence and the existence of SA fluorescence due to reporter encapsulation.

Each assay plate had positive controls for 100% leakage as well. These controls were placed in wells B1-B3. The equations above for percent leakage require normalization to a standard in order to compare different MAPs. Two positive controls were used during the screening of the peptide library. Triton 100-X was used as an indicator of complete membrane lysing. In this case, there would be a large fluorescence signal from ANTS and a small signal from SA. The ultimate goal of this screen, however, was to search for peptides which retained or exceeded the pore-forming abilities of MelP5. For this reason, we prepared wells containing 0.5nmoles of MelP5 in addition to the wells containing Triton 100X. To make the peptides further comparable we could normalize the signal in each well to either the signal caused by triton or by MelP5 for a given plate. The modified equation for percent leakage was the following Equation 6.1:

$$\%FRETleakage = \left(\frac{I_{SA,controls}-I_{SA,peptide}}{I_{SA,controls}}\right)/\left(\frac{I_{SA,controls}-I_{SA,MelP5}}{I_{SA,controls}}\right)$$

Equation 6.1 The percent leakage equals the SA signal in the control wells $I_{SA,controls}$ minus the signal in the peptide wells $I_{SA,peptide}$ divided by the control well signal, scaled by the control well signal minus the MelP5 control $I_{SA,MelP5}$ divided by the control well signal. Additionally we could use triton ($I_{SA,Triton}$) instead of MelP5.

The choice of standard influenced our determination of a true "positive" result from the screen.

## 6.4 Selecting Positive Result Peptides from the Library Screen

We screened over 10,000 beads from this library, the results of which are shown in Figure 6.5. These figures show a colored representation of how far away from the average result each bead was. The results tended to cluster around what we would see for MelP5, 100% leakage in ANTS/DPX containing vesicle assays and 15-20% leakage in TBD containing vesicle assays. In this screen, positive results were identified as gain-of-function peptides, ones that retained or showed increased leakage in the TBD assay at pH 5. Positive results also needed to exhibit pH-sensitivity, and thus would show little ANTS/DPX leakage at pH 7. We defined cutoff values for these peptides to be as follows: positive results must have less than 20% ANTS/DPX leakage at pH 7 and must be at least as active as MelP5 at pH 5. Though we defined these initial parameters, we also tried to develop a method of ranking peptides within our range of "positive" results.
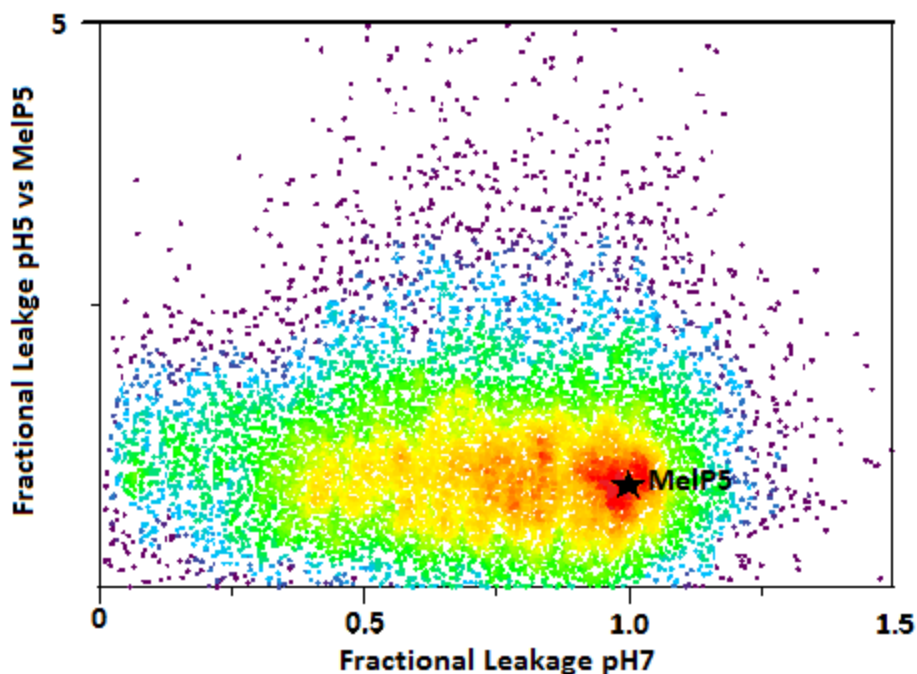


Figure 6.5 Total Screen Data scaled to MelP5. Figure 6.5 shows the screen data of all peptide beads. These data are plotted as Fractional leakage at pH7 relative to the fractional leakage of large molecules (TBD) at pH5. MelP5 is shown as a black star in the center and peptides increasingly further from the average (MelP5) are shown in gradients from red to purple.
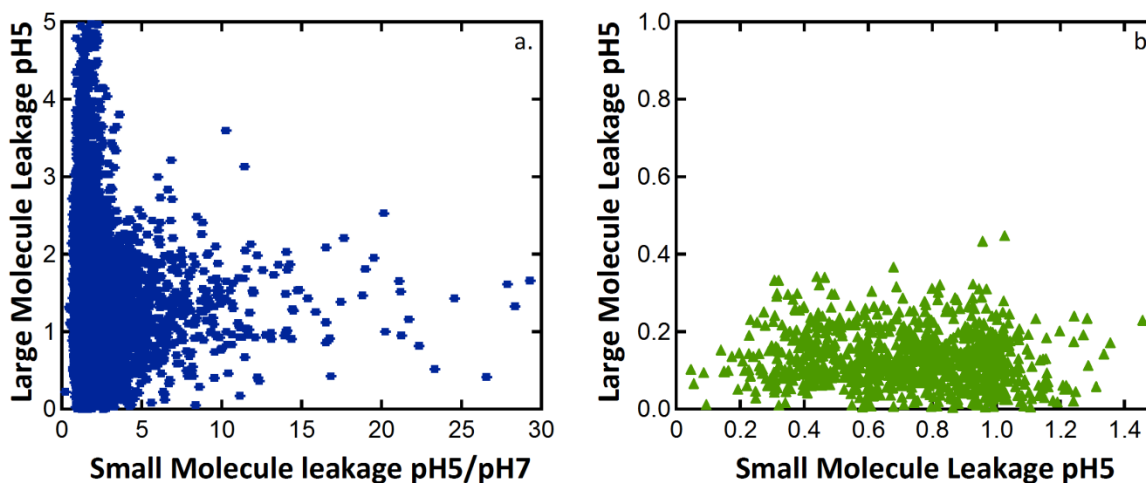
Figure 6.6 Methods of Determining Positives/False positives. Figure 6.6a shows a plot of the screen data as the ratio of pH5/pH7 small molecule leakage vs large molecule leakage at pH5. True positive results have a high pH5/pH7 ratio and cause significant large molecule leakage. Figure 6.6b illustrates the presence of false positives in the data. Certain peptides showed equal or greater preference for large molecule leakage as compared to small molecule leakage.

One method of ranking peptides came from the relative leakage of ANTS/DPX at pH 7 as compared to leakage at pH 5. In our two-step assay we were able to determine ANTS/DPX leakage at pH 7 and at pH 5 because the two assays did not interfere with each other. Positive results with percent leakage of ANTS/DPX less than 20% at pH 7 should have an increased percent leakage of ANTS/DPX at pH 5. Indeed, many of the peptides showed greatly increased small solute leakage at low pH conditions. Figure 6.6a shows the data from the screen plotted as the ratio of pH 5 ANTS/DPX leakage to pH 7 ANTS/DPX leakage versus TBD leakage relative to MelP5. Several peptides exhibit an extraordinarily large ratio of pH5/pH7 leakage because they caused little to no leakage at pH 7. Given the fact that the lipid concentration was increased four-fold (from 1mM to 4mM), such peptides could be greater than several orders of magnitude more active in endosomes as opposed to on the cell membrane. These data also provided a method of eliminating false positive results from the screen. Figure 6.6b

shows a small subset of the data plotted as pH 5 ANTS/DPX leakage versus pH 5 TBD leakage.  For some beads, the TBD leakage was greater than MelP5 but the ANTS/DPX leakage did not increase.  Due to the fact that TBD is a larger molecule and that the encapsulating vesicles had the same composition we saw no logical reason for a peptide to cause less ANTS/DPX leakage than TBD leakage.  These results therefore were "false positives" and were filtered out or ignored as part of the screen.

As mentioned above, in order to rank true positives we examined their activity relative to MelP5.  The data from Figure 6.5 were future separated into small subsections or "epochs" in order to find outliers from the group of peptides examined within each epoch (Figure 6.6).  Amongst these outliers we were able to select peptides that had either substantial large molecule leakage or minimal small molecule leakage.  Below is a table of several peptides which we selected as the best positive results due to their having optimal biophysical characteristics.  These peptides were named: pHD118, pHD34, and pHD108.  Each peptide showed only a small amounts of leakage at pH 7 and large amounts of leakage at pH5.  In addition, we selected several peptides which appeared to be either constitutively active, causing leakage at all pH values and constitutively inactive or loss-of-function causing no leakage.  We continued to screen and select more peptides but at this stage we decided to determine the sequence of our positive and negative results.

Figure 6.6 Location of Positive Result Peptides from Figure 6.5
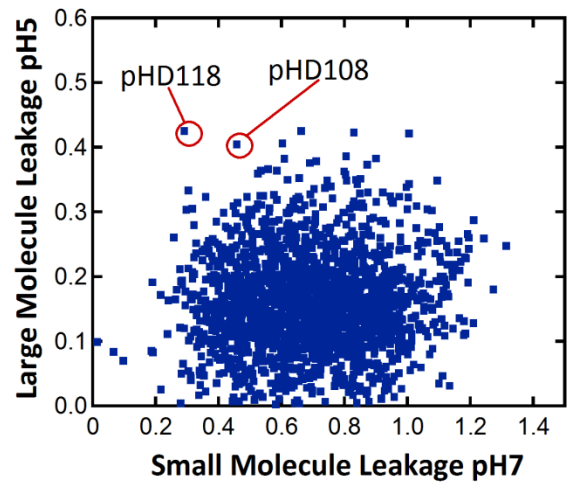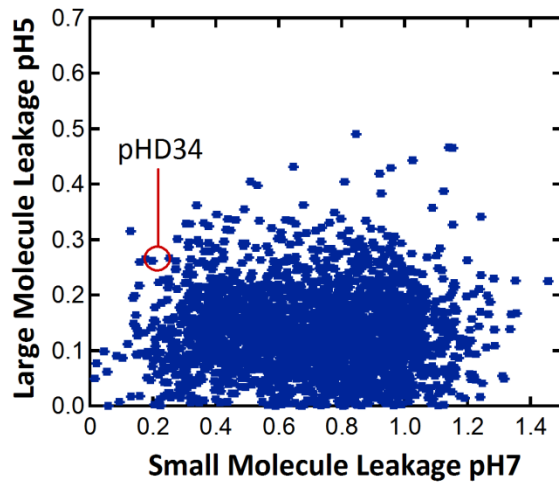
6.5 Sequencing Positive Result Peptides

Combinatorial libraries, though convenient for generating a large number of unique sequences, suffer from one major drawback: we don't know which sequence is on which bead. Each bead contains one unique sequence, which allowed us to sequence the peptides using one of two methods. For the peptides which were negative results, we opted to sequence using an enzyme digest and mass spectroscopy methods. For our positive results, we chose to sequence peptides using Edman degradation. Each method has advantages and disadvantages which lead us to use one method for sequencing negatives and the other method for sequencing the positives. Overall each method has been extensively verified and proved reliable in determining peptide sequences.

For negative results we decided to sequence peptides using an enzyme digest and mass spectroscopy. In developing this method we noted that the parent sequence, MelP5 can be divided into subsections between leucine residues with about one varied reside in each subsection. We knew that if we could break a peptide down into these small sections we could determine the change in mass for each subsection and therefore identify the sequence. We used Pepsin, an enzyme which can break peptide bonds at the C-terminus of leucine residues, for this purpose. The assay solutions in wells with unique peptides were removed and washed three times with methanol. Beads were then placed in a 0.5 mL eppendorf tube to which the following components were added: 1.6 uL of 1 mg/mL pepsin in Millipore water, 2 uL of 25% formic acid and 6.4 uL of Millipore water. Formic acid at this concentration was found to be enough to

activate pepsin, which only has enzymatic activity at pH 1-2, and also the formic acid was compatible with liquid chromatography mass spectroscopy (LC/MS). After degradation, the reaction was quenched with 10 uL of 5% sodium hydroxide, which is also compatible with LC/MS. The samples were injected into a Waters LC/MS, which allowed for the identification of various fragments of the peptides. Figure 6.7 below shows an example chromatogram for the parent sequence MelP5. The peaks in the chromatogram were characteristic for various fragments of the peptide sequence. These peaks could be fit to a known sequence by matching to fragment ions of these peaks as shown below. Mass spectroscopy based sequencing of peptides provided a quick method that required small amounts of material (less than 1 pmole of peptides). The main drawback was that the sequences were not determined by individual amino acid but rather they required analysis of the fragment ions to produce a sequence.
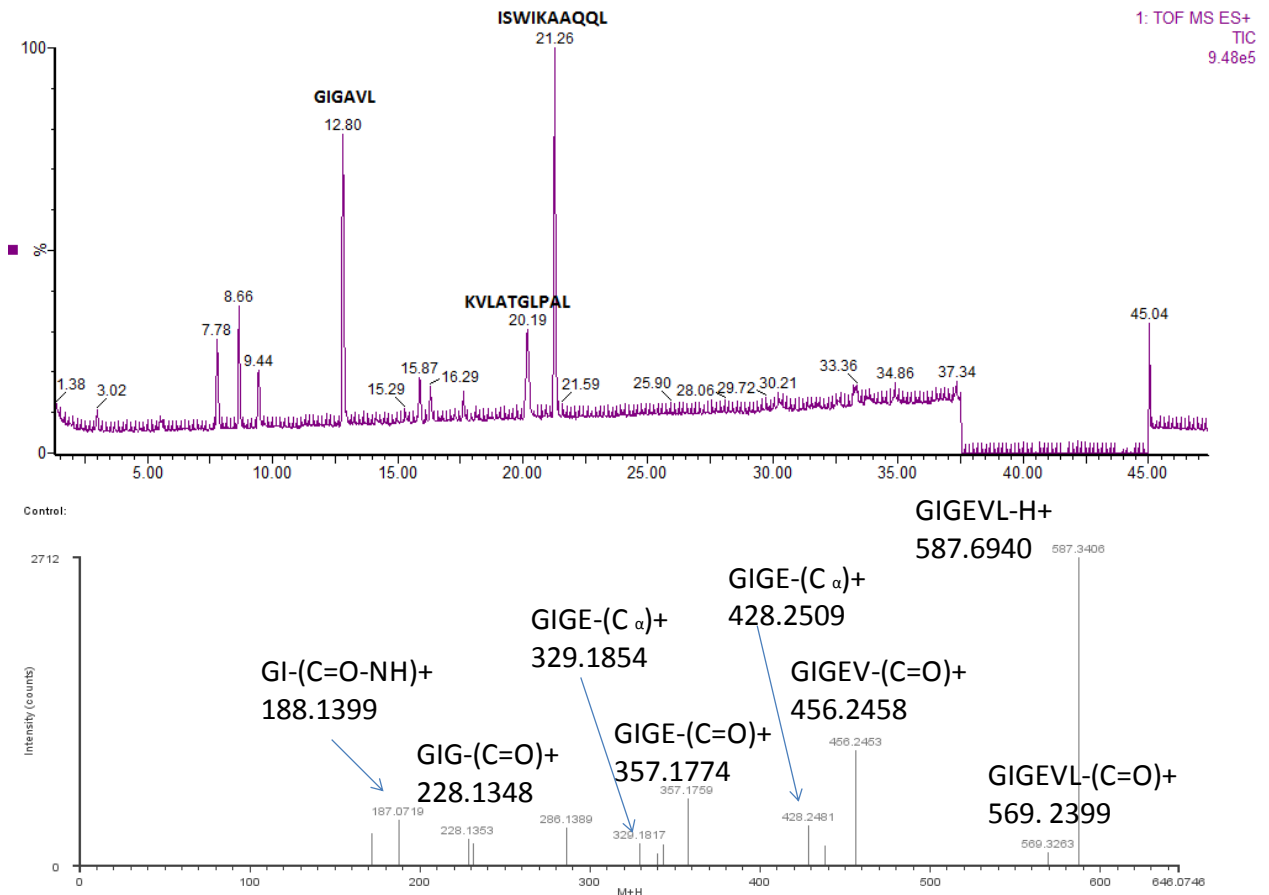
Figure 6.7 Example LC/MS data of Peptides. This data highlights the protocol used to sequence peptides through LC/MS. The chromatogram at the top is of a MelP5-pepsin digest with fragments labeled. Below is a method showing fitting of masses to fragment ion data.

Unknown peptide sequences on beads can be determined by each individual amino acid using Edman degradation. This technique relies on chemical cleavage of each amino acid in the sequence from the bead in a sequential manner. We chose to sequence positive results from our library screen using Edman degradation because it was the most reliable method for determining peptide sequences.[97] This sequencing work was performed in collaboration with Dr Jodie Franklin at the Johns Hopkins Medical Institute. Working with Dr Franklin we were able to determine the sequences of several positive result peptides such as pHD118, pHD34 and pHD108. This method, while reliable, was more material consuming and time intensive as opposed to mass

spectroscopy sequencing methods.  Still, we were able to very accurately determine the sequences of these peptides, which allowed us to use them for further biophysical characterization and cell based studies.

<u>Summary of Chapter 6</u>

We have an understanding of the biophysical mechanisms upon which an ideal endosomal escape causing peptide would work.  We screened our peptide library using a two step assay, searching for peptides which caused little to no small solute leakage at pH 7 and extensive amounts of large molecule leakage at pH 5.  From our knowledge of MelP5 activity we determined that positive results from our screen would have less than 20% leakage of ANTS/DPX at pH7 but greater than 15-20% leakage in the TBD assay at pH 5.  We further categorized these peptides relative to each other based on the ratio of pH 5 to pH 7 ANTS/DPX leakage and the extent of TBD leakage beyond the amount caused by MelP5.  These positive peptides therefore contained a compromise between the desired characteristics of pH-sensitivity and large-scale pore formation.  We utilized both Mass Spectroscopy as well as Edman degradation techniques to sequence these peptides.  Once we determined the optimal peptide sequences from our library, we set out to confirm their activity with further biophysical studies as well as cell based assays.

Chapter 7 Biophysical and Cell-based Studies of Positive Screen Results

Do our biophysical characterization methods accurately reflect real-life biological systems? This is a question that pertains to every experiment in biophysics and engineering. Our attempt at inducing synthetic molecular evolution succeeded in producing peptides with an ideal biophysical mechanism of activity for endosomal escape. The three peptides we selected showed a minimum of a two times increase in ANTS/DPX (small molecule) leakage at pH 5 over pH 7 and also showed greater TBD (large molecule) leakage than MelP5 at pH 5. From this point we sought to prove the connection between our model lipid vesicle system and real biological systems. To confirm that these peptides could be useful as endosomal escape agents we characterized them using the model methods described in Chapters 2-5. We determined both the partitioning free energy at low pH as well as the secondary structure over a pH range. These peptides exhibited pH-sensitivity in a range close to that of late endosomes. In addition we examined the pH-dependant leakage of TBD caused by these peptides and found that in low pH environments they cause a significant amount of TBD leakage even at low concentrations. The last step was to prove a correlation between the ideal mechanism of activity and biological significance. We examined the delivery of both small molecules and macromolecules to two different types of cells, CHO and HUVEC cells. Our peptides facilitated the delivery of small molecules and macromolecules to cells. We noted that the effects, however, were at concentrations that were higher than we anticipated. Due to this fact, we reexamined

our model systems and discovered limitations and improvements which provide the basis for future screens and studies.

7.1 Partitioning Free Energies of Positive Result Peptides

Peptides with the ideal endosomal escape causing mechanism should bind to membranes only in low pH environments. This fact was postulated in Chapter 4. Studies with MelP5_Δ4 and MelP5_Δ6 confirmed that low partitioning free energy is correlated to the inhibition of small molecule leakage. It was therefore important to establish that the first part of our idealized mechanism applied to these new peptides: pHD118, pHD34, and pHD108. Could these peptides bind to a model endosomal membrane, lipid vesicles, in a pH-dependant manner? We utilized two methods to determine the binding coefficients and partitioning free energies in model vesicle systems of PC, 90% PC 10% PG, and 75% PC 25% CH. The first method followed the same protocols as described in Chapter 4 above for measuring binding. We added 10uM of a given peptide to 10 mM sodium phosphate buffer at pH 7 with 100 mM potassium chloride and to 10 mM sodium acetate buffer at pH 5 with 100 mM potassium chloride. Increasing amounts of vesicles were added to the solution and the change in tryptophan fluorescence intensity was measured. The titration method worked well for POPC and POPC:PG vesicles but not for vesicles containing cholesterol. Cholesterol is known to interfere with the changes in tryptophan signal with peptides such as Melittin.[98] We devised a new method to determine the rate of peptide binding to PC:CH vesicles. We mixed 10 uM peptide with 500 uM PC:CH vesicles and then filtered out the vesicles using 100 kDa molecular weight cutoff filter units. This allowed us to measure the fluorescence signal from the tryptophan both before vesicle addition as well as after, allowing us to determine the partitioning coefficient as per the following equation:

$$K_x = \frac{I_o - I_{ft}}{I_{ft}} * \frac{[L]}{55.3}$$

Equation 7.1  The mole fraction partitioning coefficient is equal to the initial fluorescence intensity of tryptophan (at 335nm) $I_o$ minus the fluorescence intensity of the flow-through water ($I_{ft}$) divided by the flow-through intensity times the ratio of the lipid concentration (in molar) to the molarity of water (55.3M)

These methods provided a way of determining the binding free energies of our peptides to various different vesicles at two different pH values.

The binding data from these experiments is shown below in Table 7.1.  Peptides pHD 118, pHD 34, and pHD 108 much like MelP5_Δ4 and MelP5_Δ6 had low partitioning free energies in pH 7 buffer.  For a vesicle concentration of 1 mM (1:100 peptide:lipid ratio) between 0.5-3% of peptide would be bound to membranes at pH 7.  Each of these peptides bound to membranes much more favorably at pH 5 with an average ΔΔG of -4.1 kcal/mole lower free energy.  At this low pH value 100% binding of the peptides bound to POPC lipid membranes.  The peptides bound nearly as strongly as MelP5 to lipid vesicles composed of POPC, around ΔG of -8.0 kcal/mol versus -8.9 kcal/mole.  The optimal peptides selected from this screen fit the binding component of our ideal mechanism of activity in POPC-based membranes.

| Peptide | PC (pH5) | PC (pH7) | PC:PG | PC:CH |
|---|---|---|---|---|
| pHD118 | -8.14 | -4.38 | -7.52 | -7.04 |
| pHD34 | -7.84 | -3.42 | -7.53 | --- |
| pHD108 | -8.02 | -3.75 | -7.84 | -6.88 |
| MelP5 | -8.10 | -8.90 | -8.31 | -8.81 |

Table 7.1 Free Energies of Peptide-Membrane Binding Interactions in kcal/mole. This table shows the binding free energies for the three positive result peptides and MelP5. The binding of MeP5 to PC membranes was much more favorable than the binding of any other peptide at pH7. MelP5 also did not show a significant drop in activity depending on lipid composition. Peptides pHD34, pHD118 and pHD108 bound to membranes less favorably at pH7 and also showed decreased binding to PC:CH membranes on the order of +1.1 kcal/mole.

Cell membranes are not solely composed of POPC, because of this we tested the binding of our peptides to PC:PG vesicles as well as PC:CH vesicles. We knew that the POPG lipid head group contains a negatively charged head group. We were unsure if the charge on this group would interfere with the peptides' ability to bind to vesicle membranes. Experimental data showed that the peptides did bind slightly less favorably to vesicles containing 10% POPG. The ΔΔG of these interactions was +0.4 kcal/mole on average. This change in partitioning free energy would not inhibit the binding of our peptides to membranes at 1mM vesicle concentration. We concluded that the effects of POPG in the membrane were negligible. What appeared to significantly affect that binding free energy was the presence of Cholesterol in the membrane. The partitioning free energy of the peptides increased by an average ΔΔG of +1.1 kcal/mol. The parent sequence, MelP5, only had a ΔΔG of +0.1 kcal/mol when cholesterol was included in vesicles. At a peptide:lipid ratio of 1:100 (1mM) this might not correspond to a significant difference, but at one order of magnitude lower concentration of 0.1 mM this could mean the difference between 100% bound peptide versus 25% bound peptide. The total concentration of lipids in a seeded slide of cells

may vary anywhere between 10 uM to 1 mM. If the ultimate application of these peptides were use as transfection reagents, the change in activity cause by different lipid compositions of different cell types may prove to be important. Overall, peptides did bind to membranes in a pH-dependant manner, begging the need to study their ability to assume secondary structure at different pH values.

## 7.2 Secondary Structure of Positive Result Peptides

Peptides pHD118, pHD34, and pHD118 bound to membranes in pH-dependant manner; did the form secondary structure in a pH-dependant manner as well? We repeated the methods described in Chapter 4 for measuring the secondary structure using circular dichroism. Solutions of peptides in 10mM Sodium Phosphate or 10mM Sodium Acetate buffer were prepared at 10uM in pH values ranging from pH 7 to pH 4. After an initial scan from 260nm to 185nm 1 mM POPC vesicles (peptide:lipid ratio of 1:100), were added to each sample. We recorded the CD spectrum from 260nm to 185nm again after this addition of vesicles. We anticipated that this method would allow us to investigate the relationship between vesicle binding and alpha helical structure formation. Each of these peptides has a strong alpha helical propensity similar to MelP5. We anticipated that these peptides would, in fact, become alpha helical at some low pH value.

Our results suggest that all three of these peptides form alpha helical secondary structure preferentially at low pH values. As shown in Figure 7.1, at pH 7 all of the positive result peptides exhibit a random coil structure with a characteristic minimum at 200nm. As the pH of the samples decreases, the peptides become increasingly alpha helical. We took the value at 222nm for each pH and normalized it to the value at pH 4 to be a representation of the % alpha helical content for these L-amino acid peptides. We plotted this value as a function of pH in Figure 7.1d. Analyzing these results we determined that the effective pKa of activity was pH 5.5 for peptides pHD118 and pHD34 and slightly lower at pH 5.0 for peptide pHD108. These values were higher than

the values found for MelP5_Δ4 and MelP5_Δ6 (pH4.8-4.6). Our peptide library contained members with activity that was more complexly controlled than simply relying on the pKa of the amino acid side groups. We determined that our three positive results peptides required not only a low pH value to become protonated and form alpha helices but also certain other factors as well.
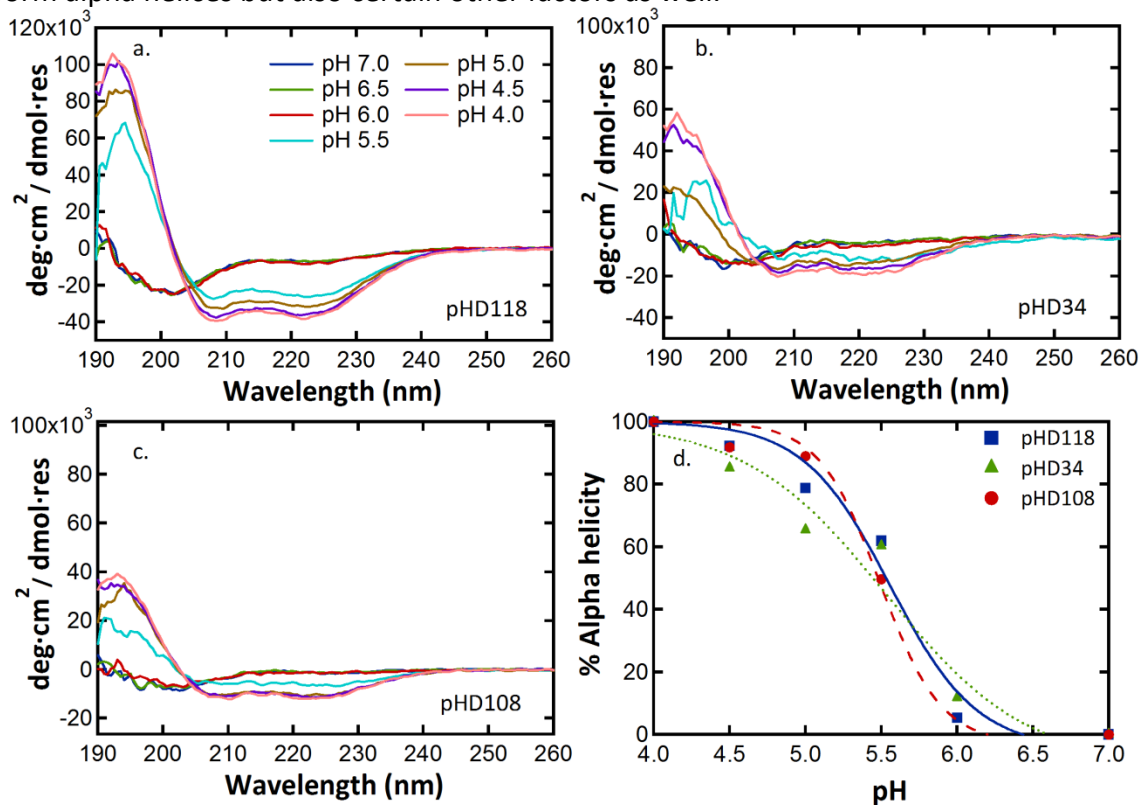


<u>Figure 7.1</u> CD Data of pHD Peptides with Vesicles. These data show the CD spectra of pHD118, pHD34, and pHD108 in the presence of 1mM vesicles. As shown in 7.1d, as the pH decreases the percent alpha helicity increases. These results indicate that the peptides obtain secondary structure with a midpoint of aproximatly pH 5.5 as determined by fitting to a sigmoid function.

Complex mechanisms of control were seen not only between the rationally designed peptides and the positive screen results but also within the screen results themselves. For peptides pHD34 and pHD118 peptides formed alpha helical secondary structure with decreasing pH with or without vesicles. This meant that our peptides formed an alpha helical structure in solution when they became protonated. This result

was not surprising because some MAPs, like melittin, are hypothesized to be soluble in aqueous solutions by forming a oligomers, thus gaining a slight amount of alpha helical content.[99] The pattern of structure formation with pHD34 and pHD118 supports the existence of oligomer structures in buffer. This leads to having alpha helical structure in the absence of lipids. The third peptide, pHD108, was different. This peptide did not form a significant amount of alpha helices in solution alone. Even at pH 4 the percent alpha helicity relative to the maximum was only 25%. With the addition of 1mM lipid vesicles, however, the alpha helical content increased dramatically. For example, the depth of the well at 222nm increased 3-fold at pH5 with the addition of 1mM lipids from -4000 deg·cm$^2$/dmol·residue to -13000 deg·cm$^2$/dmol·residue. Peptide pHD108 exhibited the same pattern of lipid-dependant secondary structure formation as MelP5; it was a monomer in solution. We found, however, that titrating in increasing amounts of lipid, at pH5 for example, did not increase the depth of the well at 222nm. Taken together these data showed that we could achieve part of the ideal mechanism of activity, pH-dependant binding and alpha helical structure formation.
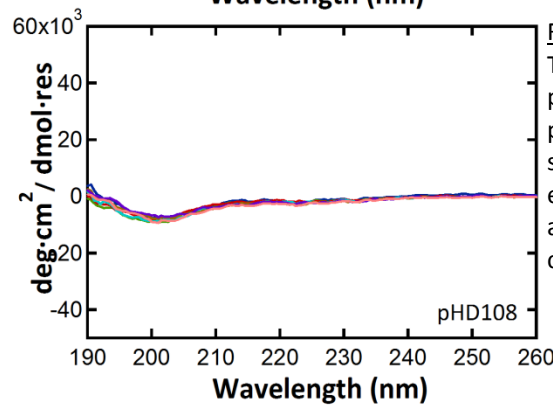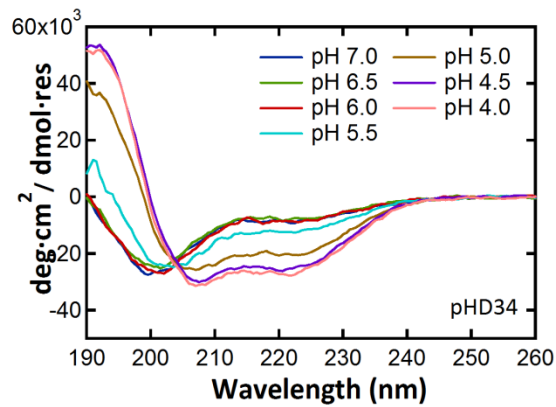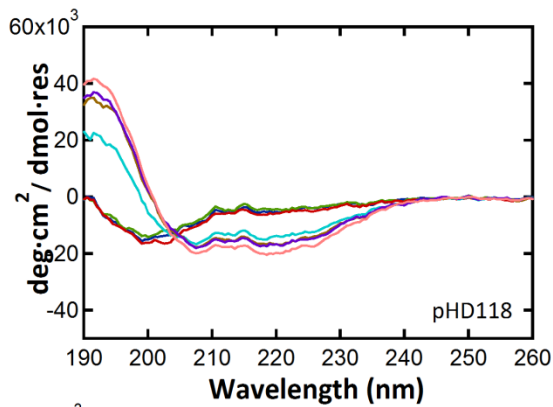
Figure 7.2 CD Data of pHD Peptides without Vesicles. These are the CD spectra of peptides pHD118, pHD34 and pHD108. Both peptides pHD118 and pHD34 show alpha helical signals at low pH in solution alone, suggesting a Melittin-like aggregation event. The third peptide, pHD108, shows only a well at 200nm (unlike Figure 7.1), suggesting it is random coil in solution at all pH values.

7.3 Biophysical Characterization of Positive Result Peptides by Leakage Assays

The three peptides we selected were chosen because of their ability to allow the passage of macromolecules across POPC membranes at low pH values. Knowing that these peptides had our ideal mechanism of activity, we looked to determine the pKa of this activity. We asked two questions, one about the minimum concentration required of peptide activity and the other about the pH value at which the peptides become active. We hypothesized that these peptides could cause efficient endosomal escape. This meant that the peptides should be active at very low concentrations (low peptide:lipid ratios) and that they should exhibit a drastic change in activity when they transition from a neutral pH environment to an environment past their pKa. To answer these questions we turned back to our model cell membrane system; lipid vesicles encapsulating TBD vesicles.

In addressing the first question we produced TBD vesicles in 10mM pH 5 sodium acetate 100mM potassium chloride buffer to find the minimum active concentration. Our peptides were screened for large scale disruption abilities at pH 5 at an average concentration of 2.5uM. We reasoned that the minimum active concentration must be lower than this value. We added each peptide to 3mM vesicles and determined percent leakage as described by Equation 2.3. All peptides showed greater than 50% leakage at 3uM concentration (1:1000 peptide:lipid ratio) (Figure 7.3). Amazingly, these peptides vastly outperformed MelP5, which only caused 10-20% leakage at a 3uM concentration in these experiments. These peptides proved to not only be as active as MelP5 but, in fact, were more active. The peptides caused detectable leakage at concentrations of

0.3-0.6uM, almost an order of magnitude lower than in the assay. As a control

experiment, we performed the same assay but first blocked the binding sites on SA with

biotin. In these control experiments the signal from SA did not change, indicating that

the peptides were not inducing aggregation of the reporters. This gave us the hope that

positive library screen results could actually be active in the nanomolar range at the

correct pH value.
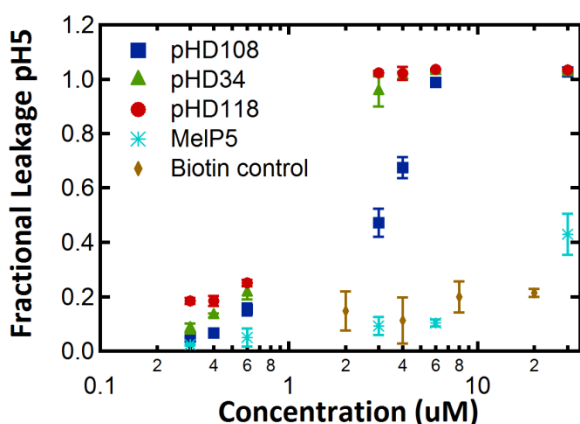


Figure 7.3 Fraction Leakage of Large Molecules at pH5. Figure 7.3 shows the leakage of TBD caused by pHD108, pHD118, and pHD34 as a function of concentrations. Above 3uM peptides caused greater than 50% leakage, which was an order of magnitude better than the parent sequence, MelP5. When SA was first blocked with biotin, no significant change in signal was recorded, indicating that the peptides do not promote the binding of TBD to SA.

Our second question pertained to what the correct pH range of activity was for

these peptides. Again we encapsulated TBD as a reporter molecule in our model POPC

lipid vesicles. We discovered that these peptides bound to membranes with different

free energies depending on the composition of the membrane. Due to this, we assayed

the leakage from PC lipid vesicles as well as PC:PG and PC:CH vesicles, all over the range

from pH 7 to pH 4. We set the active concentration to be 3uM and used 3mM vesicles

to afford ourselves a 1:1000 peptide:lipid ratio. At this concentration the peptides

should easily disrupt membranes and allow the escape of TBD molecules. Our results

show that the pKa values for the pHD peptides did not vary much. Peptides pHD118 and

pHD34 had a pKa of 5.75 in POPC vesicles and pHD108 had a pKa of 6.0. For vesicles

containing 10% POPG the pKa was essentially the same as with POPC vesicles, between

6.0-5.75. This was unsurprising because the binding free energies differ by less than 0.5

kcal/mole. What was surprising, however, was the difference in pKa between peptides

in solution with POPC vesicles and peptides in solution with POPC:CH vesicles. The

active pKa of the peptides dropped by an entire pH unit from pH 6.0-5.75 to pH 5.0-4.5.

This made sense considering that the peptides bound more favorably to vesicles in the

absence of cholesterol. The peptides were able to cause 100% leakage at low pH values

even in spite of the cholesterol in the membranes. The pKa likely shifted because much

more of the peptide needed to become protonated in order to achieve the active

concentration. The effect of cholesterol raised the question of how well our model

systems mimicked actual cell endosomes.
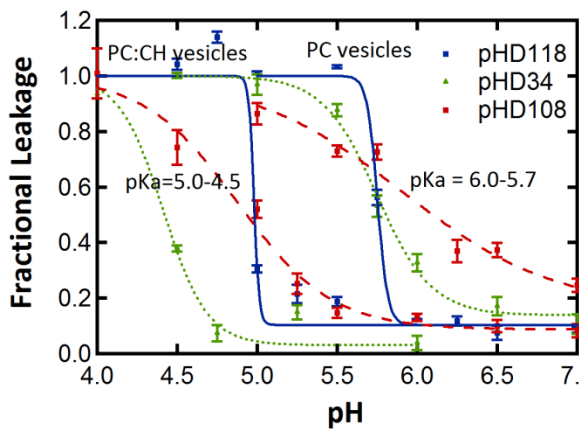


Figure 7.4 Fractional Leakage of TBD vs pH. These data show the fraction leakage of large molecules (TBD) with respect to pH at a peptide:lipid ratio of 1:1000. As the pH decreases, the fractional leakage increases from nearly 0 to 100%. The pKa in PC vesicles was determined to be between pH 6.0 and 5.7 for pHD118, pHD34 and pHD108. The pKa in PC:CH vesicles shifted nearly 1 pH unit lower to pH 5.0 to pH 4.5. These data are in congruence with the data regarding binding free energies in different lipid compositions.

Cell Based Assays with Positive Result Peptides

As a final component of this work we set out to determine if peptides could induce endosomal escape in a pH dependant manner. We tested whether or not our peptides were cytotoxic at neutral pH and at what pH could they become cytotoxic. We looked at the permeabilization of cell membranes to large molecules at both pH 5 and pH 7. Finally, we performed an endosomal escape assay to examine whether or not large molecules could escape endosomes in the presence of our peptides. Through these methods we characterized the actually biological response of real cells to our peptides.

We determined the cytotoxcicity of our peptides to Chinese Ovarian Hampster (CHO) cells as well as several other cell types. In CHO cells we used Sytox Green as an indicator of cell death. Sytox Green is a molecule that cannot readily diffuse across cell membranes. In the instance of cell permeabilization, Sytox Green can penetrate the cell membrane and bind to nucleotides within the cell, which increases its fluorescence.[100] We seeded CHO cells at $5*10^3$ cells/well in 8 chamber slides and cultured the cells in DMEM media for 3 days. For the assay, DMEM was replaced with Phosphate Buffered Saline adjusted to pH values in a range from pH7 to pH4 and Sytox Green was added to a final concentration of 1μM. We added peptides to the cells in a concentration of 300μM and determined a percentage of cell death as a function of the percent of fluorescently labeled cells observed in a microscope. We found that even at a concentration of 300μM, no cells were labeled with Sytox Green, indicating that the peptides were not cytotoxic at pH 7. As the pH of the solution decreases, the peptides

gradually switched from being innocuous to being completely cytotoxic. In addition to Sytox labeling, significant cell detachment from the surface was observed. Interestingly, the pH at which the cells transitioned from being inactive to being cytotoxic fell closer to the pKa in POPC:CH vesicles as opposed to the pKa in POPC vesicles (Figure 7.5). Mammalian cells contain 25% cholesterol; the lower pKa of activity in cells was an effect of cholesterol in the membrane. We therefore made a link between our biophysical models and activity in cells. Sytox green is only a small molecule; we wanted to show that our peptides could allow the passage of large molecules into these cells.
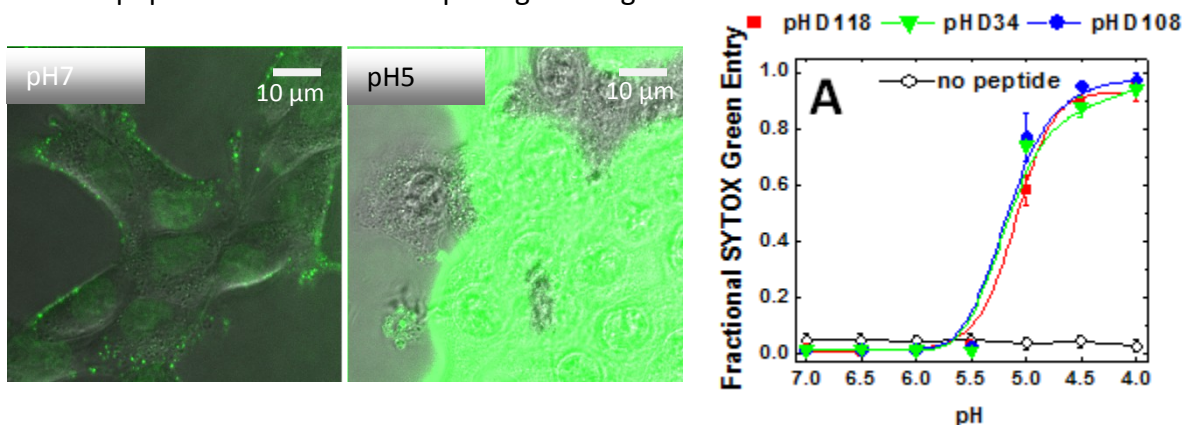


Figure 7.5 Sytox Green Staining of Cells. Figure 7.5 shows the methodology of Sytox Green Assay of cell permeabilization. In pH7 PBS buffer with 100µM peptide, cells exhibit small background signal of Sytox Green with small, punctuate regions on the surface indicating endosomal uptake of the dye. In pH5 PBS buffer with 100uM peptide, cells exhibit a saturating amount of Sytox Green labeling. The third panel shows Sytox Green labeling, given as % fluoresceing cells, as a function of pH for peptides pHD118, pHD34 and pHD108. The midpoint pH was found to be the same as the point of pKa for large molecule leakage in PC:CH vesicles, confirming a connection between vesicle model membranes and biological membranes.

We studied the ability of fluorescently labeled 3kDa Dextran molecules to enter these cells in the presence of our peptide to show that these peptides could allow macromolecular passage. Again, we cultured CHO cells at $5*10^3$ cells/well in 8 chamber slides in DMEM media for 3 days. In these experiments, DMEM media was removed and PBS adjusted to pH5 was added to the cells. Peptides were added to the solution at

100µM-300µM along with 1µM Fluorescein labeled 3kDa dextran.  Cells were incubated in this mixture at 37C for 15 minutes, after which time the mixture was removed and replaced with pH7 PBS.  We added 1uM of TAMRA labeled 3kDa dextran to this solution and allowed the cells to incubate at 37C for 15 minutes.  We imaged these cells using a Confocal Fluorescent Microscope, exciting the sample at 488nm for Fluorescein and at 561nm for TAMRA.  We found that Fluorescein signal was confined to the inside of the cells, indicating that at pH5 the peptides were able to cause disruptions in the membrane large enough to allow the passage of the dextran molecules (Figure 7.6).  The TAMRA signal was excluded from the cells, also indicating that when the solution pH increased to pH 7, the cells no longer contained large disruptions.  From this we concluded that our peptides were both able to activate at low pH and disrupt membranes and were able to deactivate when exposed to a higher pH solution. Peptides pHD118, pHD108, and pHD34 hold the capability of being used as a systemic delivery agent which would activate in low pH environments such as an endosome and would later deactivate inside of the cytosol.  With these results we were further encouraged to attempt studies to examine whether or not our peptides caused efficient endosomal escape.
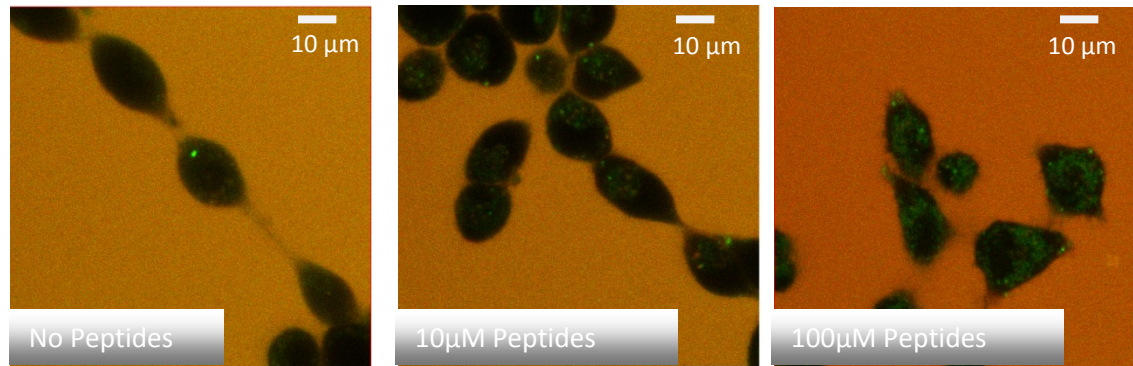
<u>Figure 7.6</u> Penetration of Cells by Large Molecules. These are representative images of the method discussed above wherein 3kDa Fluorescein Dextran (FD) was added to cells in pH 5 PBS buffer followed by washing with pH 7 PBS and addition of 3kDa TAMRA Dextran TA. Without peptides, no significant amount of Dextran accumulates inside of the cells. With 10uM and 100uM peptides, however, the 3kDa FD which was added at pH5 gets into cells and the 3kDa TA dextran added at pH7 is excluded. This shows that the peptides cause large scale disruptions in mammalian cells membranes to allow macromolecular delivery at low pH.

In our final assay, we tested the ability of pHD118, pHD108 and pHD34 to cause the escape of macromolecules from endosomes. We cultured CHO cells at $5*10^3$ in 8 chambered slides with DMEM media for 3 days. After this time period we switched to DMEM media lacking Fetal Bovine Serum (FBS) because this protein is known to interfere with uptake of dextrans. To induce endocytosis, we added a mixture of TAMRA labeled Arg9 (Arg9TA) and Alexafluor488 3kDa dextran to the cells along with 100uM peptides. Arg9TA can bind to the surface of the cells and induce endosomal uptake of the dextrans and peptides from solution. We incubated cells with this solution for up to 3 hours and imaged the cells for TAMRA and Alexafluor488 signals at time points of 15 min, 1 hour, and 3 hours. We found that for control samples, Arg9TA bound to cell membranes and remained trapped inside of endosomes for the entire time period of this study. Without the peptide, Alexfluor488 Dextran molecules remained confined to small endosomes within the cell (Figure 7.7). When peptides

were included in the samples, endosomes appeared to be much larger, and signal from

the Arg9TA was much less localized.  Signal from the Alexafluor488 Dextran appeared

less localized as well and disappeared into the background at long timepoints.  The

peptides enabled the escape of dextrans on the order of 3kDa in size.  This size range

could be appropriate for siRNA and other macromolecules.
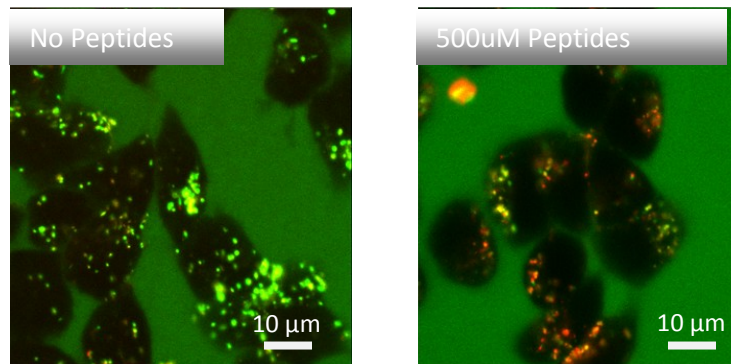


Figure 7.7 Endosomal Escape of Macromolecules Caused by pHD Peptides. Figure 7.9 shows example images of endosomal escape assays conducted with 500μM peptide.  In this experiment, without peptide Alexafluor488 10kDa dextran and Arg9-TA are clearly trapped inside of endosomes, showing as yellow/green.  With the peptide, after 1-3 hours, vesicles appear mostly red, indicating that the Arg9TA is bound to the endosomal membrane but that Alexafluor488 has escaped.

## Summary of Chapter 7

In examining the positive results from our screen we were able to establish a relationship between our biophysical characterization methods and cell based systems. We saw that these peptides functioned by the ideal mechanism of becoming protonated at low pH, binding to membranes, and associating to cause disruptions. These results were confirmed in both POPC vesicles as well as in CHO cells. Importantly, the difference between the pKa in POPC and the pKa in cells proved to be the same as the difference between POPC vesicles and POPC:CH vesicles. We were able to justify the results we saw in cells simply by adding cholesterol to our model membrane system. Moreover, we succeeded in creating a peptide which can be used with other delivery systems to cause endosomal escape of macromolecule drug therapies.

<u>Conclusions</u>

Membrane Active Peptides hold the key to unlocking an array of useful medicines that cannot otherwise enter the cell. We have shown that MAPs can be categorized by means of biophysical characterization techniques. In Chapter 1 we discussed how MAPs can be either transiently destabilizing or stable pore forming peptides. In Chapter 2 we examined how the extent of membrane activity can be determined by secondary reporter leakage assays. We used this information in Chapter 3 to design a peptide which would have ideal large, stable pore forming characteristics. We found that our rationally designed peptides did not work as intended; stable pore formation and pH-sensitivity are not simply additive properties as determined in Chapter 4. We used this information to design a peptide library in Chapter 5 which we then screened for a peptide with a combination of large pore forming and pH-sensitive activities in Chapter 6. Finally, in Chapter 7, we examined several positive result peptides and found that our biophysical characterization techniques can be used to predict activity in biological systems. We recommend that the insights generated within this body of work be used to develop new drug delivery methods using our peptides as guiding key for nanoparticle drug delivery systems and as the basis for future generations of Membrane Active Peptides.

Citations List

[1] Alberts, B., Johnson, A., Lewis, J., Raff, M., Roberts, K., and Walter, P. (2002) Membrane Structure, In *Molecular Biology of the Cell*, pp 584-614, Garland Science, New York, New York.

[2] Cullis, P. R., and Dekruijff, B. (1979) Lipid Polymorphism and the Functional Roles of Lipids in Biological-Membranes, *Biochim Biophys Acta 559*, 399-420.

[3] Nagle, J. F., and Tristram-Nagle, S. (2000) Structure of lipid bilayers, *Bba-Rev Biomembranes 1469*, 159-195.

[4] Gersten, J. I., and Smith, F. W. (2001) Polymers, In *The Physics and Chemistry of Materials*, John Wiley & Sons, Inc, New York, New York.

[5] Goldfine, H. (1984) Bacterial-Membranes and Lipid Packing Theory, *J Lipid Res 25*, 1501-1507.

[6] Hancock, R. E. W., and Lehrer, R. (1998) Cationic peptides: a new source of antibiotics, *Trends Biotechnol 16*, 82-88.

[7] Kang, S. J., Kim, D. H., Mishig-Ochir, T., and Lee, B. J. (2012) Antimicrobial Peptides: Their Physicochemical Properties and Therapeutic Application, *Arch Pharm Res 35*, 409-413.

[8] Nelson, D. L., and Cox, M. (2008) *Lehninger Principals of Biochemistry*, 5 ed., W.H. Freeman, New York, New York.

[9] Margulis, L. (1976) Genetic and Evolutionary Consequences of Symbiosis, *Exp Parasitol 39*, 277-349.

[10] Gill, S. J., and Wadso, I. (1976) Equation of State Describing Hydrophobic Interactions, *P Natl Acad Sci USA 73*, 2955-2958.

[11] Singer, S. J., and Nicolson, G. L. (1972) Fluid Mosaic Model of Structure of Cell-Membranes, *Science 175*, 720-&.

[12] Catterall, W. A. (2000) From ionic currents to molecular mechanisms: The structure and function of voltage-gated sodium channels, *Neuron 26*, 13-25.

[13] Dimroth, P., Kaim, G., and Matthey, U. (2000) Crucial role of the membrane potential for ATP synthesis by F1Fo ATP synthases, *J Exp Biol 203*, 51-59.

[14] Hancock, J. T. (2005) *Cell Signaling*, 2 ed., Oxford University Press, Oxford, United Kingdom.

[15] Kroemer, G., Galluzzi, L., Vandenabeele, P., Abrams, J., Alnemri, E. S., Baehrecke, E. H., Blagosklonny, M. V., El-Deiry, W. S., Golstein, P., Green, D. R., Hengartner, M., Knight, R. A., Kumar, S., Lipton, S. A., Malorni, W., Nunez, G., Peter, M. E., Tschopp, J., Yuan, J., Piacentini, M., Zhivotovsky, B., and Melino, G. (2009) Classification of cell death:

recommendations of the Nomenclature Committee on Cell Death 2009, *Cell Death Differ 16*, 3-11.

[16] Darzynkiewicz, Z., Bruno, S., Delbino, G., Gorczyca, W., Hotz, M. A., Lassota, P., and Traganos, F. (1992) Features of Apoptotic Cells Measured by Flow-Cytometry, *Cytometry 13*, 795-808.

[17] Boyer, R. F. (2005) *Concepts in Biochemistry*, 3 ed., Wiley, New York, New York.

[18] Murphy, R. F., Schmid, J., and Fuchs, R. (1993) Endosome Maturation - Insights from Somatic-Cell Genetics and Cell-Free Analysis, *Biochem Soc T 21*, 716-720.

[19] Huotari, J., and Helenius, A. (2011) Endosome maturation, *Embo J 30*, 3481-3500.

[20] Medina, D. L., Fraldi, A., Bouche, V., Annunziata, F., Mansueto, G., Spampanato, C., Puri, C., Pignata, A., Martina, J. A., Sardiello, M., Palmieri, M., Polishchuk, R., Puertollano, R., and Ballabio, A. (2011) Transcriptional Activation of Lysosomal Exocytosis Promotes Cellular Clearance, *Dev Cell 21*, 421-430.

[21] Bartel, D. P. (2004) MicroRNAs: Genomics, biogenesis, mechanism, and function, *Cell 116*, 281-297.

[22] Varkouhi, A. K., Scholte, M., Storm, G., and Haisma, H. J. (2011) Endosomal escape pathways for delivery of biologicals, *J Control Release 151*, 220-228.

[23] van de Wetering, P., Moret, E. E., Schuurmans-Nieuwenbroek, N. M. E., van Steenbergen, M. J., and Hennink, W. E. (1999) Structure-activity relationships of water-soluble cationic methacrylate/methacrylamide polymers for nonviral gene delivery, *Bioconjugate Chem 10*, 589-597.

[24] Cho, Y. W., Kim, J. D., and Park, K. (2003) Pollycation gene delivery systems: escape from endosomes to cytosol, *J Pharm Pharmacol 55*, 721-734.

[25] Sunshine, J. C., Peng, D. Y., and Green, J. J. (2012) Uptake and Transfection with Polymeric Nanoparticles Are Dependent on Polymer End-Group Structure, but Largely Independent of Nanoparticle Physical and Chemical Properties, *Mol Pharmaceut 9*, 3375-3383.

[26] Sun, T. M., Du, J. Z., Yan, L. F., Mao, H. Q., and Wang, J. (2008) Self-assembled biodegradable micellar nanoparticles of amphiphilic and cationic block copolymer for siRNA delivery, *Biomaterials 29*, 4348-4355.

[27] Mann, D. A., and Frankel, A. D. (1991) Endocytosis and Targeting of Exogenous Hiv-1 Tat Protein, *Embo J 10*, 1733-1739.

[28] Abes, R., Arzumanov, A., Moulton, H., Abes, S., Ivanova, G., Gait, M. J., Iversen, P., and Lebleu, B. (2008) Arginine-rich cell penetrating peptides: Design, structure-activity, and

applications to alter pre-mRNA splicing by steric-block oligonucleotides, *J Pept Sci 14*, 455-460.

[29] Vives, E., Brodin, P., and Lebleu, B. (1997) A truncated HIV-1 Tat protein basic domain rapidly translocates through the plasma membrane and accumulates in the cell nucleus, *J Biol Chem 272*, 16010-16017.

[30] He, J., Kauffman, W. B., Fuselier, T., Naveen, S. K., Voss, T. G., Hristova, K., and Wimley, W. C. (2013) Direct Cytosolic Delivery of Polar Cargo to Cells by Spontaneous Membrane-translocating Peptides, *J Biol Chem 288*, 29974-29986.

[31] Richard, J. P., Melikov, K., Vives, E., Ramos, C., Verbeure, B., Gait, M. J., Chernomordik, L. V., and Lebleu, B. (2003) Cell-penetrating peptides: a re-evaluation of the mechanism of cellular uptake., *Biophys J 84*, 212a-212a.

[33] Hatakeyama, H., Ito, E., Akita, H., Oishi, M., Nagasaki, Y., Futaki, S., and Harashima, H. (2009) A pH-sensitive fusogenic peptide facilitates endosomal escape and greatly enhances the gene silencing of siRNA-containing nanoparticles in vitro and in vivo, *J Control Release 139*, 127-132.

[34] Kakudo, T., Chaki, S., Futaki, S., Nakase, I., Akaji, K., Kawakami, T., Maruyama, K., Kamiya, H., and Harashima, H. (2004) Transferrin-modified liposomes equipped with a pH-sensitive fusogenic peptide: An artificial viral-like delivery system, *Biochemistry-Us 43*, 5618-5628.

[35] An, M., Wijesinghe, D., Andreev, O. A., Reshetnyak, Y. K., and Engelman, D. M. (2010) pH-(low)-insertion-peptide (pHLIP) translocation of membrane impermeable phalloidin toxin inhibits cancer cell proliferation, *P Natl Acad Sci USA 107*, 20246-20250.

[36] Merrifield, R. B. (1963) Solid Phase Peptide Synthesis .1. Synthesis of a Tetrapeptide, *J Am Chem Soc 85*, 2149-&.

[37] Sessa, G., Weissman.G, Freer, J. H., and Hirschho.R. (1968) Effects of Melittin (Bee Venom) on Natural and Artificial Membranes, *Fed Proc 27*, 248-&.

[38] Chapman, D., Cherry, R. J., Finer, E. G., Hauser, H., Phillips, M. C., Shipley, G. G., and Mcmullen, A. I. (1969) Physical Studies of Phospholipid/Alamethicin Interactions, *Nature 224*, 692-&.

[39] Subbarao, N. K., Parente, R. A., Szoka, F. C., Nadasdi, L., and Pongracz, K. (1987) Ph-Dependent Bilayer Destabilization by an Amphipathic Peptide, *Biochemistry-Us 26*, 2964-2972.

[40] Krauson, A. J., He, J., and Wimley, W. C. (2012) Gain-of-Function Analogues of the Pore-Forming Peptide Melittin Selected by Orthogonal High-Throughput Screening, *J Am Chem Soc 134*, 12732-12741.

[41] Hanke, W., Methfessel, C., Wilmsen, H. U., Katz, E., Jung, G., and Boheim, G. (1983) Melittin and a Chemically Modified Trichotoxin Form Alamethicin-Type Multistate Pores, *Biochim Biophys Acta 727*, 108-114.

[42] Li, W. J., Nicol, F., and Szoka, F. C. (2004) GALA: a designed synthetic pH-responsive amphipathic peptide with applications in drug and gene delivery, *Adv Drug Deliver Rev 56*, 967-985.

[43] Brogden, K. A. (2005) Antimicrobial peptides: Pore formers or metabolic inhibitors in bacteria?, *Nat Rev Microbiol 3*, 238-250.

[44] Yang, L., Harroun, T. A., Weiss, T. M., Ding, L., and Huang, H. W. (2001) Barrel-stave model or toroidal model? A case study on melittin pores, *Biophys J 81*, 1475-1485.

[45] He, L. H., Robertson, J. W. F., Li, J., Karcher, I., Schiller, S. M., Knoll, W., and Naumann, R. (2005) Tethered bilayer lipid membranes based on monolayers of thiolipids mixed with a complementary dilution molecule. 1. Incorporation of channel peptides, *Langmuir 21*, 11666-11672.

[46] Lin, J., Merzlyakov, M., Hristova, K., and Searson, P. C. (2008) Impedance spectroscopy of bilayer membranes on single crystal silicon, *Biointerphases 3*, Fa33-Fa40.

[47] Li, E., Merzlyakov, M., Lin, J., Searson, P., and Hristova, K. (2009) Utility of surface-supported bilayers in studies of transmembrane helix dimerization, *J Struct Biol 168*, 53-60.

[48] Gritsch, S., Nollert, P., Jahnig, F., and Sackmann, E. (1998) Impedance spectroscopy of porin and gramicidin pores reconstituted into supported lipid bilayers on indium-tin-oxide electrodes, *Langmuir 14*, 3118-3125.

[49] Montal, M., and Mueller, P. (1972) Formation of Bimolecular Membranes from Lipid Monolayers and a Study of Their Electrical Properties, *P Natl Acad Sci USA 69*, 3561-3566.

[50] Raguse, B., Braach-Maksvytis, V., Cornell, B. A., King, L. G., Osman, P. D. J., Pace, R. J., and Wieczorek, L. (1998) Tethered lipid bilayer membranes: Formation and ionic reservoir characterization, *Langmuir 14*, 648-659.

[51] Lin, J., Szymanski, J., Searson, P. C., and Hristova, K. (2010) Effect of a Polymer Cushion on the Electrical Properties and Stability of Surface-Supported Lipid Bilayers, *Langmuir 26*, 3544-3548.

[52] Lin, J. I., Szymanski, J., Searson, P. C., and Hristova, K. (2010) Electrically Addressable, Biologically Relevant Surface-Supported Bilayers, *Langmuir 26*, 12054-12059.

[53] Lin, J., Motylinski, J., Krauson, A. J., Wimley, W. C., Searson, P. C., and Hristova, K. (2012) Interactions of Membrane Active Peptides with Planar Supported Bilayers: An Impedance Spectroscopy Study, *Langmuir 28*, 6088-6096.

[54] Valincius, G., McGillivray, D. J., Febo-Ayala, W., Vanderah, D. J., Kasianowicz, J. J., and Losche, M. (2006) Enzyme activity to augment the characterization of tethered bilayer membranes, *J Phys Chem B 110*, 10213-10216.

[55] Heinrich, F., Ng, T., Vanderah, D. J., Shekhar, P., Mihailescu, M., Nanda, H., and Losche, M. (2009) A New Lipid Anchor for Sparsely Tethered Bilayer Lipid Membranes, *Langmuir 25*, 4219-4229.

[56] Smart, O. S., Goodfellow, J. M., and Wallace, B. A. (1993) The Pore Dimensions of Gramicidin-A, *Biophys J 65*, 2455-2460.

[57] Wiedman, G., Herman, K., Searson, P., Wimley, W. C., and Hristova, K. (2013) Electrical Response of Bilayers to the Bee Venom Toxin Melittin, *Biophys J 104*, 65a-65a.

[58] Coronado, R., and Latorre, R. (1983) Phospholipid-Bilayers Made from Monolayers on Patch-Clamp Pipettes, *Biophys J 43*, 231-236.

[59] Portlock, S. H., Clague, M. J., and Cherry, R. J. (1990) Leakage of Internal Markers from Erythrocytes and Lipid Vesicles Induced by Melittin, Gramicidin-S and Alamethicin - a Comparative-Study, *Biochim Biophys Acta 1030*, 1-10.

[60] Fox, R. O., and Richards, F. M. (1982) A Voltage-Gated Ion Channel Model Inferred from the Crystal-Structure of Alamethicin at 1.5-a Resolution, *Nature 300*, 325-330.

[61] Eisenberg, D. (1984) 3-Dimensional Structure of Membrane and Surface-Proteins, *Annu Rev Biochem 53*, 595-623.

[62] Nicol, F., Nir, S., and Szoka, F. C. (2000) Effect of phospholipid composition on an amphipathic peptide-mediated pore formation in bilayer vesicles, *Biophys J 78*, 818-829.

[63] Hristova, K., Dempsey, C. E., and White, S. H. (2001) Structure, location, and lipid perturbations of melittin at the membrane interface, *Biophys J 80*, 801-811.

[64] Kuchinka, E., and Seelig, J. (1989) Interaction of Melittin with Phosphatidylcholine Membranes - Binding Isotherm and Lipid Headgroup Conformation, *Biochemistry-Us 28*, 4216-4221.

[65] Ladokhin, A. S., Wimley, W. C., and White, S. H. (1995) Leakage of membrane vesicle contents: Determination of mechanism using fluorescence requenching, *Biophys J 69*, 1964-1971.

[66] Fletcher, J. E., and Jiang, M. S. (1993) Possible Mechanisms of Action of Cobra Snake-Venom Cardiotoxins and Bee Venom Melittin, *Toxicon 31*, 669-695.

[67] Wiedman, G., Fuselier, T., He, J., Searson, P. C., Hristova, K., and Wimley, W. C. (2014) Highly Efficient Macromolecule-Sized Poration of Lipid Bilayers by a Synthetically Evolved Peptide, *J Am Chem Soc 136*, 4724-4731.

[68] Almeida, P. F., and Pokorny, A. (2009) Mechanisms of Antimicrobial, Cytolytic, and Cell-Penetrating Peptides: From Kinetics to Thermodynamics, *Biochemistry-Us 48*, 8083-8093.

[69] Macdonald, R. C., Macdonald, R. I., Menco, B. P. M., Takeshita, K., Subbarao, N. K., and Hu, L. R. (1991) Small-Volume Extrusion Apparatus for Preparation of Large, Unilamellar Vesicles, *Biochim Biophys Acta 1061*, 297-303.

[70] Wheaten, S. A., Ablan, F. D. O., Spaller, B. L., Trieu, J. M., and Almeida, P. F. (2013) Translocation of Cationic Amphipathic Peptides across the Membranes of Pure Phospholipid Giant Vesicles, *J Am Chem Soc 135*, 16517-16525.

[71] De Graef, M., and McHenry, M. E. (2007) *Structure of materials : an introduction to crystallography, diffraction and symmetry*, Cambridge University Press, Cambridge.

[72] Fry, D. W., White, J. C., and Goldman, I. D. (1978) Rapid Separation of Low-Molecular Weight Solutes from Liposomes without Dilution, *Anal Biochem 90*, 809-815.

[73] Ladokhin, A. S., Selsted, M. E., and White, S. H. (1997) Bilayer interactions of indolicidin, a small antimicrobial peptide rich in tryptophan, proline, and basic amino acids, *Biophys J 72*, 794-805.

[74] Ellens, H., Bentz, J., and Szoka, F. C. (1985) H+-Induced and Ca-2+-Induced Fusion and Destabilization of Liposomes, *Biochemistry-Us 24*, 3099-3106.

[75] Armstrong, J. K., Wenby, R. B., Meiselman, H. J., and Fisher, T. C. (2004) The hydrodynamic radii of macromolecules and their effect on red blood cell aggregation, *Biophys J 87*, 4259-4270.

[76] Ladokhin, A. S., Selsted, M. E., and White, S. H. (1997) Sizing membrane pores in lipid vesicles by leakage of co-encapsulated markers: Pore formation by melittin, *Biophys J 72*, 1762-1766.

[77] Weinstein, J. N., Yoshikami, S., Henkart, P., Blumenthal, R., and Hagins, W. A. (1977) Liposome-Cell Interaction - Transfer and Intracellular Release of a Trapped Fluorescent Marker, *Science 195*, 489-492.

[78] Jones, L. J., Upson, R. H., Haugland, R. P., PanchukVoloshina, N., Zhou, M. J., and Haugland, R. P. (1997) Quenched BODIPY dye-labeled casein substrates for the assay of protease activity by direct fluorescence measurement, *Anal Biochem 251*, 144-152.

[79] Helm, C. A., Knoll, W., and Israelachvili, J. N. (1991) Measurement of Ligand Receptor Interactions, *P Natl Acad Sci USA 88*, 8169-8173.

[80] Wimley, W. C., and White, S. H. (1996) Experimentally determined hydrophobicity scale for proteins at membrane interfaces, *Nat Struct Biol 3*, 842-848.

[81] Shai, Y. (1999) Mechanism of the binding, insertion and destabilization of phospholipid bilayer membranes by alpha-helical antimicrobial and cell non-selective membrane-lytic peptides, *Bba-Biomembranes 1462*, 55-70.

[82] Anaspec. (2014) pK and pl Values of Amino Acids, Anaspec.

[83] Beschiaschvili, G., and Seelig, J. (1990) Melittin Binding to Mixed Phosphatidylglycerol Phosphatidylcholine Membranes, *Biochemistry-Us 29*, 52-58.

[84] Parente, R. A., Nadasdi, L., Subbarao, N. K., and Szoka, F. C. (1990) Association of a Ph-Sensitive Peptide with Membrane-Vesicles - Role of Amino-Acid-Sequence, *Biochemistry-Us 29*, 8713-8719.

[85] Ladokhin, A. S., Jayasinghe, S., and White, S. H. (2000) How to measure and analyze tryptophan fluorescence in membranes properly, and why bother?, *Anal Biochem 285*, 235-245.

[86] Marieb, E. N. (2006) *Essentials of human anatomy & physiology*, 8th ed., Pearson/Benjamin Cummings, San Francisco.

[87] Sigma-Aldrich. (2014) Buffer Reference Center, Sigma-Aldrich.

[88] Wimley, W. C., Creamer, T. P., and White, S. H. (1996) Solvation energies of amino acid side chains and backbone in a family of host-guest pentapeptides, *Biochemistry-Us 35*, 5109-5124.

[89] Whitmore, L., and Wallace, B. A. (2008) Protein secondary structure analyses from circular dichroism spectroscopy: Methods and reference databases, *Biopolymers 89*, 392-400.

[90] Wiedman, G., Hristova, K., and Wimley, W. (2015) Testing the limits of rational design by engineering pH sensitivity into membrane active peptides, *Biochimica et Biophysica Acta (BBA) - Biomembranes*.

[91] Oneil, K. T., and Degrado, W. F. (1990) A Thermodynamic Scale for the Helix-Forming Tendencies of the Commonly Occurring Amino-Acids, *Science 250*, 646-651.

[92] Kohn, W. D., Kay, C. M., and Hodges, R. S. (1995) Protein Destabilization by Electrostatic Repulsions in the 2-Stranded Alpha-Helical Coiled-Coil Leucine-Zipper, *Protein Sci 4*, 237-250.

[93] Zidovetzki, R. (2014) Helical Wheel Projections.

[94] Kaiser, E., Colescot.Rl, Bossinge.Cd, and Cook, P. I. (1970) Color Test for Detection of Free Terminal Amino Groups in Solid-Phase Synthesis of Peptides, *Anal Biochem 34*, 595-&.

[95] Bochet, C. G. (2002) Photolabile protecting groups and linkers, *J Chem Soc Perk T 1*, 125-142.

[96] Duzgunes, N., Faneca, H., and de Lima, M. C. P. (2010) Methods to Monitor Liposome Fusion, Permeability, and Interaction with Cells, *Methods Mol Biol 606*, 209-232.

[97] Edman, P. (1949) A Method for the Determination of the Amino Acid Sequence in Peptides, *Arch Biochem 22*, 475-476.

[98] Raghuraman, H., and Chattopadhyay, A. (2004) Interaction of melittin with membrane cholesterol: A fluorescence approach, *Biophys J 87*, 2419-2432.

[99] John, E., and Jahnig, F. (1992) A Synthetic Analog of Melittin Aggregates in Large Oligomers, *Biophys J 63*, 1536-1543.

[100] Roth, B. L., Poot, M., Yue, S. T., and Millard, P. J. (1997) Bacterial viability and antibiotic susceptibility testing with SYTOX Green nucleic acid stain, *Appl Environ Microb 63*, 2421-2431.

# Gregory R. Wiedman

**Address:**          3526 Greenmount Ave
                      Baltimore, MD, 21218
                      Telephone: 610-529-6056
                      E-mail: gwiedman@jhu.edu

## Education:
2011-15 PhD in Materials Science Engineering, Johns Hopkins University
2009-10 M.S.E. in Engineering and Nanotechnology, University of Pennsylvania
2006-10 B.S.E. in Bioengineering, University of Pennsylvania

## Awards and Accomplishments:
- Preparing Future Faculty for Teaching (PFFT) Fellow CIRTL (2013-2015)
- IGERT Fellow Johns Hopkins University (2011-2015)
- Johns Hopkins University Institute for Nanobiotechnology Member
- Nanotech Minor council member and NanoDay coordinator (2007-2010)
- UPENN Nanobio Interface Center Member
- 2009-2010 UPENN Dean's List
- UPENN Engineering Entrepreneurship Speakers Award

## Memberships:
- American Chemical Society
- Biophysical Society
- American Society for Testing Materials

## Research Experience:

**August 2011-Pressent**
Doctoral Candidate at the Department of Materials Science Engineering at Johns Hopkins University
Advisor: Prof. Kalina Hristova
- Developed protocols for quantifying pH-sensitive leakage from vesicles
- Designed high-throughput screens for peptides to induce endosomal escape
- Studied effects of translocating and pore-forming peptides on various cell lines and their implications of gene delivery
- Mentored Undergraduate and Masters students in lab as well as oversaw several Senior Design projects

**January 2008-Juanuary 2011**
Research Assistant at the Department of Biochemistry and Biophysics at the University of Pennsylvania
Advisor: Prof. Bohdana M. Discher
- Designed proteins for membrane electron transfer/light harvesting
- Purified proteins using HPLC and various other techniques

- Characterized protein-cofactor assembly using UV-VIS spectroscopy, Redox Titrations, Analytical Ultracentrifugation, Mass Spectroscopy, Circular Dichroism, Fluorescence Spectroscopy, Stopped-Flow etc.
- Sample preparation for AFM measurements and molecular electronics applications

**September 2009-September 2010**
Senior Design Research Assistant at the Immunology Department of University of Pennsylvania
Advisor: Nathalie Scholler MD PhD
- Generated and purified single chain antibodies
- Developed novel system for Nanoparticle-antibody functionalization
- Researched and demonstrated Nanoparticle binding to tumor receptor expressing mouse cells

**December 2006-December 2007**
Research Assistant at the Department of Chemistry of University of Pennsylvania
Advisor: Michael Therien PhD
- Synthesized block-copolymers and self-assembled polymersomes
- Characterized polymersome size, shape, and size distribution.
- Synthesized and purified porphyrin molecules

**<u>Teaching Experience:</u>**

**October 2014-December 2014**
Lecturer for Whiting School of Engineering at Johns Hopkins University
Advisor: Dr Edward Scheinerman
- Designed the course EN.500.111.03 Finding the Cure Methods in Drug Discovery
- Delivered lesson plans with numerous active learning techniques
- Designed formative and summative assessments for students
- Provided resources for students to find their own research opportunities.

**August 2012-May 2013**
Teaching Assistant for Department of Materials Science at Johns Hopkins University
Advisor: Prof Todd Hufnagel and Prof. Kalina Hristova
- Created lesson plans and lead laboratory exercises
- Created answer keys and tests for student evaluation
- Held study sessions and review sessions for assistance outside of the classroom
- Mentored Undergraduate and Masters students

**January 2011-May 2011**
Substitute Teacher and Test-prep instruction for Nueva Esperanza Academy, Philadelphia PA.
Director: Mr. Michael Kelly, Assistant Principal
- Mentored minority and at-risk students from the Philadelphia region.
- Created individualized lesson plans from targeted student educational needs.
- Provided instruction to students on a classroom, small group, and individual level

- Helped to design and improve test-preparation program for State Assessment Exam which lead to an increase from 40 to 60% proficiency rating for the school.

## Publications

(1) **Wiedman G**, Fuselier T, He J, Searson PC, Wimley WC, Hristova K. Highly efficient macromolecular-sized poration of lipid bilayers by a synthetically evolved peptide. *JACS.* 136(12): 4724-4731 (2014)

(2) **Wiedman G**, Searson P, Wimley WC, Hristova K. Testing the limits of rational design by engineering pH-sensitivity into Membrane Active Peptides. *BBA In Press*

(3) **Wiedman G**, Herman K, Searson P, Wimley WC, Hristova K. The electrical response of bilayers to the bee venom toxin melittin: evidence for transient bilayer permeabilization. *Biochim Biophys Acta.* 1828(5): 1357-64 (2013).

(4) Chen C, **Wiedman G**, Khan A., Ulmschneider MB. Absorption and folding of melittin onto lipid bilayer membranes via atomic detail microsecond molecular dynamic simulations. *Biochemica Biophysica Acta* (2014).

(5) Cruz J, Mihailescu M, **Wiedman G**, Herman K, Searson P, Wimley WC, Hristova K. A membrane-translocating peptide penetrates into bilayers without significant bilayer perturbations. *Biophys J.* 104(11)2419-28 (2013).

(6) Huang W, Zhang Y, Yang S, **Wiedman G**, Liu Y, Guo W, Hemker K, Hristova K, Kymissis IJ, Katz HE. A High-Capacitance Nonionic Dielectric for Self-Healable, Printable, and Flexible Organic Field Effect Transistors and Chemical Sensors. *Submitted Advanced Functional Materials*

## Presentations:

(1) **Gregory R. Wiedman**, Taylor Fuselier, Jing He, Peter Searson, William C Wimley, Kalina Hristova: "A Novel Class of Pore-Forming Peptide". Biophysical Society Meeting, San Francisco, California, 2014.

(2) **Gregory R. Wiedman**, Katherine Herman, Peter Searson, William C Wimley, Kalina Hristova: "Melittin and Membrane Active Peptides as Drugs: a study of Electrical Impedance". American Chemical Society Meeting, New Orleans, Louisiana, 2013.

(3) **Gregory R. Wiedman**, Katherine Herman, Peter Searson, William C Wimley, Kalina Hristova: "An Electrochemical Impedance Spectroscopy Study of membrane Active Peptides". Biophysical Society Meeting, Philadelphia, Pennsylvania, 2013.

(4) **Gregory R. Wiedman**, Katherine Herman, Peter Searson, William C Wimley, Kalia Hristova: "Effect of melittin and a gain-of-function Melittin analogue on bilayer properties: and electrical impedance study." Biophysical Society Meeting, San Diego, California, 2012.

(5) **Gregory R. Wiedman**, Katherine Herman, Peter Searson, William Wimley, Kalina Hristova: "Pore Forming Peptides". ACS Colloids Meeting, Johns Hopkins University, 2012

(6) Sarah E. Chobot, **Gregory R. Wiedman**, Christopher C Moser, Bohdana M. Discher P. Leslie Dutton: "Design and Characterization of an Enzymatically Active Amphiphilic Maquette Protein" *Biochemistry* 98(3), 639 (2010).

(7) Sarah E. Chobot, Ross L. Anderson, Lee A. Solomon, **Gregory R. Wiedman**, J. Wand, Mike L. Klein, Chris C. Moser. Bohdana M. Discher, P. Leslie Dutton : "De novo synthetic models for light capture and catalysis", presentation for NSF MRSEC review, 2010.

(8) Kolin C Hribar and **Gregory R. Wiedman**, Andrew Prantner, Chaitanya Divgi, Nathalie Scholler: "Gold Nanorods Conjugated to Tumor-specific Antibody for the Targeting of Ovarian Cancer", Bioengineering Department Senior Design Presentation, 2010

(9) **Gregory R. Wiedman,** Paul O'Brien, Sarah E. Chobot, Sanjini U Nanayakkara, Kendra M Kathan, Dawn A Bonnell, P. Leslie Dutton and Bohdana M. Discher**:** "Structural Design,

Assembly, and Engineering of Oxidoreductases in Energy Conversion", University of Pennsylvania Biochemistry and Biophysics Departmental Retreat, 2009.


**<u>Other Expertise</u>**:

- Extensive experience in the field of protein design and characterization
- Imaging and spectroscopy techniques including UV-VIS, fluorescence, CD and IR spectroscopy, confocal microscopy, SEM, and AFM
- Developed proficiency in molecular biology techniques such as bacteria cultivation/cell growth, Western Blot, ELISA assays, and Flow Cytometry, MS, and LC/MS
- Trained in techniques of materials production such as chemical synthesis of proteins/biomolecules, CVD, Microfabrication and various other materials techniques.
- Gained excellent communication and coordination skills in project design.

Gregory Wiedman Biography

       I was born to my parents Robert and Judith Wiedman on January 7th, 1987.  I was raised in Delaware County in the greater Philadelphia area in Pennsylvania with my siblings Justin, Allison, Nicholas, and Luke Wiedman.  I attended Springfield High School and the University of Pennsylvania where I received a Bachelor's of Science in Engineering in Bioengineering and a Master's of Science In Engineering in Nanotechnology.  During my time at Hopkins I have been a member of the Institute for Nanobiotechnology, a Preparing Future Faculty for Research Fellow as well as a member of both the Biophysical Society and the American Chemical Society.  I have designed and taught classes as part of the INBT, the Materials Science Department, as well as being the instructor of record for EN.500.111.03 "Finding the Cure Methods in Drug Discovery".  I took great pleasure in the work I conducted at The Johns Hopkins University and I hope that those reading this work will have also receive such enjoyment.